Powerful Spatial Multiple Testing via Borrowing Neighboring Information

Linsui Deng¹, Kejun He^{1*}, Xianyang Zhang^{2*}

¹The Center for Applied Statistics, Institute of Statistics and Big Data,
Renmin University of China, Beijing, China

²Department of Statistics, Texas A&M University, College Station, USA

Abstract

Clustered effects are often encountered in multiple hypothesis testing of spatial signals. In this paper, we propose a new method, termed two-dimensional spatial multiple testing (2d-SMT) procedure, to control the false discovery rate (FDR) and improve the detection power by exploiting the spatial information encoded in neighboring observations. The proposed method provides a novel perspective of utilizing spatial information by gathering signal patterns and spatial dependence into an auxiliary statistic. 2d-SMT rejects the null when a primary statistic at the location of interest and the auxiliary statistic constructed based on nearby observations are greater than their corresponding thresholds. 2d-SMT can also be combined with different variants of the weighted BH procedures to improve the detection power further. A fast step-down algorithm is developed to accelerate the search for optimal thresholds in 2d-SMT. In theory, we establish the asymptotical FDR control of 2d-SMT under weak spatial dependence. Extensive numerical experiments demonstrate that the 2d-SMT method combined with various weighted BH procedures achieves the most competitive performance in FDR and power trade-off.

Keywords: Empirical Bayes; False discovery rate; Near epoch dependence; Side information.

1 Introduction

Large-scale multiple testing with spatial structure has become increasingly important in various areas, e.g., functional Magnetic Resonance Imaging (fMRI) research, genome-wide association study, environmental studies, and astronomical surveys. The essential task is identifying locations that exhibit significant deviations from the background to build scientific interpretations. Since thousands or even millions of spatially correlated hypotheses tests

^{*}Correspondence: kejunhe@ruc.edu.cn and zhangxiany@stat.tamu.edu.

are often conducted simultaneously, incorporating informative spatial patterns to provide a powerful multiplicity adjustment for dependent multiple hypothesis testing is becoming a significant challenge.

There has been a growing literature on spatial signal detection with false discovery rate control (FDR, Benjamini and Hochberg, 1995). Heller et al. (2006) and Sun et al. (2015) proposed to perform multiple testing on cluster-wise hypotheses by aggregating locationwise hypotheses to increase the signal-to-noise ratio. Benjamini and Heller (2007), Sun et al. (2015) and Basu et al. (2018) defined new error rates to reflect the relative importance of hypotheses associated with different clusters. For instance, a hypothesis corresponding to a larger cluster is more important than the one associated with a smaller cluster. Scott et al. (2015) considered a two-group mixture model with the prior null probability dependent on the auxiliary spatial information. Yun et al. (2022) proposed a spatial-adaptive FDRcontrolling procedure by exploiting the mirror conservativeness of the p-values under the null and the spatial smoothness under the alternative. Tansey et al. (2018) enforced spatial smoothness by imposing a penalty on the pairwise differences of log odds of hypotheses being signals between adjacent locations. Along a related line, Genovese et al. (2006) suggested to weight p-values or equivalently assign location-specific cutoffs by leveraging the tendency of hypotheses being null. This idea has been further developed in a few recent papers to incorporate different types of structural and covariate information. See, e.g., Ignatiadis et al. (2016), Li and Barber (2019), Cai et al. (2021), Zhang and Chen (2022) and Cao et al. (2022).

In many applications, signals tend to exhibit in clusters. As a result, hypotheses around a non-null location are more likely to be under the alternative than under the null. One way to account for spatially clustered signals is to screen out the locations where the average signal strength of the neighbors captured by an auxiliary statistic is weak (Shen et al., 2002). The locations passing the screening step are subjected to further analysis. This procedure suffers from the so-called selection bias as the downstream statistical inference needs to account for

the selection effect from the screening step. A simple remedy is sample splitting (Wasserman and Roeder, 2009; Liu et al., 2022b), where a subsample is used to perform screening, and the remaining samples are utilized for the downstream inference. Sample splitting is intuitive and easy to implement, but it inevitably sacrifices the detection power because it does not excavate complete information. Furthermore, there are often no completely independent observations to conduct sample splitting in spatial settings.

We propose a new method named the two-dimensional spatial multiple testing (2d-SMT) procedure that fundamentally differs from the existing spatial multiple testing procedures. 2d-SMT consists of a two-dimensional rejection region built on two statistics, an auxiliary statistic $T_1(s)$ and a primary statistic $T_2(s)$, for each hypothesis. The first dimension utilizes the auxiliary information constructed from the neighbors of a location of interest to perform feature screening, which helps to increase the signal density and lessen the multiple testing burdens in the second dimension. The second dimension then uses a statistic computed from the data at the location of interest to pick out signals. 2d-SMT declares the hypothesis at location s to be non-null if $T_1(s) \geq t_1$ and $T_2(s) \geq t_2$. The optimal cutoffs t_1^* and t_2^* are chosen to achieve the maximum number of discoveries while controlling the FDR at the desired level. The 2d-SMT procedure involves the following main ingredients, designed to improve its robustness and efficiency:

- Accounting for the dependence between the auxiliary statistic and the primary statistics, which alleviates the selection bias;
- Borrowing spatial signal information through an empirical Bayes approach;
- Speeding up the search for the bivariate cutoff through an efficient step-down algorithm. 2d-SMT explores spatial information from a completely different perspective than the existing weighted procedures. It thus can be combined with these methods to improve their power further. Examples of these weighted procedures include the group BH procedure (GBH, Hu et al., 2010), independent hypothesis weighting (IHW, Ignatiadis et al., 2016), structure

adaptive BH algorithm (SABHA, Li and Barber, 2019), and locally adaptive weighting and screening approach (LAWS, Cai et al., 2021). The readers are referred to Section 2.7 for more details.

In a related study, Yi et al. (2021) proposed the 2dFDR approach to detect the association between omics features and covariates of interest in the presence of confounding factors. 2dFDR borrows information from confounder-unadjusted test statistics to boost the power in omics association testing with confounder-adjustment. In contrast, 2d-SMT is designed for the spatial multiple testing problem by borrowing information from neighboring observations. We develop a fast algorithm to overcome the computational bottleneck in finding the 2d cutoff values, which can be applied to both 2dFDR and 2d-SMT. Finally, it is worth mentioning that our asymptotic analysis allows weak spatial dependence, which goes beyond the independence assumption in Yi et al. (2021).

The rest of the paper is organized as follows. Section 2 develops the 2d-SMT procedure, including the oracle procedure, the feasible procedure with estimated covariance structure, and the extension by combining it with various weighted BH procedures. Section 3 discusses some implementation details and proposes an efficient algorithm to find the optimal thresholds. Section 4 establishes the asymptotic FDR control of the 2d-SMT procedure. In Section 5, extensive simulation studies demonstrate the effectiveness of the 2d-SMT procedure. Section 6 illustrates the method using an ozone dataset. Section 7 concludes and points out a few future research directions. Some additional details of the numerical experiments and technical proofs are presented in a separate online supplementary file.

2 Method

Consider a random field $\{X(s): s \in \mathcal{S}\}$ defined on a spatial domain $\mathcal{S} \subseteq \mathbb{R}^K$ with $K \geq 1$ that takes the form of

$$X(s) = \mu(s) + \epsilon(s), \tag{1}$$

where $\mu(s)$ is an unobserved process of interest and $\epsilon(s)$ is a mean-zero stationary Gaussian process. We are interested in examining whether $\mu(s)$ belongs to an indifference region \mathcal{A} . For example, $\mathcal{A} = \{\mu \in \mathbb{R} : \mu \leq \mu_0\}$ for a one-sided test and $\mathcal{A} = \{\mu \in \mathbb{R} : |\mu| \leq \mu_0\}$ for a two-sided test, where μ_0 is some pre-specified value. The unobserved process $\mu(s)$, together with the indifference region \mathcal{A} , induces a background statement $\theta(s) = \mathbf{1}\{\mu(s) \notin \mathcal{A}\}$ on the spatial domain \mathcal{S} . We define $\mathcal{S}_0 = \{s \in \mathcal{S} : \theta(s) = 0\}$ and $\mathcal{S}_1 = \{s \in \mathcal{S} : \theta(s) = 1\}$ as the sets of null and non-null locations respectively. We focus on the point-wise analysis, where we are interested in testing the hypothesis

$$\mathcal{H}_{0,s}: \mu(s) \in \mathcal{A}$$
 versus $\mathcal{H}_{a,s}: \mu(s) \notin \mathcal{A}$.

At each location $s \in \mathcal{S}$, we make a decision $\delta(s)$, where $\delta(s) = 1$ if $\mathcal{H}_{0,s}$ is rejected and $\delta(s) = 0$ otherwise. Let $\Delta_1 = \{s \in \mathcal{S} : \delta(s) = 1\}$ be the set of rejections associated with the decision rule δ . The false discovery rate (FDR) is defined as

$$FDR = \mathbb{E}\left(\frac{|\Delta_1 \cap \mathcal{S}_0|}{1 \vee |\Delta_1|}\right),\,$$

where $|\cdot|$ denotes the cardinality of a generic set and $\Delta_1 \cap \mathcal{S}_0$ is the set of false rejections.

We next present a novel spatial multiple testing procedure that borrows neighboring information to improve the power of signal detection without sacrificing the FDR control.

2.1 Motivation

For clarity, we focus our discussions on the one-sided test in the rest of this paper, i.e.,

$$\mathcal{H}_{0,s}: \mu(s) \leq 0$$
 versus $\mathcal{H}_{a,s}: \mu(s) > 0$.

For each location $s \in \mathcal{S}$, we define a set of its neighborhood as $\mathcal{N}(s) \subseteq \mathcal{S} \setminus \{s\}$. Because of the spatial dependence and smoothness encountered in many real applications, the set of

neighboring observations $\{X(v): v \in \mathcal{N}(s)\}$ is expected to provide useful side information on determining the state of $\theta(s)$. To formalize this idea, we consider two statistics, namely the auxiliary statistic

$$T_1(s) = \frac{1}{\tau(s)} \sum_{v \in \mathcal{N}(s)} X(v) \tag{2}$$

based on the averaged observed values in the neighborhood of s and the primary statistic $T_2(s) = \sigma^{-1}(s)X(s)$ based on the observation from the location of interest, where $\sigma^2(s) = \text{var}\{\epsilon(s)\}$ and $\tau^2(s) = \sum_{v,v' \in \mathcal{N}(s)} \text{cov}\{\epsilon(v), \epsilon(v')\}$. Under the null $\mathcal{H}_0(s)$, we have

$$\begin{pmatrix} T_1(s) \\ T_2(s) \end{pmatrix} = \begin{pmatrix} \xi(s) \\ \sigma^{-1}(s)\mu(s) \end{pmatrix} + \begin{pmatrix} V_1(s) \\ V_2(s) \end{pmatrix},$$

where $\xi(s) = \tau^{-1}(s) \sum_{v \in \mathcal{N}(s)} \mu(v)$ and

$$\begin{pmatrix} V_1(s) \\ V_2(s) \end{pmatrix} \sim \mathcal{N} \left(\begin{pmatrix} 0 \\ 0 \end{pmatrix}, \begin{pmatrix} 1 & \rho(s) \\ \rho(s) & 1 \end{pmatrix} \right)$$

with $\rho(s) = \{\sigma(s)\tau(s)\}^{-1} \sum_{v \in \mathcal{N}(s)} \operatorname{cov}\{\epsilon(s), \epsilon(v)\}$. Our method is motivated by the following two-stage procedure. Specifically, at stage 1, we use the auxiliary statistic $T_1(s)$ to screen out the nulls based on the belief that observations around a non-null location are likely to take larger values on average. At stage 2, we use $T_2(s)$ to pick out signals among those who survive from stage 1. Given the thresholds (t_1, t_2) for the two stages, the procedure can be described as follows:

- Stage 1. Use the auxiliary statistic $T_1(s)$ to determine a preliminary set of signals $\mathcal{D}_1 = \{s \in \mathcal{S} : T_1(s) \geq t_1\}.$
- Stage 2. Reject $\mathcal{H}_{0,s}$ for $T_2(s) \geq t_2$ and $s \in \mathcal{D}_1$. As a result, the final set of discoveries is given by $\mathcal{D}_2 = \{s \in \mathcal{S} : T_1(s) \geq t_1, T_2(s) \geq t_2\}.$

Due to the screening step that reduces the multiple testing burden for the second stage,

we expect the above procedure to be more powerful than the traditional procedure based only on the primary statistic. Indeed, the traditional 1d rejection region is a special case of the 2d rejection region $\{s \in \mathcal{S} : T_1(s) \geq t_1, T_2(s) \geq t_2\}$ by setting $t_1 \leq \min_{s \in \mathcal{S}} T_1(s)$, i.e., the screening stage preserves all locations. If we select the two thresholds one by one, then the choice of t_2 needs to account for the selection effect from the first stage. Here we propose a new method to address this issue by simultaneously selecting the two thresholds, which we name it the 2-dimensional (2d) procedure.

2.2 Approximation of the false discovery proportion

Note that $\mathcal{H}_{0,s}$ is rejected when $T_1(s) \geq t_1$ and $T_2(s) \geq t_2$. Recalling that \mathcal{S}_0 is the set of true nulls, FDP is then given by

$$FDP(t_1, t_2) = \frac{\sum_{s \in S_0} \mathbf{1} \{ T_1(s) \ge t_1, T_2(s) \ge t_2 \}}{1 \lor R(t_1, t_2)},$$

where $R(t_1, t_2) = \sum_{s \in \mathcal{S}} \mathbf{1} \{T_1(s) \ge t_1, T_2(s) \ge t_2\}$ corresponds to the total number of rejections. As $\mu(s) \le 0$ for $s \in \mathcal{S}_0$, we have

$$FDP(t_1, t_2) \le \frac{\sum_{s \in S_0} \mathbf{1} \{V_1(s) + \xi(s) \ge t_1, V_2(s) \ge t_2\}}{1 \lor R(t_1, t_2)}.$$

Replacing the number of false rejections in the numerator of the RHS above by its expected value, we obtain the approximated upper bound on the FDP as

$$FDP(t_1, t_2) \lesssim \frac{\sum_{s \in \mathcal{S}_0} \mathbb{P}\left\{V_1(s) + \xi(s) \ge t_1, V_2(s) \ge t_2\right\}}{1 \vee R(t_1, t_2)}.$$
 (3)

The major challenge here is the estimation of the expected number of false rejections given by $\sum_{s \in S_0} \mathbb{P} \{V_1(s) + \xi(s) \geq t_1, V_2(s) \geq t_2\}$, which involves a large number of nuisance parameters $\xi(s)$'s. To overcome the difficulty, we shall adopt a Bayesian viewpoint by assuming that $\{\xi(s) : s \in S\}$ follow a common prior distribution. The Bayesian viewpoint allows

us to borrow spatial information across different locations to directly estimate the expected number of false rejections without estimating individual $\xi(s)$ at each location explicitly.

2.3 Nonparametric empirical Bayes

Suppose $\xi(s)$ are independently generated from a common prior distribution G_0 . We aim to estimate G_0 based on the set of auxiliary statistics $\{T_1(s): s \in \mathcal{S}\}$ through the nonparametric empirical Bayes (NPEB) approach. It can be achieved by maximizing the marginal distribution of $T_1(s) = \xi(s) + V_1(s)$, which is given by $f_{G_0}(x) = \int \phi(x-u)dG_0(u)$ with ϕ denoting the density function of standard normal distribution.

Classical empirical Bayes methods often assume independence among the observations, which is violated in our case due to the spatial dependence. To reduce the dependence, we select a subset $\widetilde{\mathcal{S}}$ of \mathcal{S} such that any two points in $\widetilde{\mathcal{S}}$ have a distance larger than some threshold c_0 (so that the dependence between $T_1(v)$ and $T_1(v')$ for any $v, v' \in \widetilde{\mathcal{S}}$ is sufficiently weak). Following Kiefer and Wolfowitz (1956) and Jiang and Zhang (2009), we consider the general maximum likelihood estimator (GMLE) defined as

$$\widetilde{G}_{\widetilde{S}} = \underset{G \in \mathcal{G}}{\operatorname{arg\,max}} \sum_{s \in \widetilde{S}} \log f_G\{T_1(s)\},$$
(4)

where \mathcal{G} represents the set of all probability distributions on \mathbb{R} and $f_G(x) = \int \phi(x-u)dG(u)$ is the convolution between G and ϕ . The optimization in (4) can be cast as a convex optimization problem that can be efficiently solved by modern interior point methods. The readers are referred to Koenker and Mizera (2014) and Koenker and Gu (2017) for more detailed discussions.

2.4 2d spatial multiple testing procedure

We now describe a procedure to select two thresholds simultaneously. Define

$$L\{t_1, t_2, \xi(s), \rho(s)\} = \mathbb{P}\{V_1(s) + \xi(s) \ge t_1, V_2(s) \ge t_2 \mid \xi(s)\}.$$

Given the GMLE $\widetilde{G}_{\widetilde{S}}$ in (4) as the prior distribution and in view of (3), we consider an approximated upper bound for $FDP(t_1, t_2)$ as

$$\widetilde{\mathrm{FDP}}(t_1, t_2) := \frac{\sum_{s \in \mathcal{S}} \int L\left\{t_1, t_2, x, \rho(s)\right\} d\widetilde{G}_{\widetilde{\mathcal{S}}}(x)}{1 \vee R(t_1, t_2)}.$$

For a desired FDR level $q \in (0,1)$, the proposed 2d-SMT procedure chooses the optimal threshold such that

$$(\widehat{t}_1^{\star}, \widehat{t}_2^{\star}) = \underset{(t_1, t_2) \in \mathcal{F}_q}{\arg \max} R(t_1, t_2), \tag{5}$$

where
$$\mathcal{F}_q = \{(t_1, t_2) \in \mathbb{R}^2 : \widetilde{\text{FDP}}(t_1, t_2) \leq q\}.$$

We argue that 2d-SMT is, in general, more powerful than the classical BH procedure based on the primary statistics alone. The intuition is that for a small enough t_1 , the first dimension does not screen out any null hypothesis and only the second dimension is effective in identifying signals. In this case, we note that

$$\int L\{t_1, t_2, x, \rho(s)\} d\widetilde{G}_{\widetilde{S}}(x) \approx \mathbb{P}\{V_2(s) \ge t_2\} \text{ and } R(t_1, t_2) = \sum_{s \in S} \mathbf{1}\{T_2(s) \ge t_2\},$$

which implies that

$$\widetilde{\text{FDP}}(t_1, t_2) \approx \frac{\sum_{s \in \mathcal{S}} \mathbb{P}\{V_2(s) \ge t_2\}}{1 \vee \sum_{s \in \mathcal{S}} \mathbf{1}\{T_2(s) \ge t_2\}}.$$
(6)

Finding the optimal cutoff $t_2^{\#}$ that maximizes the number of rejections while controls the RHS of (6) at level q is equivalent to applying the BH procedure to the primary statistics. Since the 2d-SMT procedure has the flexibility to choose an additional cutoff t_1 to maximize the number of rejections, it guarantees to make more rejections. As we will show in Section 4, 2d-SMT procedure provides asymptotic FDR control, and thus the higher number of rejections typically translates into a higher power.

Remark 1. Shen et al. (2002) and Huang et al. (2021) considered the case where μ has

a sparse wavelet representation. The goal is to test the global null $\mu(s) = 0$ for all s and detect the significant wavelet coefficients while controlling the FDR. Observing that the wavelet coefficients within each scale and across different scales are related, they screened the wavelet coefficients based on the largest adjacent wavelet coefficients to gain more power. The generalized degrees of freedom determine the number of locations for the subsequent FDR-controlling procedure. Our approach can be potentially applied to their settings by exploring the signal structure encoded in the neighboring wavelet coefficients.

2.5 Estimating the null proportion

It is well known that when the number of signals is a substantial proportion of the total number of hypotheses, the BH procedure will be overly conservative. We develop a new estimator of the proportion of true null hypotheses in our setting, which is a modification of Storey's approach (Storey, 2002; Storey et al., 2004). As a motivation, we assume that $T_2(s)$ approximately follows the mixture model

$$T_2(s) \sim \pi_0 \mathcal{N}(\mu_0(s), 1) + (1 - \pi_0) \mathcal{N}(\mu_1(s), 1),$$

where $\mu_0(s) \leq 0$, $\mu_1(s) > 0$, and π_0 denotes the prior probability that $s \in \mathcal{S}_0$. Let Φ be the cumulative distribution function (CDF) of the standard normal distribution. Fixing some $\lambda \in \mathbb{R}$, we have

$$\mathbb{P}\{T_{2}(s) < \lambda\} = \pi_{0}\mathbb{P}\{\mathcal{N}(\mu_{0}(s), 1) < \lambda\} + (1 - \pi_{0})\mathbb{P}\{\mathcal{N}(\mu_{1}(s), 1) < \lambda\}$$
$$\geq \pi_{0}\mathbb{P}\{\mathcal{N}(\mu_{0}(s), 1) < \lambda\}$$
$$> \pi_{0}\Phi(\lambda),$$

where the second line is tighter if $(1 - \pi_0)\mathbb{P}\{\mathcal{N}(\mu_1(s), 1) < \lambda\}$ is closer to zero and the third line becomes equality when $\mu_0(s) = 0$. The above derivation suggests a conservative

estimator for π_0 given by

$$\widehat{\pi}_0 := \frac{\sum_{s \in \mathcal{S}} \mathbf{1}\{T_2(s) < \lambda\}}{|\mathcal{S}| \Phi(\lambda)} \approx \frac{\mathbb{P}\{T_2(s) < \lambda\}}{\Phi(\lambda)} \ge \pi_0.$$
 (7)

2.6 A feasible procedure

So far we have assumed that the spatial covariance function $k(s,s') = \text{cov}\{\epsilon(s),\epsilon(s')\}$ of the error process is known. In practice, we need to estimate the spatial covariance function $\text{cov}\{\epsilon(s),\epsilon(s')\}$, which has been widely investigated in the literature (Sang and Huang, 2012; Padoan and Bevilacqua, 2015; Sommerfeld et al., 2018; Katzfuss and Guinness, 2021); see Section S.V of the Supplementary Materials for more details. Given the estimated covariance function, we let $\widehat{T}_1(s)$ and $\widehat{T}_2(s)$ respectively denote the feasible statistics of $T_1(s)$ and $T_2(s)$ by replacing $(\sigma(s), \tau(s), \rho(s))$ with their estimates $(\widehat{\sigma}(s), \widehat{\tau}(s), \widehat{\rho}(s))$. Define the nonparametric empirical Bayes estimate of G_0 based on $\{\widehat{T}_1(s): s \in \widetilde{S}\}$ as $\widehat{G}_{\widetilde{S}}(u)$. We propose the following FDP estimate which accounts for the null proportion using the idea in Section 2.5,

$$\widehat{\text{FDP}}_{\lambda,\widetilde{\mathcal{S}}}(t_1, t_2) := \frac{\sum_{s \in \mathcal{S}} \mathbf{1}\{\widehat{T}_2(s) < \lambda\}}{m\Phi(\lambda)} \frac{\sum_{s \in \mathcal{S}} \int L\{t_1, t_2, x, \widehat{\rho}(s)\} d\widehat{G}_{\widetilde{\mathcal{S}}}(x)}{1 \vee \widehat{R}(t_1, t_2)}, \tag{8}$$

where $\widehat{R}(t_1, t_2) = \sum_{s \in \mathcal{S}} \mathbf{1}\{\widehat{T}_1(s) \geq t_1, \widehat{T}_2(s) \geq t_2\}$. Thus, given the desired FDR level $q \in (0, 1)$, the optimal rejection thresholds are defined as

$$(\widetilde{t}_1^{\star}, \widetilde{t}_2^{\star}) = \underset{(t_1, t_2) \in \mathcal{F}_q}{\arg \max} \widehat{R}(t_1, t_2), \tag{9}$$

where $\mathcal{F}_q = \{(t_1, t_2) \in \mathbb{R}^2 : \widehat{\text{FDP}}_{\lambda, \widetilde{\mathcal{S}}}(t_1, t_2) \leq q\}$. The left panel in Figure 1 exemplifies the thresholds for the BH and 2d-SMT procedures with the nominal FDR level at 10%. Compared to the BH procedure, the 2d-SMT procedure realizes a lower threshold for $T_2(s)$ (the red vertical line) because it excludes locations exhibiting weak neighboring signals with a threshold for $T_1(s)$ (the red horizontal line). The lower threshold for $T_2(s)$ in 2d-SMT

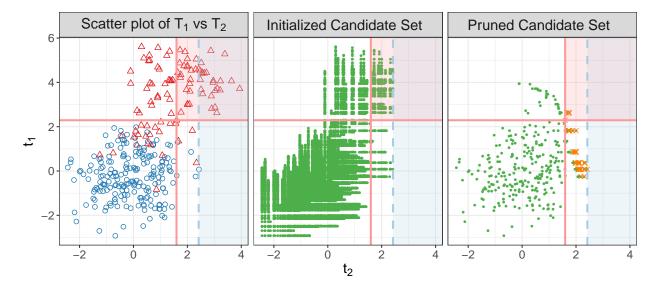


Figure 1: An illustration of the proposed 2d-SMT procedure and fast step-down algorithm. The spatial domain S includes 300 points. The red triangle (\triangle) and blue circle (\circ) in the left panel denote non-null and null locations, respectively. The solid and dashed lines are the thresholds for 2d-SMT procedure and BH procedure, respectively. The orange cross (\times) in the right panel corresponds to the cutoff whose corresponding FDP is less than 0.1. The set \mathcal{T}' in the middle panel contains 14,534 points, whereas the set after our proposed pruning steps in the right panel significantly reduces the number of candidates to 345.

leads to more true rejections in this example.

2.7 Spatial varying null proportions and cutoffs

Our proposed 2d-SMT is a flexible framework that can accommodate weighted BH procedures (wBH), a broad class of multiple testing procedures. wBH leverages the hypothesis heterogeneity by assigning location-specific cutoffs. According to wBH, $\mathcal{H}_{0,s}$ will be rejected with the rule $p(s) := 1 - \Phi(\widehat{T}_2(s)) \leq \min\{\tau, w(s)t\}$, $\tau \in (0, 1]$, where τ is the censoring level for all p-values and w(s) is a location-specific weight that encodes external information for location s. Apparently, the rejection rule is equivalent to assigning location-specific cutoffs to the primary statistics, i.e., $\widehat{T}_2(s) \geq \Phi^{-1}(1 - \min\{\tau, w(s)t\})$. Inspired by the idea behind wBH, we extend 2d-SMT by allowing location-specific cutoffs to further incorporate external information on the prior null probability and signal distribution. Specifically, we reject $\mathcal{H}_{0,s}$ whenever $\widehat{T}_1(s) \geq c(t_1, s)$ and $\widehat{T}_2(s) \geq c(t_2, s)$, where $c(t, s) = \Phi^{-1}(1 - \min\{\tau, w(s)t\})$. With

some abuse of notation, we let

$$\widehat{\text{FDP}}_{\lambda,\widetilde{\mathcal{S}}}(t_1, t_2) := \frac{\sum_{s \in \mathcal{S}} \widehat{\pi}_0(s) \int L\left\{c(t_1, s), c(t_2, s), x, \widehat{\rho}(s)\right\} d\widehat{G}_{\widetilde{\mathcal{S}}}(x)}{1 \vee \widehat{R}(t_1, t_2)}, \tag{10}$$

where $\widehat{\pi}_0(s)$ is an estimate of the null proportion $\pi_0(s) = \mathbb{P}\{\theta(s) = 0\}$ at location s. We reject $\mathcal{H}_{0,s}$ if $T_1(s) \geq c(\widetilde{t}_1^{\star}, s)$ and $T_2(s) \geq c(\widetilde{t}_2^{\star}, s)$, where $(\widetilde{t}_1^{\star}, \widetilde{t}_2^{\star})$ is the solution to (9) with the FDP estimate given in (10).

There have been extensive recent studies on the choice of w(s) in wBH. Examples include GBH (Hu et al., 2010), IHW (Ignatiadis et al., 2016; Ignatiadis and Huber, 2021), SABHA (Li and Barber, 2019) and LAWS (Cai et al., 2021). The weights in these examples are either proportional to $1/\pi_0(s)$ or $\{1 - \pi_0(s)\}/\pi_0(s)$, where $\pi_0(s)$ can be estimated using various approaches. In the spatial setting, we often use the location associated with each hypothesis as the external covariate to estimate $\pi_0(s)$.

3 Implementation Details

In this section, we discuss a few crucial points for the implementation of our method. First of all, the auxiliary statistic $\widehat{T}_1(s)$ requires the specification of a pre-chosen neighborhood $\mathcal{N}(s)$ for each location. In our implementation, we let $\mathcal{N}(s)$ be the set of the κ -nearest neighbors around location s, and find that 2d-SMT is not quite sensitive to the choice of κ and deliver satisfactory power improvement provided $2 \leq \kappa \leq 7$; see Section S.I.2 of the Supplementary Materials for more details. Generally, the neighborhood $\mathcal{N}(s)$ can be determined using external/side information that is independent of the data $\{X(s): s \in \mathcal{S}\}$.

Second, the auxiliary statistics used in NPEB estimation, $\{\widehat{T}_1(s) : s \in \widetilde{\mathcal{S}}\}$, should be from far enough spatial locations to weaken their spatial dependency. In practice, we choose $\widetilde{\mathcal{S}} \subset \mathcal{S}$ whose neighbors have no overlaps.

Third, when the signal is sparse, the estimation of the number of false rejections in 2d-SMT procedure may be unstable. Inspired by the idea of Knockoff+, we add a small offset to

improve the selection stability. More precisely, we replace $\sum_{s\in\mathcal{S}} \int L\{t_1,t_2,x,\widehat{\rho}(s)\} d\widehat{G}_{\widetilde{\mathcal{S}}}(x)$ in (8) by $\sum_{s\in\mathcal{S}} \int L\{t_1,t_2,x,\widehat{\rho}(s)\} d\widehat{G}_{\widetilde{\mathcal{S}}}(x)+q$, where q is the target FDR level. This replacement improves the selection stability for sparse signals but does not influence the performance of power and FDR control for dense signals.

Finally, finding the optimal thresholds in 2d-SMT requires solving the discrete constrained optimization problem (9). Due to the discrete nature of (9), the solution can be obtained if we replace \mathcal{F}_q by

$$\{(t_1, t_2) \in \mathcal{T} : \widehat{\text{FDP}}_{\lambda, \widetilde{\mathcal{S}}}(t_1, t_2) \le q\},$$

where $\mathcal{T} = \{(\widehat{T}_1(s), \widehat{T}_2(s')) : s, s' \in \mathcal{S}\}$ is the set of all candidate cutoff values. A naive grid search algorithm would require evaluating $\widehat{\text{FDP}}_{\lambda,\widetilde{\mathcal{S}}}$ at $|\mathcal{S}|^2$ different values, which is computationally prohibitive for a large number of spatial locations. To overcome the computational bottleneck, we propose a fast step-down algorithm to utilize the specific structure of (9) through the following three steps. We briefly introduce the basic idea below and defer the comprehensive discussion to Section S.VI of the Supplementary Materials.

Step 1. We maintain the cutoffs that achieve the minimum FDP among all the cutoffs realizing the same rejection sets. The derivation in Section S.VI of the Supplementary Materials suggests that we only need to consider the following set of candidate cutoff values:

$$\mathcal{T}' = \left\{ (\widehat{T}_1(s_l), \widehat{T}_2(s_k)) : \widehat{T}_1(s_l) \le \widehat{T}_1(s_k) \text{ and } l \le k, \ k = 1, 2, \dots, m \right\} \cup \left\{ (\infty, \infty) \right\}.$$

Step 2. Let $\widetilde{t}_2^{\#}$ be the minimum value satisfying $\widehat{\text{FDP}}_{\lambda,\widetilde{\mathcal{S}}}(-\infty,t_2) \leq q$. It is not hard to see that the optimal cutoff for the primary statistic in 2d-SMT is no more than $\widetilde{t}_2^{\#}$. Hence we can reduce the set of candidate cutoffs to $\mathcal{T}'' = \left\{ (t_1,t_2) \in \mathcal{T}' : t_2 \leq \widetilde{t}_2^{\#} \right\}$.

Step 3. Denote the elements in \mathcal{T}'' by $(t_{1,i,j}, t_{2,i})$ for $i = 1, 2, ..., \check{m}$ and $j = 1, ..., m_i$, where \check{m} is the number of $\widehat{T}_2(s)$'s that are smaller than or equal to $\widetilde{t}_2^\#$. Suppose the points are

sorted in the following way: (1) $t_{2,1} > t_{2,2} > \cdots > t_{2,\tilde{m}}$; (2) $t_{1,i,1} > t_{1,i,2} > \cdots > t_{1,i,m_i}$ for all $1 \le i \le \tilde{m}$. Our algorithm involves two loops. In the outer loop, we search the cutoff for the primary statistic, while in the inner loop, we search the cutoff for the auxiliary statistic. The key idea here is to skip those cutoffs in the inner loop that are impossible to procedure a value of $\widehat{\text{FDP}}$ equal to or below the level q. For example, consider a cutoff $(t_{1,i,j},t_{2,i})$ which induces R rejections with $\widehat{\text{FDP}}_{\lambda,\tilde{\mathcal{S}}}(t_{1,i,j},t_{2,i}) = 2q$. Then the next cutoff, denoted as $(t_{1,i,j'},t_{2,i})$, needs to induce at least 2R rejections to ensure that $\widehat{\text{FDP}}_{\lambda,\tilde{\mathcal{S}}}(t_{1,i,j'},t_{2,i}) \le q$. When there is no tie, increasing j by k brings exactly k more rejections. Therefore, the next possible cutoff to be examined is $(t_{1,i,j+R},t_{2,i})$. The middle and left panels in Figure 1 illustrate how the set of candidate cutoff values can be reduced by Step 3.

Algorithm 1 Fast Step-down Algorithm.

```
Input: Test Statistics \{(\widehat{T}_1(s), \widehat{T}_2(s)) : s \in \mathcal{S}\}; target FDR level q;
 Initialization:
  1: Initialize (\widetilde{t}_1^{\star}, \widetilde{t}_2^{\star}, R_{\max}, \text{FDP}_{\min}) = \left(-\infty, \widetilde{t}_2^{\#}, \widehat{R}(-\infty, \widetilde{t}_2^{\#}), \widehat{\text{FDP}}_{\lambda, \widetilde{\mathcal{S}}}(-\infty, \widetilde{t}_2^{\#})\right)
 Search Step:
  1: for i = 1, 2, ..., m do
              Calculate R = \widehat{R}(t_{1,i,1}, t_{2,i});
  2:
  3:
             Set j = 1 + \max(0, R_{\max} - R);
              while j \leq m_i do
  4:
                    Calculate R = \widehat{R}(t_{1,i,j}, t_{2,i}) and \widehat{\text{FDP}} = \widehat{\text{FDP}}_{\lambda, \widetilde{S}}(t_{1,i,j}, t_{2,i}) according to (8);
  5:
                    if R = R_{\text{max}} and \widehat{\text{FDP}} < \widehat{\text{FDP}}_{\text{min}} or R > R_{\text{max}} and \widehat{\text{FDP}} \le q then
  6:
                           (\widetilde{t}_1^{\star}, \widetilde{t}_2^{\star}, R_{\max}, \text{FDP}_{\min}) = (t_{1,i,j}, t_{2,i}, R, \widehat{\text{FDP}});
  7:
                           Update j = j + 1;
  8:
                    else
 9:
                           Calculate R_{\text{req}} = \lceil \widehat{\text{FDP}} \times R/q \rceil;
10:
                           Update j = j + \max(1, R_{\text{req}} - R);
11:
12:
                    end if
13:
             end while
14: end for
 Output: Rejection threshold (\widetilde{t}_1^{\star}, \widetilde{t}_2^{\star}).
```

4 Asymptotic results

In this section, we investigate the asymptotic property of the proposed 2d-SMT procedure. We observe $\{X(s): s \in \mathcal{S}_m\}$, where $\mathcal{S}_m = \{s_1, s_2, \cdots, s_m\} \subseteq \mathcal{S} \subseteq \mathbb{R}^K$. We denote by

 $S_{0,m} = S_m \cap S_0$ with $m_0 = |S_{0,m}|$ the set of null locations and let $S_{1,m} = S_m \cap S_1$ with $m_1 = |S_{1,m}|$ be the set of non-null locations. We further let $\widetilde{S}_m \subseteq S_m$ with $|\widetilde{S}_m| = \widetilde{m}$ be the set of locations for implementing the NPEB. Our asymptotic analysis requires the following regularity conditions.

Assumption 1 (Spatial Domain). The spatial domain $S \subset \mathbb{R}^K$ is infinitely countable. Further, there exist $0 < \Delta_l < \Delta_u < \infty$, such that for every element in S, the distance to its nearest neighbor is bounded from below and above respectively by Δ_l and Δ_u , i.e.,

$$\Delta_l \le \inf_{\substack{s' \in \mathcal{S} \\ s' \ne s}} \operatorname{dist}(s, s') \le \Delta_u, \ \forall s \in \mathcal{S},$$

where $dist(\cdot, \cdot)$ denotes the Euclidean distance of two points.

Assumption 1 states that the distance between any location in S and its nearest neighbor is moderately uniform. One example satisfying Assumption 1 is the lattice $S = \mathbb{Z}^K$ where $\Delta_l = \Delta_u = 1$. Particularly, the lower bound ensures $\max_{s,s' \in S_m} \operatorname{dist}(s,s')$ tends to infinity as m increases.

Assumption 2 (Neighborhood). For each location s in S, its neighborhood $\mathcal{N}(s) \subset S \setminus \{s\}$ used in 2d-SMT is its nearest neighbors with size uniformly upper bounded by some positive integer $N_{nei} \in \mathbb{N}^+$, i.e., $0 < |\mathcal{N}(s)| < N_{nei}$, $\forall s \in S$.

Assumption 2 specifies the neighborhood set of each location and requires the number of locations in each neighborhood to be bounded.

Assumption 3 (Second-order Structure). The variance and covariance of the error process $\epsilon(s)$ satisfy

- (a) There exist positive constants $B_{ud,\sigma}$, $B_{up,\sigma}$, $B_{ud,\tau}$, and $B_{up,\tau}$, such that $B_{ud,\sigma} \leq \inf_{s \in \mathcal{S}} \sigma(s) \leq \sup_{s \in \mathcal{S}} \sigma(s) < B_{up,\sigma}$ and $B_{ud,\tau} \leq \inf_{s \in \mathcal{S}} \tau(s) \leq \sup_{s \in \mathcal{S}} \tau(s) < B_{up,\tau}$ for all $s \in \mathcal{S}$;
- (b) The estimated covariance of X are uniformly weakly consistent with a polynomial rate, i.e., $\sup_{s,s'\in\mathcal{S}_m} |\widehat{\operatorname{cov}}\{\epsilon(s),\epsilon(s')\}| = o_{\mathbb{P}}(m^{-q})$ for some q>0.

Assumptions 3(a) requires the variance of the error process to be bounded away from zero and infinity. Assumption 3(b) imposes requirement on the convergence rate of the covariance function estimate, which is satisfied by many commonly-used estimators. For example, the maximum likelihood estimator achieves the desired rate of convergence with q = 1/2 when the parametric covariance function is locally Lipschitz continuous (Mardia and Marshall, 1984).

To describe the spatial dependence structure, we adopt the near epoch dependency (NED) that was first introduced to the spatial analysis in Jenish and Prucha (2012) and has become popular since then. Denote by \mathcal{V} a spatial domain such that $\mathcal{S} \subseteq \mathcal{V} \subset \mathbb{R}^K$ for $K \geq 1$. Let $\{Y(v), v \in \mathcal{V}\}$ be a random field and set $\mathfrak{F}(S) = \sigma\{Y(s), s \in S\}$ as the σ -field generated by Y(s) for $s \in S \subset \mathcal{V}$.

Definition 1 (Near Epoch Dependency). Let $X = \{X(s), s \in \mathcal{S}_m\}$ be a random field with $\|X(s)\|_p < \infty$ where $\|X(s)\|_p = (\mathbb{E}|X(s)|^p)^{1/p}$, $p \geq 1$. Define $Y = \{Y(s), s \in \mathcal{V}_m\}$ as a random field where $\mathcal{S}_m \subseteq \mathcal{V}_m$ and let $\mathbf{d} = \{d_m(s), s \in \mathcal{S}_m\}$ be a set of finite positive constants. Then, the random field X is said to be $L_p(\mathbf{d})$ -near-epoch dependent on the random field Y if

$$||X(s) - \mathbb{E} \{X(s) \mid \mathfrak{F}(S)\}||_p \le d_m(s)\psi(r),$$

where $S \subset \mathcal{V}_m$, $r = \max\{t \geq 0 : B(s;t) \subseteq S\}$ with B(s;t) being a ball centered around s with radius t, and $\psi(r) \geq 0$ is some non-increasing sequence with $\lim_{r\to\infty} \psi(r) = 0$. Here $\psi(r)$ and $d_m(s)$ are called NED coefficients and NED scaling factors, respectively. We say X is $L_p(\mathbf{d})$ -NED of size $-\lambda$ if $\psi(r) = O(r^{-\mu})$ for some $\mu > \lambda > 0$. Furthermore, if $\sup_m \sup_{s \in \mathcal{S}_m} d_m(s) < \infty$, then X is said to be uniformly L_p -NED on Y.

Assumption 4 (Uniform Near Epoch Dependency). $X = \{X(s), s \in \mathcal{S}_m\}$ is uniformly L_p - $NED \ on \ Y = \{Y(s) : s \in \mathcal{V}_m\}$ of size $-\lambda$, for $\lambda > 0$, $p \geq 2$, where Y(s) are independently distributed.

In Definition 1, B(s;t) is the maximum ball that is completely included in S. The quantity $||X(s) - \mathbb{E}\{X(s) \mid \mathfrak{F}(S)\}||_p$ satisfies a generalized non-decreasing property with respect to S. Specifically, if $||X(s) - \mathbb{E}\{X(s) \mid \mathfrak{F}(S)\}||_p \leq d_m(s)\psi(r)$, we then have $||X(s) - \mathbb{E}\{X(s) \mid \mathfrak{F}(V)\}||_p \leq d_m(s)\psi(r)$ for any $S \subseteq V \subseteq S$. We can choose $d_m(s) = 2||X(s)||_p$ as the scaling factor such that $0 \leq \psi(r) \leq 1$. In addition, if X is L_p -NED on Y, then X is also L_q -NED on Y with the same $\{d_m(s)\}$ and $\psi(r)$ for any $q \leq p$. The condition $p \geq 2$ in Assumption 4 guarantees that the variance of $\mathbb{E}\{X(s) \mid \mathfrak{F}(S)\}$ converges to that of X(s) as S expands.

Under the NED assumption, we can approximate X(s) with $\mathbb{E}[X(s) \mid \mathfrak{F}\{B(s;r)\}]$ and in turn approximate $T_1(s)$ with

$$T_1^*(s;r) = \mathbb{E}\left[T_1(s) \mid \mathfrak{F}\left\{\bigcup_{v \in \mathcal{N}(s)} B(v;r)\right\}\right] / \zeta_r(s), \tag{11}$$

where $\zeta_r^2(s) = \text{var}\left(\mathbb{E}\left[T_1(s) \mid \mathfrak{F}\left\{\bigcup_{v \in \mathcal{N}(s)} B(v; r)\right\}\right]\right)$. We further require the conditional statistics to be normally distributed as required by the theory for NPEB.

Assumption 5 (Normality). For any $S \subset \mathcal{V}$, $\mathbb{E}\{X(s) \mid \mathfrak{F}(S)\}$ is normally distributed.

Spatial linear autoregression model with Gaussian white noise satisfies Assumptions 4 and 5 (Jenish, 2012). Under Assumptions 4 and 5, $\{T_1^*(s;r):s\in\widetilde{\mathcal{S}}_m\}$ defined in (11) are independent and normal distributed random variables with unit variance if r>0 satisfies

$$\bigcup_{v \in \mathcal{N}(s)} B(v; r) \cap \bigcup_{v \in \mathcal{N}(s')} B(v; r) = \emptyset, \quad s, s' \in \widetilde{\mathcal{S}}_m.$$
 (12)

Under Assumptions 1 and 2, setting $r = \widetilde{\Delta}_{l,m}/2 - N_{nei}\Delta_u$ indicates (12), where

$$\widetilde{\Delta}_{l,m} = \inf_{s,s' \in \widetilde{\mathcal{S}}_m} \operatorname{dist}(s,s'). \tag{13}$$

Assumption 6 (Subset for NPEB). The subset for implementing NPEB, $\widetilde{\mathcal{S}}_m \subset \mathcal{S}_m$, satisfies $\tilde{m}^{1/(\lambda p)}\{\log(\tilde{m})\}^{-1/(2\lambda)} = o(\widetilde{\Delta}_{l,m}) \text{ and } \tilde{m} \to \infty \text{ as } m \to \infty, \text{ where } \widetilde{\Delta}_{l,m} \text{ is defined as in (13).}$

The condition about \tilde{m} and $\widetilde{\Delta}_{l,m}$ in Assumption 6 trades off the number of $\widetilde{\mathcal{S}}_m$ and

the distance between them, which becomes milder when increasing the strength of near epoch dependency, i.e., λ or p. In fact, we can choose $\widetilde{\mathcal{S}}_m$ satisfying Assumption 6 under Assumptions 1 and 2; see Section S.IV.1 of the Supplementary Materials for more details.

Assumption 7 (Null Proportion). $m_0/m \to \pi_0 \in (0,1)$, as $m \to \infty$.

Assumption 8 (Prior Distribution). (a) There exists a positive constant ν_0 such that $\{\xi(s)\}_{s\in\mathcal{S}_m}$ is a sequence of i.i.d. random variables with the distribution G_0 on $[-\nu_0,\nu_0]$; (b) Let $G_{\tilde{m}}(u) = \tilde{m}^{-1} \sum_{s\in\tilde{\mathcal{S}}_m} \mathbf{1}\{\xi(s) \leq u\}$ be the empirical distribution of the unknown means. Suppose $d_H(f_{G_{\tilde{m}}}, f_{G_0}) = o_{\mathbb{P}}(1)$, for any $\tilde{m} \to \infty$, where $f_G(x) = \int \phi(x-u)dG(u)$ and $d_H^2(f,g) = 2^{-1} \int \{\sqrt{f(x)} - \sqrt{g(x)}\}^2 dx$ is the squared Hellinger distance between two densities f and g.

Assumption 7 requires the asymptotic null proportion to be strictly between zero and one, which rules out the case of very sparse signals. We adopt a Bayesian viewpoint by assuming that $\xi(s)$ has a prior distribution G_0 . Assumption 8(b) states that the empirical distribution of $\xi(s)$ for $s \in \widetilde{\mathcal{S}}_m$ is close to G_0 in the sense that $d_H(f_{G_m}, f_{G_0})$ converges in probability to zero.

Assumption 9 (Asymptotic True/False Rejection Proportion). As m_0 and m_1 tend to infinity, we have

$$\frac{\sum_{s \in \mathcal{S}_{0,m}} \mathbf{1} \left\{ T_1(s) \ge t_1, T_2(s) \ge t_2 \right\}}{m_0} := \frac{V_m(t_1, t_2)}{m_0} \xrightarrow{a.s.} K_0(t_1, t_2),$$

$$\frac{\sum_{s \in \mathcal{S}_{1,m}} \mathbf{1} \left\{ T_1(s) \ge t_1, T_2(s) \ge t_2 \right\}}{m_1} := \frac{S_m(t_1, t_2)}{m_1} \xrightarrow{a.s.} K_1(t_1, t_2),$$

for every $(t_1, t_2) \in \mathbb{R} \times \mathbb{R}$, where

$$K_{0}(t_{1}, t_{2}) = \lim_{m_{0} \to \infty} \frac{\sum_{s \in \mathcal{S}_{0,m}} \int L\{t_{1}, t_{2}, x, \rho(s)\} dG_{0}(x)}{m_{0}}$$

$$= \lim_{m \to \infty} \frac{\sum_{s \in \mathcal{S}_{m}} \int L\{t_{1}, t_{2}, x, \rho(s)\} dG_{0}(x)}{m},$$
(14)

and both $K_0(t_1, t_2)$ and $K_1(t_1, t_2)$ are non-negative continuous functions of (t_1, t_2) .

Let $K_1(-\infty, t_2)$ be the limit of $\sum_{s \in S_{1,m}} \mathbf{1} \{T_2(s) \ge t_2\} / m_1$ as m_1 goes to infinity. We define

$$FDP_{\lambda}^{\infty}(t_1, t_2) := \frac{F(\lambda)K_0(t_1, t_2)}{\Phi(\lambda)K(t_1, t_2)},$$
(15)

where $K(t_1, t_2) = \pi_0 K_0(t_1, t_2) + (1 - \pi_0) K_1(t_1, t_2)$ and $F(\lambda) = \pi_0 \Phi(\lambda) + (1 - \pi_0) \{1 - K_1(-\infty, \lambda)\}.$

Assumption 10 (Existence of Cutoffs). There exist t_1^{\star} and t_2^{\star} such that $\text{FDP}_{\lambda}^{\infty}\left(t_1^{\star},0\right) < q$, $\text{FDP}_{\lambda}^{\infty}\left(0,t_2^{\star}\right) < q$, and $K\left(t_1^{\star},t_2^{\star}\right) > 0$.

Assumption 9 states the asymptotic convergence of the processes defined based on the numbers of true and false rejections. The second equation in (14) holds when the error process is stationary and the locations are generated from a homogeneous point process that is independent of $\theta(s)$'s. Assumption 10 reduces the searching region for the optimal threshold to a rectangle. The FDR of 2d-SMT procedure is given by

$$\widetilde{\mathrm{FDR}}_{m} = \mathbb{E}\left[\frac{\widehat{V}_{m}\left(\widetilde{t}_{1}^{\star}, \widetilde{t}_{2}^{\star}\right)}{\widehat{V}_{m}\left(\widetilde{t}_{1}^{\star}, \widetilde{t}_{2}^{\star}\right) + \widehat{S}_{m}\left(\widetilde{t}_{1}^{\star}, \widetilde{t}_{2}^{\star}\right)}\right],$$

where $(\widetilde{t}_1^{\star}, \widetilde{t}_2^{\star})$ is defined in (9), $\widehat{V}_m(t_1, t_2) = \sum_{s \in \mathcal{S}_{0,m}} \mathbf{1}\{\widehat{T}_1(s) \geq t_1, \widehat{T}_2(s) \geq t_2\}$ and $\widehat{S}_m(t_1, t_2) = \sum_{s \in \mathcal{S}_{1,m}} \mathbf{1}\{\widehat{T}_1(s) \geq t_1, \widehat{T}_2(s) \geq t_2\}$ represent the numbers of false and true rejections, respectively.

Theorem 1. Under Assumptions 1–10, we have $\limsup_{m\to\infty} \widetilde{\mathrm{FDR}}_m \leq q$.

Theorem 1 states that 2d-SMT procedure asymptotically controls the FDR. The proof of Theorem 1, which is deferred to Section S.II of the Supplementary Materials, relies on two facts: (i) (8) is an asymptotically conservative estimator of the true FDR; (ii) (8) satisfies the uniform law of large numbers over the rectangle encompassed by $t_1 \leq t_1^*$ and $t_2 \leq t_2^*$. See the Supplementary Materials for the detailed arguments.

5 Simulation Studies

We conduct extensive simulation studies to evaluate the performance of the proposed 2d-SMT procedure. We consider various simulation settings, including (1) 1d and 2d spatial domains; (2) known and unknown covariance structures; (3) different signal shapes; and (4) simple and composite nulls. We investigate the specificity and sensitivity of different methods under different scenarios by varying the signal intensities, magnitudes, and degrees of dependency.

5.1 Competing Methods

We compare the 2d procedure with the following competing methods.

- ST: Storey's procedure (Storey, 2002, qvalue package, v2.18.0);
- IHW: Independent hypothesis weighting (Ignatiadis et al., 2016; Ignatiadis and Huber, 2021, IHW package, v1.14.0);
- SABHA: Structure adaptive BH procedure with the stepwise constant weights (Li and Barber, 2019, https://rinafb.github.io/code/sabha.zip);
- LAWS: Locally adaptive weighting and screening (Cai et al., 2021, https://www.tandfonline.com/doi/suppl/10.1080/01621459.2020.1859379);
- AdaPT: Adaptive p-value thresholding procedure (Lei et al., 2018, adaptMT package, v1.0.0);
- dBH: Dependence-adjusted BH procedure (Fithian and Lei, 2020, dBH package, https://github.com/lihualei71/dbh).

As discussed in Section 2.7, our idea can combine with the ST, SABHA, and IHW methods to further enhance their power by borrowing neighboring information. We denote the corresponding procedures by 2D (ST), 2D (SA), and 2D (IHW), respectively, and include them in the numerical comparisons. Throughout, we focus on testing the one-sided hypotheses $\mathcal{H}_{0,s}: \mu(s) \leq 0$ versus $\mathcal{H}_{a,s}: \mu(s) > 0$. We set the nominal FDR level at q = 10% and report

the FDP and power (the number of true discoveries divided by the total number of signals) by averaging over 50 simulation runs. For the set of neighbors $\mathcal{N}(s)$ of the location s, we can use the κ -nearest neighbors for each s. A sensitivity analysis of κ is conducted in Section S.I.2 of the Supplementary Materials and empirically suggests κ to be an integer between 2 and 7. In our simulation studies, we use $\kappa = 4$.

5.2 One-Dimensional Domain

In this section, we consider the process $X(s) = \mu(s) + \epsilon(s)$ defined on the one-dimensional domain $\mathcal{S} = [0, 30]$. We observe the process X(s) at 900 locations that are evenly distributed over the domain \mathcal{S} . We introduce three data generating mechanisms for the signal process $\mu(s)$ and consider three signal sparsity levels within each mechanism.

- Scenario I: $\mu(s) = \gamma \mu_0(s)$, where γ determines the magnitude and $\mu_0(s)$ is generated from B-spline basis functions to control the signal densities and locations. Three different shapes of $\mu_0(s)$ are considered, which correspond to the sparse, medium, and dense signal cases, respectively.
- Scenario II: $\mu(s) = \gamma \delta(s)$ with $\delta(s) \sim \text{Bernoulli}(\bar{\pi}_0(s))$. The non-null probability functions $\bar{\pi}_0(s)$ exhibit similar patterns as those of $\mu_0(s)$ described in Scenario I.
- Scenario III: $\mu(s) = \gamma G(s)$, where G(s) follows a Gaussian process with a constant mean $\bar{\mu}$ and the covariance function $k_{\mu}(s,s') = \sigma_{\mu}^2 \exp\{-(\|s-s'\|/\rho_{\mu})^k\}$ with k=1, $\sigma_{\mu}^2 = 3$ and $\rho_{\mu} = 0.3$. We set $\bar{\mu} = -2.5, -2, -1$ for the sparse, medium, and dense signal cases, respectively. Their corresponding non-null proportions are approximately 4%, 8%, and 25%.

The shapes of $\mu_0(s)$ in Scenario I, the generated signals $\delta(s)$ in Scenario II, and the simulated signals G(s) in Scenario III are depicted in Figures S.1(a)–S.1(c) of the Supplementary Materials, respectively. For the magnitude γ , we considered $\gamma \in \{2,3,4\}$ in Scenarios I and III, and $\gamma \in \{1,1.5,2\}$ in Scenario II. We generated the noise process $\epsilon(s)$ from a mean-zero Gaussian process with the covariance function $k_{\epsilon}(s,s';r,k,\rho_{\epsilon}) = (1-r)\mathbf{1}\{s=1,2,3,4\}$

s'} + $r \exp\{-(\|s - s'\|/\rho_{\epsilon})^k\}$. Here, r determines the relative percentage of nugget effect, ρ_{ϵ} measures the strength of dependency, and k controls the decay rate of dependence. We demonstrated three different degrees of spatial dependence through the following choices of (r, k, ρ_{ϵ}) : (1) r = 0.5, k = 1, $\rho_{\epsilon} = 0.05$ (exponential kernel); (2) r = 0.8, k = 1, $\rho_{\epsilon} = 0.1$ (exponential kernel); and (3) r = 0.6, k = 2, $\rho_{\epsilon} = 0.2$ (Gaussian kernel). The above (1)–(3) combinations of (r, k, ρ_{ϵ}) represent the weak, medium, and strong correlation among locations, respectively; see Figure S.3 of the Supplementary Materials. Here we assume only one observation is available at each location and the covariance structure is known. In the next subsection, we shall consider the situation where we have multiple observations at each location to estimate the unknown covariance structure.

We applied various methods discussed in Section 5.1 to the generated datasets, and the empirical FDP and power under Scenarios I–III are summarized in Figures 2–7 based on 50 replicates. We now comment on the simulation results. Under Scenario I, ST, IHW, SABHA, 2D (ST), and dBH controlled the FDR reasonably well across all cases. LAWS, AdaPT, 2D (IHW), and 2D (SA) were inflated for the medium and strong correlation cases, with LAWS being the worst. 2D (SA) and AdaPT were generally more powerful than the other methods, while dBH was quite conservative. As expected, the 2d procedures outperformed their 1d counterparts in terms of power. The results for Scenario II were generally similar to those in Scenario I. Under Scenario III, the empirical FDPs were close to zero, indicating all methods were conservative due to the composite null effect. The 2d procedures delivered the highest power compared to the other approaches. Overall, the 2d procedures achieved remarkable improvements in power for either the weak correlation, the sparse signal, or the feeble magnitude cases.

5.3 Two-Dimensional Domain and Unknown Covariance

In this section, we consider a spatial process $X(s) = \mu(s) + \epsilon(s)$ defined on the unit square $\mathcal{S} = [0, 5]^2$. We observe the process on a 30×30 lattice within the unit square. The noise $\epsilon(s)$

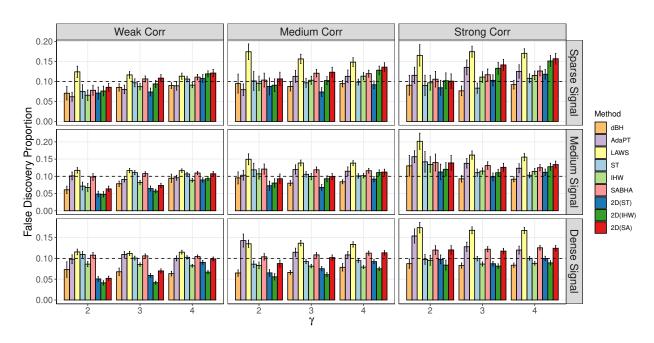


Figure 2: The mean and the standard error of FDP under Scenario I with $\gamma \in \{2, 3, 4\}$.

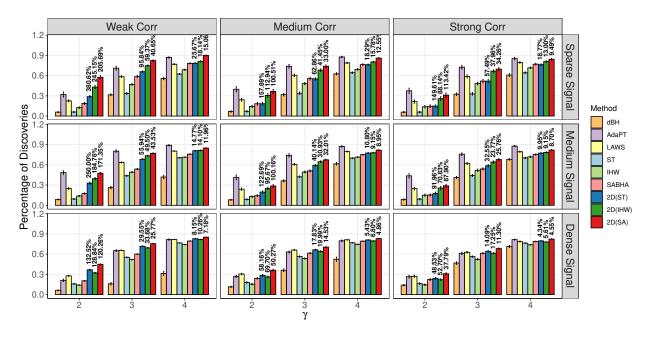


Figure 3: The mean and the standard error of power under Scenario I with $\gamma \in \{2, 3, 4\}$. The percentages on the top of bars represent the power improvement of 2d procedures compared to their 1d counterparts.

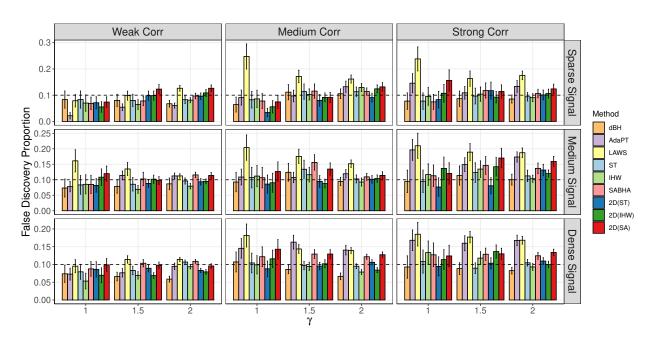


Figure 4: The mean and the standard error of FDP under Scenario II with $\gamma \in \{1, 1.5, 2\}$.

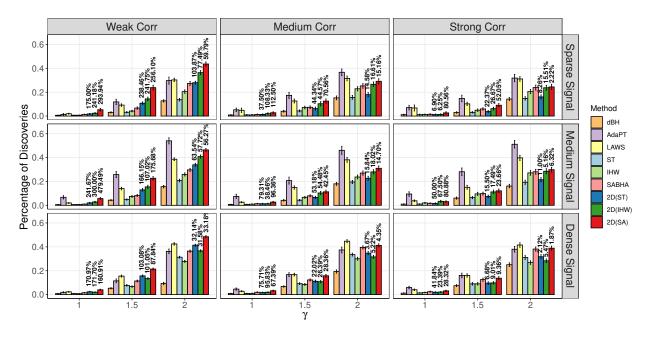


Figure 5: The mean and the standard error of power under Scenario II with $\gamma \in \{1, 1.5, 2\}$. The percentages on the top of bars represent the power improvement of 2d procedures compared to their 1d counterparts.

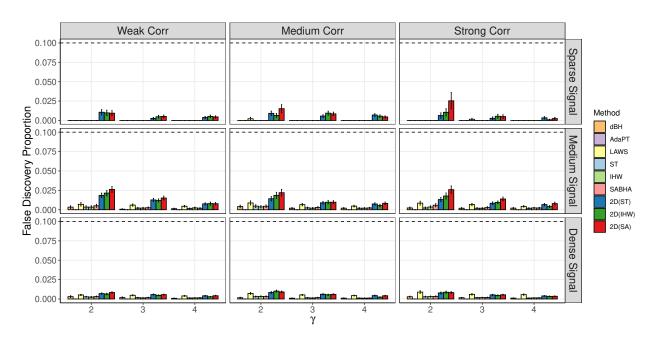


Figure 6: The mean and the standard error of FDP under Scenario III with $\gamma \in \{2, 3, 4\}$.

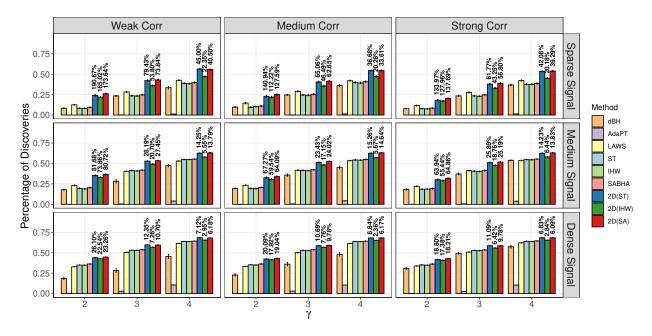


Figure 7: The mean and the standard error of power under Scenario III with $\gamma \in \{2, 3, 4\}$. The percentages on the top of bars represent the power improvement of 2d procedures compared to their 1d counterparts.

was generated from a mean-zero Gaussian process defined on $[0,5]^2$ with the same covariance function as described in Section 5.2 based on the distances between locations. Unlike Section 5.2, we now assume that the covariance structure is unknown, but three replications are available at each location. Given multiple realizations at each location, we could employ the maximum likelihood estimation with a pre-specified family of covariance functions to estimate the spatial covariance structure. The details are provided in Section S.V of the Supplementary Materials. We consider two structures for the signal process $\mu(s)$.

- Scenario IV (smooth signal): $\mu_{sm}(s) = \gamma \mu_0(s)$, where $\mu_0(s) = f_1(s_1) f_2(s_2)$ with $s = (s_1, s_2)$ and $\{f_i\}_{i=1,2}$ being generated using B-spline functions as in Scenario I.
- Scenario V (clustered signal): $\mu_{cl}(s) = \gamma \mu_0(s)$, where $\mu_0(s) \sim \text{Bernoulli}(\bar{\pi}_0(s))$ with

$$\bar{\pi}_0(s) = \begin{cases} 0.9, & \text{if } (s_1 - 1/2)^2 + (s_2 - 1/2)^2 \le (1/4)^2, \\ 0.01, & \text{otherwise.} \end{cases}$$

Three signal sparsity levels based on Scenarios IV and V were investigated: (1) sparse signal: $\mu_0(s) = \mu_{\rm cl}(s)$; (2) medium signal: $\mu_0(s) = \mu_{\rm sm}(s)$; and (3) dense signal: $\mu_0(s) = \mu_{\rm sm}(s) + \mu_{\rm cl}(s)$. The realized signal processes associated with these three sparsity levels are shown in Figure S.2 of the Supplementary Materials, and their corresponding percentages of the realized non-null locations are 5%, 17%, and 23%, respectively. For the magnitude γ , we set $\gamma \in \{0.5, 1, 1.5\}$ in both scenarios.

We report the numerical results of FDP and power of competing methods based on 50 simulation runs in Figures 8–9, respectively. Generally speaking, the 2d procedures had the best FDR and power trade-off. LAWS delivered higher power at the expense of FDR inflation. AdaPT provided reliable FDR control in all cases but their power were dominated by 2D (ST), 2D (IHW), and 2D (SA) for the sparse signal and weak correlation structures. The power improvements from the 2d procedures were most significant when

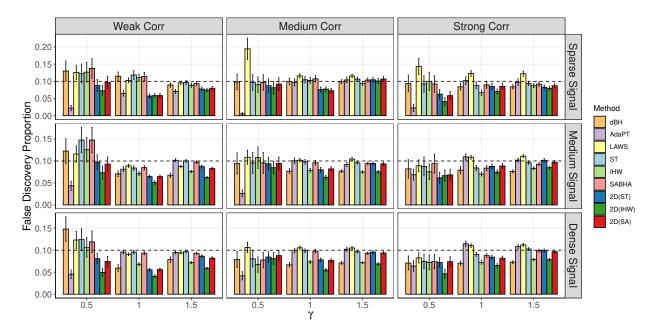


Figure 8: The mean and the standard error of FDP on the two-dimensional domain with $\gamma \in \{0.5, 1, 1.5\}.$

the correlation was weak. It is also worth mentioning that in the case of strong correlation, the underlying covariance function was based on the Gaussian kernel while we estimated the covariance structure using the exponential kernel. The 2d procedures appeared robust to the misspecification subject to the parametric family of covariance functions.

6 Ozone data analysis

Ozone has double-edged effects on human health: on the one hand, ozone in the upper atmosphere (stratospheric ozone) shields humans from harmful ultraviolet (UV) radiation; on the other hand, ozone at ground level (tropospheric ozone) can trigger a variety of adverse health effects on human, sensitive vegetation and ecosystems (Weinhold, 2008; Liu et al., 2022a). The US Environmental Protection Agency (EPA) formulates regulations to help states reduce tropospheric ozone levels in outdoor air. The majority of tropospheric ozone occurs through the reaction of nitrogen oxides (NO_x), carbon monoxide (CO), and volatile organic compounds (CO) in the atmosphere when exposed to sunlight, particularly under the UV spectrum (CO).

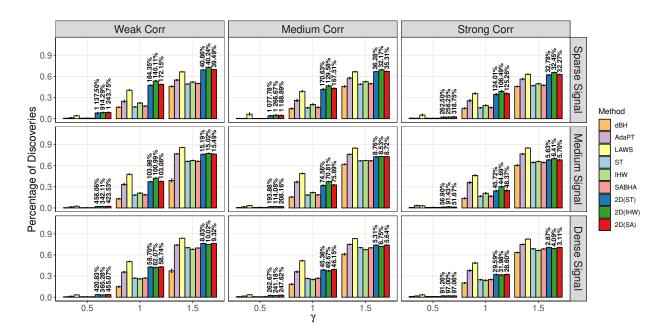


Figure 9: The mean and the standard error of power on the two-dimensional domain with $\gamma \in \{0.5, 1, 1.5\}$. The percentages on the top of bars represent the power improvement of 2d procedures compared to their 1d counterparts.

We applied our proposed 2d procedures and their 1d alternatives to identify the locations where the decreasing trend is below a pre-specified level for the Contiguous United States from 2010 to 2021. The data were the annual averages of the fourth-highest daily maximum 8-hour ozone concentrations, available at the EPA's air quality system¹. To facilitate the analysis, we retained 697 stations (i) having a single site, (ii) having full records across the years, and (iii) being recorded by the World Geodetic System (WGS84). We followed the procedures in Sun et al. (2015) to pre-process the data. For each location, we first fitted the linear model

$$\mathbf{X}(s) = \mu_0(s) + \beta(s)\mathbf{t} + \sigma_{\epsilon}(s)\boldsymbol{\epsilon}(s), \tag{16}$$

where $\mathbf{X}(s) = (X_{2010}(s), \dots, X_{2021}(s))^{\top}$ was the observed ozone level measured in parts per billion (ppb), $\mathbf{t} = (2010, 2011, \dots, 2021)^{\top}$ was the predictor capturing the time trend, $\beta(s)$ was the slope at site s, $\boldsymbol{\epsilon}(s) = (\epsilon_{2010}(s), \dots, \epsilon_{2021}(s))^{\top}$ was assumed to follow a mean-zero Gaussian process with the exponential kernel function $k_{\epsilon}(\cdot, \cdot; r, 1, \rho_{\epsilon})$, and $\sigma_{\epsilon}(s)$ was

¹http://www.epa.gov/airexplorer/index.htm

the standard deviation of noise at site s. We were interested in testing whether the ozone level declined more than β_0 ppb per year at each site, i.e., $\mathcal{H}_{0,s}:\beta(s)\geq -\beta_0$ versus $\mathcal{H}_{1,s}:\beta(s)<-\beta_0$, where $\beta_0\in\{0.1,0.2,0.3,0.4,0.5\}$. We first conducted simple linear regression and obtained the OLS estimates of $(\mu_0(s),\beta(s),\sigma_{\epsilon}(s))$, denoted as $(\widehat{\mu}_0(s),\widehat{\beta}(s),\widehat{\sigma}_{\epsilon}(s))$. Then, we obtained $(\widehat{r},\widehat{\rho}_{\epsilon})$ by fitting the kernel function to the residuals $\widehat{\epsilon}(s):=\{\mathbf{X}(s)-\widehat{\beta}(s)\mathbf{t}-\widehat{\mu}_0(s)\}/\widehat{\sigma}_{\epsilon}(s)$. Finally, the primary test statistic was calculated as $\widehat{T}_2(s)=\{\widehat{\beta}(s)+\beta_0\}/\widehat{\sigma}_{\widehat{\beta}}(s)$, and the auxiliary test statistic was given by $\widehat{T}_1(s)=\sum_{v\in\mathcal{N}(s)}\{\widehat{\beta}(v)+\beta_0\}/\widehat{\tau}(s)$, where $\mathcal{N}(s)$ was the set containing the two-nearest neighbors of s and $\widehat{\tau}(s)=\sum_{v,v'\in\mathcal{N}(s)}\widehat{\cos}\{\widehat{\beta}(v),\widehat{\beta}(v')\}$.

Locations with significant ozone level decline. We applied 2D (ST), 2D (IHW), 2D (SA), and their 1d alternatives to identify the non-null locations. We trisected the ranges of the latitude and longitude, which divided the whole area into nine different regions and allocated each site a categorical variable; see Figure S.10 of the Supplementary Materials for the division. Our analysis employed the categorical variable as the covariate in IHW and as the group indicator in SABHA. As shown in Figure 10, 2d procedures generally discovered more locations with significant decreasing ozone levels than their 1d counterparts did.

Ozone precursor. The EPA has been making efforts to reduce tropospheric ozone by executing air pollution control strategies, including formulating vehicle and transportation standards, regional haze and visibility rules, and regularly reviewing the National Ambient Air Quality Standards (NAAQS). The universal ozone precursors (NO_x, CO, and VOCs) first respond to these strategies and then influence the ozone levels. Indeed, some studies found the emissions of nitrogen dioxide (NO₂) and CO account for the increase in background ozone levels (Chin et al., 1994; Vingarzan, 2004; Han et al., 2011). Motivated by these findings, we collected the contemporaneous CO and NO₂ data from EPA and focused on the locations detected by either the 1d procedures or the 2d procedures but not both. Our goal was to scrutinize the trends of CO and NO₂ at these locations and explain our findings.

To this end, we regressed the CO and NO_2 levels on t separately and recorded the slopes to

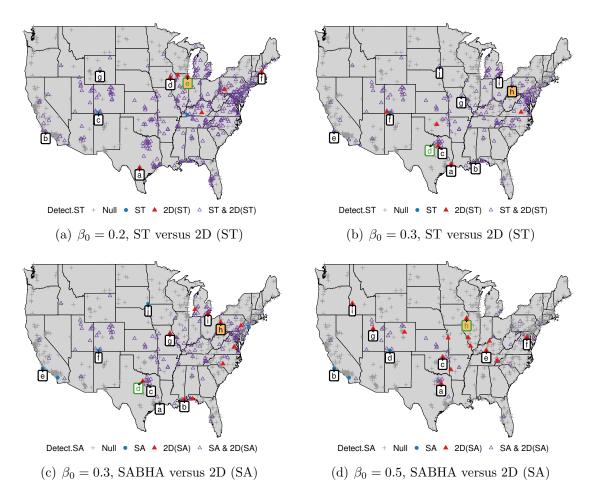


Figure 10: Results for ozone data analysis. The red triangles (\triangle), blue circles (\bullet), purple triangles (\blacktriangle), and grey plus (+) signs represent the locations detected by the 2d procedure only, the 1d procedure only, both procedures, and neither one of the procedures, respectively. The labelled locations: (i) are detected by either 1d procedures or 2d procedures but not both; and (ii) possess either CO or NO₂ records across 2010 to 2021. Within each sub-figure, the location with the orange background has the most significant CO decline among the labelled locations; meanwhile, the location with the green typeface has the most significant NO₂ decline among the labelled locations.

understand the increasing/decreasing trends of the CO and NO₂ levels. We summarized the major findings in Figure 10 and Tables S.1 and S.2 (of the Supplementary Materials). First, the locations detected only by the 2d procedures always included the ones with the most significant decline in the CO or NO₂ levels (i.e., the locations with the orange background or green typeface labels in Figure 10). See more details in Table S.1. Second, the average decline (measured by the average of the standardized slopes) of the locations detected only by

the 2d procedures was larger than that of the locations detected only by the 1d procedures. Take Figure 10(d) as an example, where we had NO₂ records at locations a, b, c, d, f, g, h and i, and CO records at locations b, c, e, f, and h. SABHA detected the locations b and d, while 2D (SA) identified the locations a, c, e, f, g, h and i. The average decline in the NO₂ levels was -3.63 for the locations detected by SABHA as compared to -4.68 for the locations detected by 2D (SA). As for CO, the average standardized slope was -0.96 for locations detected by SABHA in comparison to -1.40 for the locations identified by 2D (SA). In general, the CO and NO₂ levels tended to decrease more rapidly for those locations detected by 2D (SA) except for the case with $\beta_0 = 0.3$. See Table S.2 for more details.

Ozone data simulation. To further validate our findings and to demonstrate the effectiveness of the 2D procedures, we conducted a simulation study where we generated data mimicking the structure of the original ozone data. In particular, we generated the ozone level data from 2010 to 2021 through (16) by setting $\beta(s) = \widehat{\beta}(s)$, $\mu(s) = \widehat{\mu}(s)$, $\sigma_{\epsilon}(s) = \widehat{\sigma}_{\epsilon}(s)$, $r = \widehat{r}$, and $\rho_{\epsilon} = \widehat{\rho}_{\epsilon}$. We processed the data and conducted multiple testing in the same way as discussed before. Table 1 shows that the 2d procedures achieved equal or slightly higher power compared to the 1d alternatives.

Table 1: Mean and standard deviation of the percentage of true discoveries in the simulated data sets mimicking the ozone data. The results are based on 50 simulation runs.

Percentage of True Discoveries						
	Methodology					
eta_0	ST	IHW	SABHA	2D(ST)	2D(IHW)	2D(SA)
0.5	0.107(0.000)	0.100(0.000)	0.175(0.000)	0.107(0.000)	0.100(0.000)	0.221(0.004)
0.4	0.311(0.036)	0.302(0.040)	0.305(0.036)	0.319(0.037)	0.303(0.042)	0.322(0.038)
0.3	0.547(0.034)	0.494(0.037)	0.483(0.037)	0.556(0.033)	0.494(0.036)	0.495(0.037)
0.2	0.755(0.019)	0.660(0.021)	0.665(0.022)	0.761(0.020)	0.659(0.021)	0.674(0.022)
0.1	0.841(0.008)	0.754(0.016)	0.765(0.015)	0.845(0.009)	0.754(0.016)	0.769(0.014)

7 Discussion

This paper proposes a new FDR-controlling procedure, 2d-SMT, to improve the signal detection power by incorporating the spatial information encoded in neighboring observations. It provides a unique perspective on utilizing spatial information, which is fundamentally different from the existing covariate and structural adaptive multiple testing procedures. The spatial information is gathered through an auxiliary statistic, which is used to screen out the noise. A primary statistic from the location of interest is then used to determine the existence of the signal. 2d-SMT is particularly effective when the signals exhibit in clusters. We establish the asymptotic FDR control for 2d-SMT under weak spatial dependence and demonstrate its usefulness through simulation studies and the analysis of an ozone data set.

To conclude, we point out a few future research directions. First, as discussed in Section 2.7, the proposed 2d-SMT is flexible to combine with various weighted BH procedures. One challenge is, however, to establish a rigorous theoretical FDR control guarantee for the resulting weighted 2d-SMT procedures. Second, when implementing our methodology, we use the κ -nearest neighbors to construct the auxiliary statistic. A more delicate strategy is to apply a weighting scheme to pool sufficient information from nearby locations. Third, extending the idea in 2d-SMT to other statistical problems, such as mediation analysis in causal inference, is of interest.

References

- Basu, P., Cai, T. T., Das, K., and Sun, W. (2018), "Weighted false discovery rate control in large-scale multiple testing," *Journal of the American Statistical Association*, 113, 1172–1183.
- Benjamini, Y. and Heller, R. (2007), "False discovery rates for spatial signals," *Journal of the American Statistical Association*, 102, 1272–1281.
- Benjamini, Y. and Hochberg, Y. (1995), "Controlling the false discovery rate: A practical and powerful approach to multiple testing," *Journal of the Royal Statistical Society: Series B (Methodological)*, 57, 289–300.
- Cai, T. T., Sun, W., and Xia, Y. (2021), "LAWS: A locally adaptive weighting and screening approach to spatial multiple testing," *Journal of the American Statistical Association*, 0, 1–14.
- Cao, H., Chen, J., and Zhang, X. (2022), "Optimal false discovery rate control for large scale

- multiple testing with auxiliary information," The Annals of Statistics, 50, 807–857.
- Chin, M., Jacob, D. J., Munger, J. W., Parrish, D. D., and Doddridge, B. G. (1994), "Relationship of ozone and carbon monoxide over North America," *Journal of Geophysical Research:* Atmospheres, 99, 14565–14573.
- Fithian, W. and Lei, L. (2020), "Conditional calibration for false discovery rate control under dependence," arXiv preprint, abs/2201.1004.
- Genovese, C. R., Roeder, K., and Wasserman, L. (2006), "False discovery control with p-value weighting," *Biometrika*, 93, 509–524.
- Han, S., Bian, H., Feng, Y., Liu, A., Li, X., Zeng, F., Zhang, X., et al. (2011), "Analysis of the relationship between O3, NO and NO2 in Tianjin, China," *Aerosol and Air Quality Research*, 11, 128–139.
- Heller, R., Stanley, D., Yekutieli, D., Rubin, N., and Benjamini, Y. J. N. (2006), "Cluster-based analysis of FMRI data," *Neuroimage*, 33, 599–608.
- Hu, J., Zhao, H., and Zhou, H. (2010), "False discovery rate control with groups," *Journal of the American Statistical Association*, 105, 1215–1227.
- Huang, H.-C., Cressie, N., Zammit-Mangion, A., and Huang, G. (2021), "False discovery rates to detect signals from incomplete spatially aggregated data," *Journal of Computational and Graphical Statistics*, 30, 1081–1094.
- Ignatiadis, N. and Huber, W. (2021), "Covariate powered cross-weighted multiple testing," *Journal of the Royal Statistical Society: Series B (Statistical Methodology)*, 83, 720–751.
- Ignatiadis, N., Klaus, B., Zaugg, J. B., and Huber, W. (2016), "Data-driven hypothesis weighting increases detection power in genome-scale multiple testing," *Nature Methods*, 13, 577–580.
- Jenish, N. (2012), "Nonparametric spatial regression under near-epoch dependence," *Journal of Econometrics*, 167, 224–239.
- Jenish, N. and Prucha, I. R. (2012), "On spatial processes and asymptotic inference under near-epoch dependence," *Journal of Econometrics*, 170, 178–190.
- Jiang, W. and Zhang, C.-H. (2009), "General maximum likelihood empirical Bayes estimation of normal means," *The Annals of Statistics*, 37, 1647–1684.
- Katzfuss, M. and Guinness, J. (2021), "A general framework for Vecchia approximations of Gaussian processes," *Statistical Science*, 36, 124–141.
- Kiefer, J. and Wolfowitz, J. (1956), "Consistency of the maximum likelihood estimator in the presence of infinitely many incidental parameters," *The Annals of Mathematical Statistics*, 27, 887–906.
- Koenker, R. and Gu, J. (2017), "REBayes: An R package for empirical Bayes mixture methods," *Journal of Statistical Software*, 82, 1–26.
- Koenker, R. and Mizera, I. (2014), "Convex optimization, shape constraints, compound decisions, and empirical Bayes rules," *Journal of the American Statistical Association*, 109, 674–685.
- Lei, J., G'Sell, M., Rinaldo, A., Tibshirani, R. J., and Wasserman, L. (2018), "Distribution-free predictive inference for regression," *Journal of the American Statistical Association*, 113, 1094–1111.
- Li, A. and Barber, R. F. (2019), "Multiple testing with the structure-adaptive Benjamini-Hochberg algorithm," *Journal of the Royal Statistical Society: Series B (Statistical Methodology)*, 81, 45–74.
- Liu, W., Hegglin, M. I., Checa-Garcia, R., Li, S., Gillett, N. P., Lyu, K., Zhang, X., and Swart, N. C. (2022a), "Stratospheric ozone depletion and tropospheric ozone increases drive Southern

- Ocean interior warming," Nature Climate Change, 12, 365–372.
- Liu, W., Ke, Y., Liu, J., and Li, R. (2022b), "Model-Free Feature Screening and FDR Control With Knockoff Features," *Journal of the American Statistical Association*, 117, 428–443.
- Mardia, K. V. and Marshall, R. J. (1984), "Maximum likelihood estimation of models for residual covariance in spatial regression," *Biometrika*, 71, 135–146.
- Padoan, S. A. and Bevilacqua, M. (2015), "Analysis of random fields using CompRandFld," *Journal of Statistical Software*, 63, 1–27.
- Sang, H. and Huang, J. Z. (2012), "A full scale approximation of covariance functions for large spatial data sets," *Journal of the Royal Statistical Society: Series B (Statistical Methodology)*, 74, 111–132.
- Scott, J. G., Kelly, R. C., Smith, M. A., Zhou, P., and Kass, R. E. (2015), "False discovery rate regression: An application to neural synchrony detection in primary visual cortex," *Journal of the American Statistical Association*, 110, 459–471.
- Shen, X., Huang, H.-C., and Cressie, N. (2002), "Nonparametric hypothesis testing for a spatial signal," *Journal of the American Statistical Association*, 97, 1122–1140.
- Sommerfeld, M., Sain, S., and Schwartzman, A. (2018), "Confidence regions for spatial excursion sets from repeated random field observations, with an application to climate," *Journal of the American Statistical Association*, 113, 1327–1340.
- Storey, J. D. (2002), "A direct approach to false discovery rates," Journal of the Royal Statistical Society: Series B (Methodological), 64, 479–498.
- Storey, J. D., Taylor, J. E., and Siegmund, D. (2004), "Strong control, conservative point estimation and simultaneous conservative consistency of false discovery rates: a unified approach," *Journal of the Royal Statistical Society: Series B (Statistical Methodology)*, 66, 187–205.
- Sun, W., Reich, B. J., Cai, T. T., Guindani, M., and Schwartzman, A. (2015), "False discovery control in large-scale spatial multiple testing," *Journal of the Royal Statistical Society: Series B* (Statistical Methodology), 77, 59–83.
- Tansey, W., Koyejo, O., Poldrack, R. A., and Scott, J. G. (2018), "False discovery rate smoothing," Journal of the American Statistical Association, 113, 1156–1171.
- Vingarzan, R. (2004), "A review of surface ozone background levels and trends," *Atmospheric Environment*, 38, 3431–3442.
- Warneck, P. (2000), "Chapter 5 Ozone in the troposphere," in *Chemistry of the Natural Atmosphere*, ed. Warneck, P., Academic Press, vol. 71 of *International Geophysics*, pp. 211–263.
- Wasserman, L. and Roeder, K. (2009), "High dimensional variable selection," *Annals of statistics*, 37, 2178–2201.
- Weinhold, B. (2008), "Ozone nation: EPA standard panned by the people," *Environmental Health Perspectives*, 116, A302–A305.
- Yi, S., Zhang, X., Yang, L., Huang, J., Liu, Y., Wang, C., Schaid, D. J., and Chen, J. (2021), "2dFDR: A new approach to confounder adjustment substantially increases detection power in omics association studies," *Genome Biology*, 22, 208.
- Yun, S., Zhang, X., and Li, B. (2022), "Detection of local differences in spatial characteristics between two spatiotemporal random fields," *Journal of the American Statistical Association*, 117, 291–306.
- Zhang, X. and Chen, J. (2022), "Covariate adaptive false discovery rate control with applications to omics-wide multiple testing," *Journal of the American Statistical Association*, 117, 411–427.

Supplementary Material for "Powerful Spatial Multiple Testing via Borrowing Neighboring Information"

Linsui Deng¹, Kejun He^{1*}, Xianyang Zhang^{2*}

¹The Center for Applied Statistics, Institute of Statistics and Big Data,
Renmin University of China, Beijing, China

²Department of Statistics, Texas A&M University, College Station, USA

The supplement is organized as follows. Section S.I includes some details on the simulation studies and the additional results of the ozone data analysis. Section S.II presents two main lemmas and the proof of Theorem 1. The two main lemmas are proved in Section S.III with some preliminary lemmas and discussions. Section S.IV provides the detailed proofs of the preliminary lemmas. We discuss the estimation for the covariance of noises in Section S.V. Section S.VI thoroughly describes the details of Algorithm 1 in Section 3 of the main paper which overcomes the computational bottleneck of a naive grid search.

S.I Additional Experimental Results

This section provides additional results for the simulations and the real data analysis with some implementation details. In particular, Section S.I.1 visualizes the simulation settings in Section 5 of the main paper. In Section S.I.2, we investigate the sensitivity of 2d-SMT to the number of observations in the nearest neighbors. Section S.I.3 depicts the partition of the Contiguous United States into nine regions and presents additional results about the ozone data analysis.

S.I.1 Simulation Settings

- Figure S.1 depicts the one-dimensional signal process $\mu(s)$ for Scenarios I–III as described in Section 5.2 of the main paper. The plots are depicted with the magnitude $\gamma = 1$.
- Figure S.2 shows the two-dimensional signal process for three signal sparsity levels in Section 5.3 of the main paper. The plots are depicted with the magnitude $\gamma = 1$.
- Figure S.3 displays the spatial covariances of the noise process $\epsilon(s)$ versus the spatial distance for three dependency strengths as described in Sections 5.2 and 5.3.

^{*}Correspondence: kejunhe@ruc.edu.cn and zhangxiany@stat.tamu.edu.

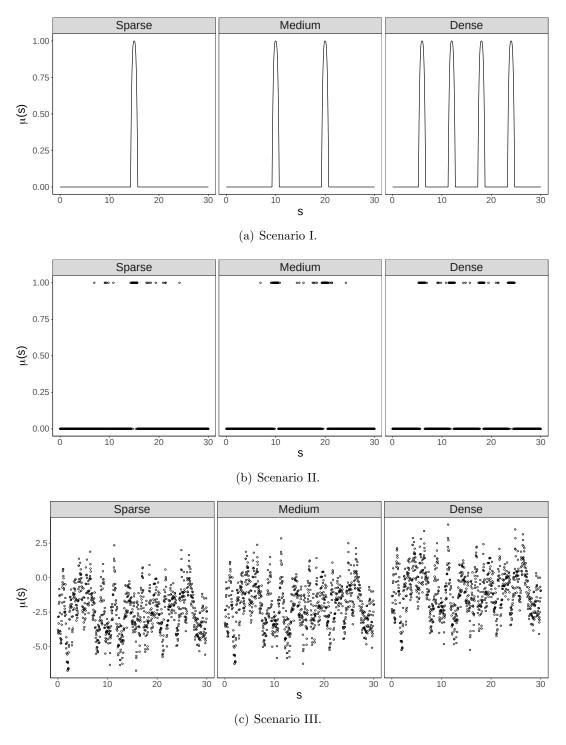


Figure S.1: The one-dimensional signal process $\mu(s)$ ($s \in [0, 30]$) with $\gamma = 1$ in Section 5.2 of the main paper. The top to bottom panels correspond to Scenarios I–III of our simulation settings respectively.

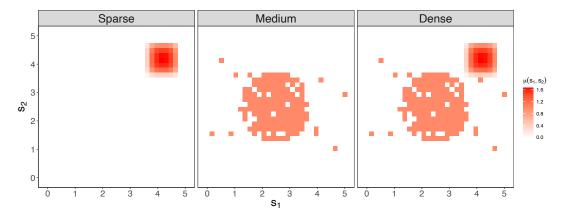


Figure S.2: The two-dimensional signal process $\mu(s_1, s_2)$ $((s_1, s_2) \in [0, 5]^2)$ with $\gamma = 1$ in Section 5.3 of the main paper. The left to right panels correspond to sparse, medium, and dense signals of our simulation settings respectively.

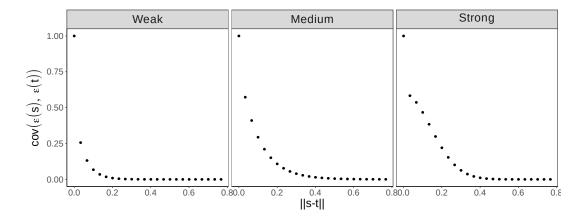


Figure S.3: The covariance structure of the noise process $\epsilon(s)$ used in our simulation studies. The x-axis is the distance between s and t, denoted as ||s-t||, and y-axis is the covariance between $\epsilon(s)$ and $\epsilon(t)$, denoted as $\cos(\epsilon(s), \epsilon(t))$. The choices of $\epsilon(t)$ for the weak, medium, and strong dependence strengths (from left to right) are: (1) $\epsilon(t)$ $\epsilon(t)$ and (2) $\epsilon(t)$ $\epsilon(t)$ $\epsilon(t)$ $\epsilon(t)$ $\epsilon(t)$ $\epsilon(t)$ are: (1) $\epsilon(t)$ $\epsilon(t)$ and (2) $\epsilon(t)$ $\epsilon(t)$ $\epsilon(t)$ $\epsilon(t)$ $\epsilon(t)$ $\epsilon(t)$ $\epsilon(t)$ $\epsilon(t)$ and (3) $\epsilon(t)$ $\epsilon(t)$ $\epsilon(t)$ $\epsilon(t)$ $\epsilon(t)$ $\epsilon(t)$ and (3) $\epsilon(t)$ $\epsilon(t)$ $\epsilon(t)$ $\epsilon(t)$ $\epsilon(t)$ $\epsilon(t)$ $\epsilon(t)$ $\epsilon(t)$ $\epsilon(t)$ and $\epsilon(t)$ and $\epsilon(t)$ $\epsilon(t)$

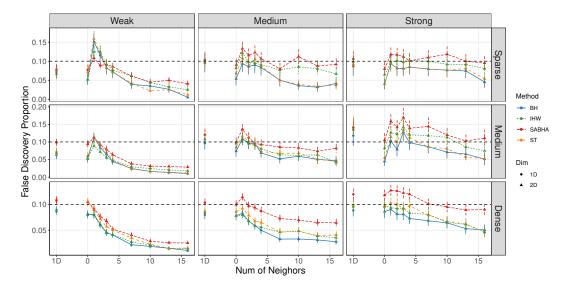


Figure S.4: The mean and the standard error of FDP under Scenario I with $\gamma = 2$. Each color represents one particular 1d procedure (the circle at the leftmost column of each plot) and its 2d counterpart (the triangles).

S.I.2 Sensitivity to the Number of Nearest Neighbors

In this section, we conduct a simulation study to investigate the sensitivity of 2d-SMT to the number of observations in $\mathcal{N}(s)$. To be concrete, we let $\mathcal{N}(s)$ be the κ -nearest neighbors for each location s. We focus on the settings in Scenarios I–III and let $\kappa \in \{1, 2, 3, 4, 7, 10, 13, 16\}$. The false discovery proportions (FDPs) and powers of BH, ST, SABHA, and IHW (with the global null proportion estimate) as well as their corresponding 2d versions are summarized in Figures S.4–S.9. The difference between the 2d procedures with zero neighbor and their 1d counterparts is that the 2d procedures add a small offset q (i.e., the FDR level) to the estimate of the number of false rejections (see Section 3 of the main paper).

Figures S.4, S.6, and S.8 show that the FDP steps up when incorporating the first neighbor, and then gradually decreases and keeps stable afterwards as more neighbors are included for all the three scenarios. As seen from Figures S.5 and S.7, including more neighbors improves the detection power for all the 2d procedures, which is significantly higher than that of the corresponding 1d counterpart under all setups of Scenarios I and II. In Figure S.9, though the detection power of the 2d procedure remains larger than the corresponding 1d counterpart, different 2d procedures behave differently for varying κ under Scenario III. In particular, the powers of 2D (IHW), 2D (ST), and 2D (BH) gradually decrease when κ is larger than 7. For 2D (SABHA), when the signal is sparse, its detection power first decreases then increases when more neighbors are included. For the medium and dense signal cases, its behavior is similar to the other 2d procedures. These findings empirically suggest that one may choose κ between 2 and 7 in 2d-SMT to control the FDP and improve the detection power.

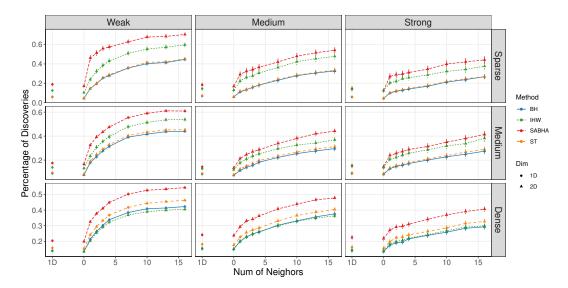


Figure S.5: The mean and the standard error of power under Scenario I with $\gamma = 2$. Each color represents one particular 1d procedure (the circle at the leftmost column of each plot) and its 2d counterpart (the triangles).

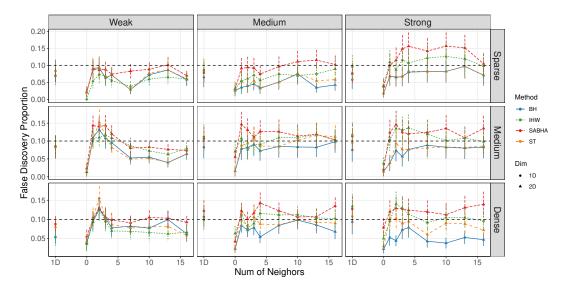


Figure S.6: The mean and the standard error of FDP under Scenario II with $\gamma = 1$. Each color represents one particular 1d procedure (the circle at the leftmost column of each plot) and its 2d counterpart (the triangles).

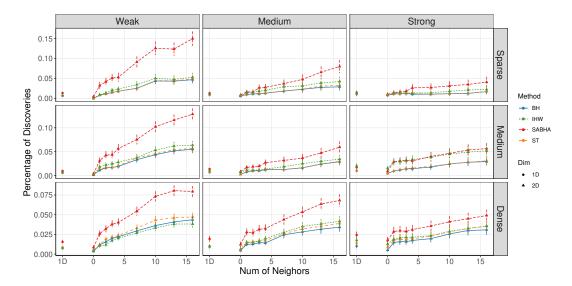


Figure S.7: The mean and the standard error of power under Scenario II with $\gamma = 1$. Each color represents one particular 1d procedure (the circle at the leftmost column of each plot) and its 2d counterpart (the triangles).

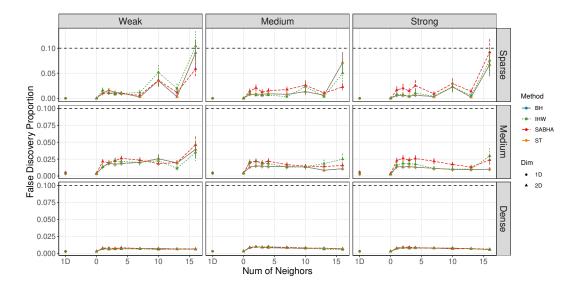


Figure S.8: The mean and the standard error of FDP under Scenario III with $\gamma=2$. Each color represents one particular 1d procedure (the circle at the leftmost column of each plot) and its 2d counterpart (the triangles).

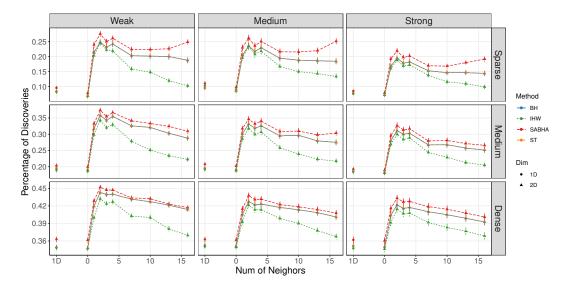


Figure S.9: The mean and the standard error of power under Scenario III with $\gamma = 3$. Each color represents one particular 1d procedure (the circle at the leftmost column of each plot) and its 2d counterpart (the triangles).

S.I.3 Additional Results for the Ozone Data Analysis

Figure S.10 uses distinct shapes and colors to illustrate the partition of the Contiguous United States into nine different regions as discussed in Section 6 of the main paper. The region to which each location belongs is treated as a categorical variable and is used as the covariate in IHW and the group indicator in SABHA. Table S.1 shows the locations with the most significant decline in the CO or NO₂ concentration levels and whether the competing methods detected them in the study of ozone level decline for various β_0 . Table S.2 presents the average standardized slopes of CO and NO₂ at the locations detected either by the 2d procedure or the 1d procedure but not both. It shows that the NO₂ concentration level at the locations detected by the 2d procedures decreases faster than their 1d counterparts on average. For CO, when the null hypothesis is $\beta_0 = 0.2$ or $\beta_0 = 0.5$, the average standardized slope of its concentration level at the locations detected by the 2d procedures remains smaller than their 1d counterparts. The only exception is when $\beta_0 = 3$, the locations detected by the 1d procedure (SABHA) have a smaller average standardized slope of CO level than those detected by 2D (SA).

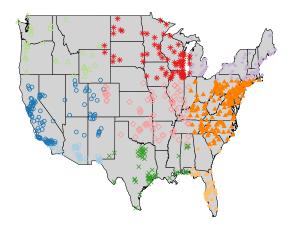


Figure S.10: The Contiguous United States is divided into nine different regions based on the latitude and longitude, i.e., each station belongs to a region coded between one and nine. The stations in the same region are depicted using the same shape and color.

Table S.1: The locations with the most significant decline in the CO or NO_2 levels. Reported are the locations where at least one of the 2d procedures gives different decisions to their corresponding 1d counterparts. The column "Stand. Coeff." represents the value of the standardized coefficient.

Ozone precursor	β_0	Lat.	Lon.	Stand. Coeff.	Methodology					
					ST	2D (ST)	IHW	2D (IHW)	SABHA	2D (SA)
СО	0.1	40.63	-75.34	-0.56	Х	✓	Х	Х	Х	Х
	0.2	42.14	-87.80	-0.94	X	✓	X	X	X	X
	0.3	41.00	-80.35	-2.19	✓	✓	✓	✓	X	✓
	0.4	36.20	-95.98	-0.85	/	✓	1	✓	X	✓
	0.5	41.53	-90.59	-3.46	X	X	X	X	X	✓
NO2	0.1	40.63	-75.34	-3.49	Х	✓	Х	Х	Х	Х
	0.2	42.14	-87.80	-4.60	X	✓	X	X	X	×
	0.3	32.87	-97.91	-43.10	✓	✓	✓	✓	X	✓
	0.4	35.41	-94.52	-7.27	X	X	X	X	X	✓
	0.5	41.53	-90.59	-9.16	X	X	X	X	X	✓

Table S.2: The average standardized slopes of CO and NO_2 at the locations where at least one of the 2d procedures gives different decisions to their corresponding 1d counterparts. Each letter refers to the specific location depicted in Figure 10 of the main paper.

		eta_0								
Ozone precursor	Methodology	0.2		0.3		0.5				
procursor		Loc.	Avr.	Loc.	Avr.	Loc.	Avr.			
	ST		_				_			
90	2D (ST)	$_{ m d,e}$	-0.48			_				
СО	SABHA	_		e, j	0.11	b	-0.96			
	2D (SA)		_	h, i	0.56	c, e, f, h	-1.40			
NO_2	ST	С	-1.30	f	-1.30	_	_			
	2D (ST)	a, e, f	-2.73	a, c	-6.44	_				
	SABHA	_		e, f, j	-2.81	b, d	-3.63			
	2D (SA)		_	b, d, g	-17.17	a, c, f, g, h, i	-4.68			

S.II Proof of Theorem 1

We introduce two lemmas, which play key roles in the proof of Theorem 1.

Lemma S.1. Under Assumptions 1–9, for any t'_1 , $t'_2 > 0$, we have

$$\sup_{|t_1| \le t_1', |t_2| \le t_2'} \left| m^{-1} \sum_{s \in \mathcal{S}_m} \int L\left\{t_1, t_2, x, \widehat{\rho}(s)\right\} d\widehat{G}_{\tilde{m}}(x) - K_0(t_1, t_2) \right| = o_{\mathbb{P}}(1).$$

Lemma S.2. Under Assumptions 1-3, 7, and 9, for any t'_1 , $t'_2 > 0$, we have

$$\sup_{|t_1| \le t_1', |t_2| \le t_2'} \left| \frac{1}{m_0} \widehat{V}_m(t_1, t_2) - K_0(t_1, t_2) \right| = o_{\mathbb{P}}(1), \tag{S.1}$$

$$\sup_{|t_1| \le t_1', |t_2| \le t_2'} \left| \frac{1}{m_1} \widehat{S}_m(t_1, t_2) - K_1(t_1, t_2) \right| = o_{\mathbb{P}}(1), \tag{S.2}$$

$$\sup_{|t_1| \le t_1', |t_2| \le t_2'} \left| \widehat{F}_m(\lambda) - F(\lambda) \right| = o_{\mathbb{P}}(1), \tag{S.3}$$

as
$$m = m_0 + m_1 \to \infty$$
, where $\widehat{F}_m(\lambda) = m^{-1} \sum_{s \in \mathcal{S}_m} \mathbf{1}\{\widehat{T}_2(s) \le \lambda\}$.

Lemma S.1 states that the estimated number of false discoveries in the proposed 2d-SMT procedure converges to the limiting process defined in Assumption 9 of the main paper. Lemma S.2 states the uniform convergence for the processes counting the numbers of false and true rejections and the empirical CDF for $\hat{T}_2(s)$. In the following derivations, we let C be a positive constant which can be different from line to line.

Proof of Theorem 1. We fix $t'_1 = t_1^*$ and $t'_2 = t_2^*$ as defined in Assumption 10. To prove Theorem 1, we first show

$$\sup_{|t_1| \le t_1^*, |t_2| \le t_2^*} \left| \widehat{\text{FDP}}_{\lambda, \widetilde{\mathcal{S}}_m} \left(t_1, t_2 \right) - \text{FDP}_{\lambda}^{\infty} \left(t_1, t_2 \right) \right| = o_{\mathbb{P}}(1), \tag{S.4}$$

and

$$\sup_{|t_{1}| \leq t_{1}^{\star}, |t_{2}| \leq t_{2}^{\star}} \left| \frac{\widehat{V}_{m}(t_{1}, t_{2})}{\widehat{V}_{m}(t_{1}, t_{2}) + \widehat{S}_{m}(t_{1}, t_{2})} - \frac{\pi_{0} K_{0}(t_{1}, t_{2})}{K(t_{1}, t_{2})} \right| = o_{\mathbb{P}}(1).$$
 (S.5)

To show (S.4), according to Lemma S.2 and Assumption 7, we have

$$\sup_{|t_1| \leq t_1^\star, |t_2| \leq t_2^\star} \left| \widehat{K}_m\left(t_1, t_2\right) - K\left(t_1, t_2\right) \right| = o_{\mathbb{P}}(1),$$

where $\widehat{K}_m(t_1, t_2) = m^{-1} \{\widehat{V}_m(t_1, t_2) + \widehat{S}_m(t_1, t_2)\}$. For any $|t_1| \leq t_1^{\star}$, $|t_2| \leq t_2^{\star}$ and large enough m, we get

$$\left|\widehat{K}_{m}(t_{1},t_{2})-K(t_{1},t_{2})\right| \leq \frac{\left|K(t_{1},t_{2})\right|}{2},$$

which implies

$$\left| \widehat{K}_m(t_1, t_2) \right| \ge \frac{|K(t_1, t_2)|}{2} \ge \frac{K(t_1^*, t_2^*)}{2} > 0$$
 (S.6)

because $\inf_{|t_1| \leq t_1^{\star}, |t_2| \leq t_2^{\star}} |K(t_1, t_2)| \geq K(t_1^{\star}, t_2^{\star}) > 0$. For large enough m, it follows that

$$\begin{split} &\left|\widehat{\text{FDP}}_{\lambda,\widetilde{\mathcal{S}}_m}\left(t_1,t_2\right) - \text{FDP}_{\lambda}^{\infty}\left(t_1,t_2\right)\right| \\ &= \frac{\left|m^{-1}K(t_1,t_2)F_m(\lambda)\sum_{s\in\mathcal{S}_m}\int L\left\{t_1,t_2,x,\widehat{\rho}(s)\right\}d\widehat{G}_{\tilde{m}}(x) - \widehat{K}_m(t_1,t_2)F(\lambda)K_0(t_1,t_2)\right|}{\Phi(\lambda)\widehat{K}_m(t_1,t_2)K(t_1,t_2)} \\ &\leq \frac{2\left|m^{-1}K(t_1,t_2)F_m(\lambda)\sum_{s\in\mathcal{S}_m}\int L\left\{t_1,t_2,x,\widehat{\rho}(s)\right\}d\widehat{G}_{\tilde{m}}(x) - \widehat{K}_m(t_1,t_2)F(\lambda)K_0(t_1,t_2)\right|}{\Phi(\lambda)K^2(t_1^*,t_2^*)} \end{split}$$

where the last inequality holds by (S.6). Thus (S.4) follows from Lemma S.1 and Lemma S.2. Similarly, we can prove (S.5).

Next we use (S.4) and (S.5) to show $\limsup_{m\to\infty}\widetilde{\mathrm{FDR}}_m \leq q$. Due to Assumption 10, we have $\mathrm{FDP}^\infty_\lambda\left(t_1^\star,0\right) < q$ and $\mathrm{FDP}^\infty_\lambda\left(0,t_2^\star\right) < q$. Then, for large enough m, we have

$$\widehat{\mathrm{FDP}}_{\lambda, \widetilde{\mathcal{S}}_m}\left(t_1^\star, 0\right) < q \ \text{ and } \ \widehat{\mathrm{FDP}}_{\lambda, \widetilde{\mathcal{S}}_m}\left(0, t_2^\star\right) < q,$$

which implies that $(\tilde{t}_1^{\star}, \tilde{t}_2^{\star})$ satisfies $|\tilde{t}_1^{\star}| \leq t_1^{\star}$ and $|\tilde{t}_2^{\star}| \leq t_2^{\star}$. Thus, we get

$$\widehat{\text{FDP}}_{\lambda,\widetilde{S}_{m}}\left(\widetilde{t}_{1}^{\star},\widetilde{t}_{2}^{\star}\right) - \frac{\widehat{V}_{m}\left(\widetilde{t}_{1}^{\star},\widetilde{t}_{2}^{\star}\right)}{\widehat{V}_{m}\left(\widetilde{t}_{1}^{\star},\widetilde{t}_{2}^{\star}\right) + \widehat{S}_{m}\left(\widetilde{t}_{1}^{\star},\widetilde{t}_{2}^{\star}\right)}$$

$$\geq \inf_{|t_{1}|\leq t_{1}^{\star},|t_{2}|\leq t_{2}^{\star}} \left\{\widehat{\text{FDP}}_{\lambda,\widetilde{S}_{m}}\left(t_{1},t_{2}\right) - \frac{\widehat{V}_{m}\left(t_{1},t_{2}\right)}{\widehat{V}_{m}\left(t_{1},t_{2}\right) + \widehat{S}_{m}\left(t_{1},t_{2}\right)}\right\}.$$
(S.7)

Rearranging the second formula, we obtain

$$\begin{split} &\inf_{|t_{1}| \leq t_{1}^{\star}, |t_{2}| \leq t_{2}^{\star}} \left\{ \widehat{\text{FDP}}_{\lambda, \widetilde{\mathcal{S}}_{m}}\left(t_{1}, t_{2}\right) - \frac{\widehat{V}_{m}\left(t_{1}, t_{2}\right)}{\widehat{V}_{m}\left(t_{1}, t_{2}\right) + \widehat{S}_{m}\left(t_{1}, t_{2}\right)} \right\} \\ &= \inf_{|t_{1}| \leq t_{1}^{\star}, |t_{2}| \leq t_{2}^{\star}} \left\{ \widehat{\text{FDP}}_{\lambda, \widetilde{\mathcal{S}}_{m}}\left(t_{1}, t_{2}\right) - \text{FDP}_{\lambda}^{\infty}\left(t_{1}, t_{2}\right) + \frac{\pi_{0}K_{0}\left(t_{1}, t_{2}\right)}{K\left(t_{1}, t_{2}\right)} \\ &- \frac{\widehat{V}_{m}\left(t_{1}, t_{2}\right)}{\widehat{V}_{m}\left(t_{1}, t_{2}\right) + \widehat{S}_{m}\left(t_{1}, t_{2}\right)} + \text{FDP}_{\lambda}^{\infty}\left(t_{1}, t_{2}\right) - \frac{\pi_{0}K_{0}\left(t_{1}, t_{2}\right)}{K\left(t_{1}, t_{2}\right)} \right\}, \end{split}$$

which converges in probability to

$$\inf_{|t_{1}| \leq t_{1}^{\star}, |t_{2}| \leq t_{2}^{\star}} \left\{ \operatorname{FDP}_{\lambda}^{\infty}\left(t_{1}, t_{2}\right) - \frac{\pi_{0} K_{0}\left(t_{1}, t_{2}\right)}{K\left(t_{1}, t_{2}\right)} \right\}$$

according to (S.4) and (S.5). As

$$-1 \leq \inf_{|t_1| \leq t_1^{\star}, |t_2| \leq t_2^{\star}} \left\{ \widehat{\text{FDP}}_{\lambda, \widetilde{\mathcal{S}}_m} \left(t_1, t_2 \right) - \frac{\widehat{V}_m \left(t_1, t_2 \right)}{\widehat{V}_m \left(t_1, t_2 \right) + \widehat{S}_m \left(t_1, t_2 \right)} \right\} \leq \widehat{\text{FDP}}_{\lambda, \widetilde{\mathcal{S}}_m} \left(\widetilde{t}_1^{\star}, \widetilde{t}_2^{\star} \right) \leq q,$$

the Lebesgues's dominated convergence theorem implies

$$\lim_{m \to \infty} \inf \mathbb{E} \left[\inf_{|t_1| \le t_1^{\star}, |t_2| \le t_2^{\star}} \left\{ \widehat{\text{FDP}}_{\lambda, \widetilde{\mathcal{S}}_m} \left(t_1, t_2 \right) - \frac{\widehat{V}_m \left(t_1, t_2 \right)}{\widehat{V}_m \left(t_1, t_2 \right) + \widehat{S}_m \left(t_1, t_2 \right)} \right\} \right]$$

$$= \inf_{|t_{1}| \leq t_{1}^{\star}, |t_{2}| \leq t_{2}^{\star}} \left\{ \text{FDP}_{\lambda}^{\infty}\left(t_{1}, t_{2}\right) - \frac{\pi_{0} K_{0}\left(t_{1}, t_{2}\right)}{K\left(t_{1}, t_{2}\right)} \right\} \geq 0,$$

where the last inequality stands due to the fact that $F(\lambda)/\Phi(\lambda) \ge \pi_0$ as indicated by (15) of the main paper. It then yields that

$$\lim_{m \to \infty} \inf \mathbb{E} \left[\widehat{\text{FDP}}_{\lambda, \widetilde{\mathcal{S}}_{m}} \left(\widetilde{t}_{1}^{\star}, \widetilde{t}_{2}^{\star} \right) - \frac{\widehat{V}_{m} \left(\widetilde{t}_{1}^{\star}, \widetilde{t}_{2}^{\star} \right)}{\widehat{V}_{m} \left(\widetilde{t}_{1}^{\star}, \widetilde{t}_{2}^{\star} \right) + \widehat{S}_{m} \left(\widetilde{t}_{1}^{\star}, \widetilde{t}_{2}^{\star} \right)} \right] \\
\geq \lim_{m \to \infty} \inf \mathbb{E} \left[\inf_{|t_{1}| \leq t_{1}^{\star}, |t_{2}| \leq t_{2}^{\star}} \left\{ \widehat{\text{FDP}}_{\lambda, \widetilde{\mathcal{S}}_{m}} \left(t_{1}, t_{2} \right) - \frac{\widehat{V}_{m} \left(t_{1}, t_{2} \right)}{\widehat{V}_{m} \left(t_{1}, t_{2} \right) + \widehat{S}_{m} \left(t_{1}, t_{2} \right)} \right\} \right] \\
= \inf_{|t_{1}| \leq t_{1}^{\star}, |t_{2}| \leq t_{2}^{\star}} \left\{ \widehat{\text{FDP}}_{\lambda}^{\infty} \left(t_{1}, t_{2} \right) - \frac{\pi_{0} K_{0} \left(t_{1}, t_{2} \right)}{K \left(t_{1}, t_{2} \right)} \right\} \geq 0,$$

where the first inequality holds because of (S.7) and the monotonicity of expectation. Finally, we obtain

$$\limsup_{m \to \infty} \widetilde{\mathrm{FDR}}_m \le \liminf_{m \to \infty} \mathbb{E} \left\{ \widehat{\mathrm{FDP}}_{\lambda, \widetilde{\mathcal{S}}_m} \left(\widetilde{t}_1^{\star}, \widetilde{t}_2^{\star} \right) \right\} \le q,$$

which completes the proof.

S.III Proofs of Lemmas S.1 and S.2

In this section, we prove Lemmas S.1 and S.2 with the help from some preliminary lemmas. In particular, Section S.III.1 presents the logic flow why the proposed estimator $\widehat{G}_{\tilde{m}}$ is able to estimate the true prior distribution of the signal process $\xi(s)$ by introducing multiple intermediate variants. Section S.III.2 states some preliminary lemmas for proving Lemma S.1. In Section S.III.3, we complete the proofs of Lemmas S.1 and S.2.

S.III.1 Notation and Proof Sketch of Lemma S.1

To better present the proof of Lemma S.1, this section briefly introduces some notation and intermediate quantities to connect the proposed general maximum likelihood estimator (GMLE) with the true G_0 . To begin with, we present a fact of GMLE that is useful in the following proof. There exists a discrete solution to (4) of the main paper with no more than $|\tilde{S}| + 1$ support points by the Carathéodory's theorem. Specifically, we can write the solution as

$$\widetilde{G}_{\widetilde{S}}(u) = \sum_{i=1}^{\widetilde{l}} \widetilde{\pi}_i \mathbf{1} \{ \widetilde{v}_i \le u \}, \quad \sum_{i=1}^{\widetilde{l}} \widetilde{\pi}_i = 1, \text{ and } \widetilde{\pi}_i > 0,$$
 (S.8)

where $\{\widetilde{v}_i\}_{i=1}^{\widetilde{l}}$ is the set of support points and $\widetilde{l} \leq |\widetilde{\mathcal{S}}| + 1$. The support of $\widetilde{G}_{\widetilde{\mathcal{S}}}$ is within the range of $\{T_1(s): s \in \widetilde{\mathcal{S}}\}$ due to the monotonicity of $\phi(x-u)$ in |x-u|, where $\phi(x)$ is the density of standard normal distribution.

Now recall from (11) of the main paper that

$$T_1^*(s;r) = \mathbb{E}\left[T_1(s) \mid \mathfrak{F}\left\{ \cup_{v \in \mathcal{N}(s)} B(v;r) \right\} \right] / \zeta_r(s),$$

where $\zeta_r^2(s) = \text{var}\left(\mathbb{E}\left[T_1(s) \mid \mathfrak{F}\left\{\cup_{v \in \mathcal{N}(s)} B(v;r)\right\}\right]\right)$. We call $\zeta_r(s)$ the normalization term since it ensures $\text{var}\{T_1^*(s;r)\} = 1$. It can be directly shown that under Assumption 5, $\{T_1^*(s;r) : s \in \widetilde{\mathcal{S}}_m\}$ are independent and normally distributed random variables with unit variance, provided that (12) of the main paper is satisfied for the subset $\widetilde{\mathcal{S}}_m$. This result fulfills the commonly-used independence assumption in the theory of nonparametric empirical Bayes (NPEB); see Zhang (2009); Jiang and Zhang (2009) for details. We will prove that $T_1^*(s;r)$ and $\widehat{T}_1(s)$ used in our implementation are close by using the near epoch dependency (NED, Assumption 4 of the main paper), the consistency of variance (i.e., showing $\widehat{\tau}(s) \to \tau(s)$), and the convergence of the normalization term (i.e., showing $\zeta_r(s) \to 1$). More precisely, we will show that $\widehat{T}_1(s)$ and $T_1^*(s;r)$ are close to each other through the following approximations:

$$\widehat{T}_1(s) \approx T_1(s) \approx T_1(s;r) \approx T_1^*(s;r),$$

where $T_1(s)$ is defined in (2) of the main paper (the auxiliary statistics with true variance); and $T_1(s;r) = T_1(s)/\zeta_r(s)$ is an intermediate variant involving the normalization term $\zeta_r(s)$ defined above. The difference between $T_1(s)$ and $\widehat{T}_1(s)$ lies on whether the normalization term is the true standard deviation of $\sum_{v \in \mathcal{N}(s)} X(v)$ or its estimate. As for $T_1(s)$ and $T_1(s;r)$, they again differ by the normalization terms $(\tau(s))$ versus $\zeta_r(s)$. The difference between $T_1(s;r)$ and its conditional version $T_1^*(s;r)$ is controlled by NED. The following intermediate quantities are the corresponding GMLEs based on $\widehat{T}_1(s)$, $T_1(s;r)$, and $T_1^*(s;r)$:

• The GMLE based on $\{\widehat{T}_1(s), s \in \widetilde{\mathcal{S}}_m\}$ is denoted as

$$\widehat{G}_{\tilde{m}}(u) = \sum_{i=1}^{\widehat{l}} \widehat{\pi}_i \mathbf{1} \left\{ \widehat{v}_i \le u \right\},\,$$

where $|\widehat{v}_i| \leq \sup_{s \in \widetilde{\mathcal{S}}_m} |\widehat{T}_1(s)|, \ \widehat{l} \leq \widetilde{m} + 1, \ \sum_{i=1}^{\widehat{l}} \widehat{\pi}_i = 1, \text{ and } \widehat{\pi}_i > 0;$

• The GMLE based on $\{T_1(s;r):s\in\widetilde{\mathcal{S}}_m\}$ is denoted as

$$\widetilde{G}_{\widetilde{m},r}(u) = \sum_{i=1}^{\widetilde{l}} \widetilde{\pi}_i \mathbf{1} \left\{ \widetilde{v}_i \leq u \right\},$$

where $|\widetilde{v}_i| \leq \sup_{s \in \widetilde{\mathcal{S}}_m} |T_1(s;r)|, \ \widetilde{l} \leq \widetilde{m} + 1, \ \sum_{i=1}^{\widetilde{l}} \widetilde{\pi}_i = 1, \ \text{and} \ \widetilde{\pi}_i > 0;$

• The GMLE based on $\{T_1^*(s;r):s\in\widetilde{\mathcal{S}}_m\}$ is denoted as

$$\widetilde{G}_{\tilde{m},r}^*(u) = \sum_{i=1}^{\widetilde{l}^*} \widetilde{\pi}_i^* \mathbf{1} \left\{ \widetilde{v}_i^* \le u \right\},\,$$

where $|\widetilde{v}_i^*| \leq \sup_{s \in \widetilde{S}_m} |T_1^*(s;r)|$, $\widetilde{l}^* \leq \widetilde{m} + 1$, $\sum_{i=1}^{\widetilde{l}^*} \widetilde{\pi}_i^* = 1$, and $\widetilde{\pi}_i^* > 0$.

Here we suppress the dependence of $\widetilde{\pi}_i$, \widetilde{v}_i , $\widetilde{\pi}_i^*$, and \widetilde{v}_i^* on r to simplify the presentation. We now describe the key idea and steps for proving Lemma S.1 as visualized in Figure S.11.

The key idea is to prove that $\widehat{G}_{\tilde{m}}$ converges to G_0 in terms of the Hellinger distance when the subset $\widetilde{\mathcal{S}}_m$ satisfies (12) of the main paper. The details will be shown in Lemma S.8. To arrive at this result, we need the following steps. On the one hand, (iv) and (v) in Figure S.11 state that $\widehat{G}_{\tilde{m}}$ approximates

$$G_{\tilde{m},r}(u) = \frac{1}{\tilde{m}} \sum_{s \in \tilde{S}_m} \mathbf{1}\{\xi(s)/\zeta_r(s) \le u\},\tag{S.9}$$

with high accuracy (see Lemmas S.5 and S.6). On the other hand, (vi) in Figure S.11 states that $G_{\tilde{m},r}(u)$ approaches

$$G_{\tilde{m}}(u) = \frac{1}{\tilde{m}} \sum_{s \in \tilde{\mathcal{S}}_m} \mathbf{1}\{\xi(s) \le u\}$$

by showing that $\zeta_r(s)$ tends to 1 as $r \to \infty$ (see Lemma S.3). Together with Assumption 8(b) of the main paper, $G_{\tilde{m},r}(u)$ converges to $G_0(u)$ as $\tilde{m} \to \infty$, which will be shown in Lemma S.7. The detailed statements of Lemmas S.3–S.8 are presented in the next subsection.

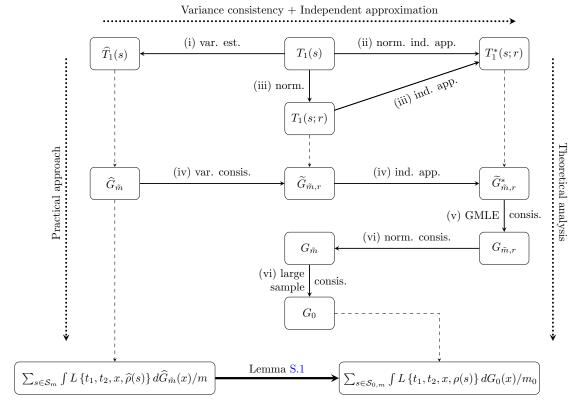


Figure S.11: The diagram of proving Lemma S.1 using the intermediate variants. The overall strategies are: (i) replacing the unknown variance with the true variance $\tau(s)$; (ii) replacing the correlated auxiliary statistics with its normalized independent approximation; (iii) analyzing the normalized independent approximation by its normalization term and independent approximation term; (iv) showing GMLE estimated from different sources are close; (v) showing GMLE $\widetilde{G}_{m,r}^*$ estimated from $T_1^*(s;r)$ converges to $G_{m,r}$; and (vi) proving that $G_{m,r}$ approaches G_0 by showing $\zeta_r(s) \to 1$ and the large sample consistency. Lemma S.1 establishes the convergence using the above strategies. Here var., est., norm., ind., app., and consis. are abbreviations for "variance", "estimation", "normalization", "independently", "approximation" and "consistency" respectively.

S.III.2 Some Preliminary Lemmas

Following the proof sketch in Section S.III.1, we now introduce some preliminary lemmas. These lemmas are in accordance with the strategies depicted in Figure S.11. In particular, Lemmas S.3 to S.5 focus on a series of properties derived from NED and the consistency of variance. Lemma S.6 provides a large deviation inequality that gives the convergence rate of $\hat{G}_{\tilde{m}}$ to $G_{\tilde{m},r}$ as defined in (S.9). Lemmas S.7 and S.8 show that $d_H(f_{\hat{G}_{\tilde{m}}}, f_{G_0}) = o_{\mathbb{P}}(1)$, which is an important step in the proof of Lemma S.1. The relations among Theorem 1 of the main paper and Lemmas S.1–S.8 are depicted in Figure S.12.

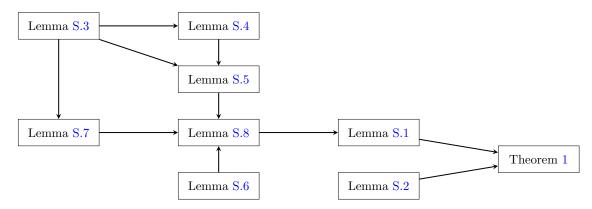


Figure S.12: The relations among Lemmas S.1–S.8 and Theorem 1.

Now, we start to present Lemmas S.3–S.8.

Lemma S.3 (Convergence of $\hat{\tau}^2(s)$). Under Assumptions 1–5, we have

- (a) $|\zeta_r^2(s) 1| \le C\psi^2(r)$ and $|1/\zeta_r^2(s) 1| \le C\psi^2(r)$ uniformly for large enough r. (b) $\sup_{s \in \tilde{\mathcal{S}}_m} |\widehat{\tau}^2(s)/\tau_r^2(s) 1| \le C\psi^2(r) + C\tilde{m}^{-q}$ uniformly for large enough r with probability tending to one as $\tilde{m} \to \infty$.
- (c) $\sup_{m} \sup_{s \in \widetilde{\mathcal{S}}_m} \eta(s; r)$ is uniformly bounded for large enough r.

Remark S.1. According to the definition of NED (see Definition 1 of the main paper), Lemma S.3(a) implies that $\zeta_r(s) \to 1$ as $r \to \infty$. It further implies

$$\sup_{s \in \mathcal{S}_m} \mathbb{E} \left\{ T_1^*(s;r) \right\}^2 = 1 + \sup_{s \in \mathcal{S}_m} \left[\mathbb{E} \left\{ T_1^*(s;r) \right\} \right]^2 \le 1 + \sup_{s \in \mathcal{S}_m} \nu_0^2 / \zeta_r^2(s) \le 1 + 2\nu_0^2 \stackrel{\triangle}{=} \nu_1^2 \quad (S.10)$$

due to Assumption 8(a) and the unit variance of $T_1^*(s;r)$ as defined in (11) of the main paper. As for Lemma S.3(b), we note that

$$\frac{\sup_{s \in \tilde{\mathcal{S}}_m} |\hat{\tau}^2(s)/\tau_r^2(s) - 1|}{1 - \sup_{s \in \tilde{\mathcal{S}}_m} |\hat{\tau}^2(s)/\tau_r^2(s) - 1|} \le \{C\psi^2(r) + C\tilde{m}^{-q}\}/[1 - \{C\psi^2(r) + C\tilde{m}^{-q}\}]
\le C\psi^2(r) + C\tilde{m}^{-q}$$
(S.11)

with high probability when r and \tilde{m} are large. Both (S.11) and (S.10) will be useful in our theoretical analysis.

Lemma S.4. Under Assumptions 1–5 and 8(a), for \tilde{m} large enough and any $\delta_1, \delta_2 > 0$, with probability at least

$$1 - \tilde{m} \exp(-\nu_1^2 \delta_1^2 / 2) - C \tilde{m} \psi^p(r) / \nu_1^p \delta_1^p - C \psi^p(r) / \delta_2^p, \tag{S.12}$$

the following events occur simultaneously.

(a)

$$\sup_{s \in \widetilde{\mathcal{S}}_m} |T_1^*(s;r)| \le \nu_1(1+\delta_1) \quad and \quad \sup_{s \in \widetilde{\mathcal{S}}_m} |T_1(s;r)| \le \nu_1(1+2\delta_1).$$

(b)

$$\tilde{m}^{-1} \sum_{s \in \tilde{\mathcal{S}}_m} |T_1(s;r) - T_1^*(s;r)| \le \delta_2 \quad and \quad \tilde{m}^{-1} \left| \sum_{s \in \tilde{\mathcal{S}}_m} T_1^2(s;r) - \left\{ T_1^*(s;r) \right\}^2 \right| \le \nu_1 \delta_2(2 + 3\delta_1).$$

(c)
$$\tilde{m}^{-1} \sum_{s \in \tilde{S}} |T_1(s; r)| \le \nu_1 (1 + \delta_1) + \delta_2,$$

and

$$\tilde{m}^{-1} \sum_{s \in \tilde{\mathcal{S}}_m} T_1^2(s; r) \le \nu_1^2 + \nu_1 \delta_2(2 + 3\delta_1) + \nu_1^2 \delta_1(2 + \delta_1).$$

Remark S.2. The three tail probabilities in (S.12) respectively correspond to the events of $\sup_{s \in \widetilde{\mathcal{S}}_m} |T_1^*(s;r) - \mathbb{E}\{T_1^*(s;r)\}| \leq \nu_1 \delta_1$, $\sup_{s \in \widetilde{\mathcal{S}}_m} |T_1^*(s;r) - T_1(s;r)| \leq \nu_1 \delta_1$, and $\tilde{m}^{-1} \sum_{s \in \widetilde{\mathcal{S}}_m} |T_1(s;r) - T_1^*(s;r)| \leq \delta_2$. In the proof, we will show that these events imply the upper bounds in (a)–(c) of Lemma S.4.

Lemma S.5. Under Assumptions 1–5 and 8(a), with probability at least (S.12), the difference of generalized log-likelihood

$$\frac{1}{\tilde{m}} \left| \sum_{s \in \tilde{S}_{m}} \log \left[\frac{f_{\tilde{G}_{\tilde{m},r}^{*}} \{T_{1}(s;r)\}}{f_{\tilde{G}_{\tilde{m},r}^{*}} \{T_{1}^{*}(s;r)\}} \frac{f_{\tilde{G}_{\tilde{m},r}} \{\hat{T}_{1}(s)\}}{f_{\tilde{G}_{\tilde{m},r}} \{T_{1}(s;r)\}} \frac{f_{\hat{G}_{\tilde{m}}} \{T_{1}^{*}(s;r)\}}{f_{\hat{G}_{\tilde{m}}} \{T_{1}(s;r)\}} \frac{f_{\hat{G}_{\tilde{m}}} \{T_{1}(s;r)\}}{f_{\hat{G}_{\tilde{m}}} \{\hat{T}_{1}(s)\}} \right] \right|$$
 (S.13)

is upper bounded by

$$C\nu_1^2 \left\{ \psi^2(r) + \tilde{m}^{-q} \right\} (1 + \delta_1^2) + C\nu_1\delta_2 (1 + \delta_1).$$

Lemma S.6. Under Assumptions 2, 5, and 8(a), conditioning on $\mathbb{E}|T_1^*(s;r)| \leq \nu_1$, if $\widehat{G}_{\tilde{m}}$ satisfies

$$\prod_{s \in \widetilde{S}} \left[\frac{f_{\widehat{G}_{\tilde{m}}} \left\{ T_1^*(s; r) \right\}}{f_{G_{\tilde{m},r}} \left\{ T_1^*(s; r) \right\}} \right] \ge e^{-2t^2 \tilde{m} c_{\tilde{m}}^2 / 15}, \tag{S.14}$$

where

$$c_{\tilde{m}} = \sqrt{\frac{\log(\tilde{m})}{\tilde{m}}} \left\{ \tilde{m}^{1/b} \sqrt{\log \tilde{m}} \left(1 \vee \nu_1 \right) \right\}^{b/(2+2b)}$$
(S.15)

for some b > 0, then there exists a universal constant t^* such that for all $t \ge t^*$ and $\log \tilde{m} \ge 2/b$,

$$\mathbb{P}\left\{d_H\left(f_{\widehat{G}_{\tilde{m}}}, f_{G_{\tilde{m},r}}\right) \ge tc_{\tilde{m}}\right\} \le \exp\left\{-\frac{t^2 \tilde{m} c_{\tilde{m}}^2}{2\log \tilde{m}}\right\} \le e^{-t^2 \log \tilde{m}}.$$

Lemma S.6 is a direct consequence of Theorem 1 in Zhang (2009). It states that $d_H(f_{\widehat{G}_{\tilde{m}}}, f_{G_{\tilde{m},r}})$ would be small enough, as long as the generalized likelihood is nearly maximized in the sense of (S.14). This result together with Lemma S.5 allows us to replace $T_1^*(s;r)$ with $\widehat{T}_1(s)$ in estimating $G_{\tilde{m},r}$.

Lemma S.7. Under Assumptions 1–5, and 8, for $\tilde{m} \to \infty$ and arbitrary $\delta_3 > 0$, we have $d_H(f_{G_{\tilde{m}}r}, f_{G_0}) \leq C\nu_1^{1/2}\psi(r) + \delta_3$,

with probability tending to one.

Lemma S.8. Under Assumptions 1–6 and 8, the GMLE based on $\{\widehat{T}_1(s), s \in \widetilde{\mathcal{S}}_m\}$ satisfies $d_H\left(f_{\widehat{G}_{\bar{m}}}, f_{G_0}\right) = o_{\mathbb{P}}(1)$ as $m \to \infty$.

Lemma S.8 is a consequence of Lemmas S.5–S.7. Its proof uses the convergence result of $d_H(f_{G_{\tilde{m},r}}, f_{G_0})$ in Lemma S.7, and shows the convergence rate in Lemma S.5 is fast enough to ensure that $\widehat{G}_{\tilde{m}}$ is an approximate GMLE of $G_{\tilde{m},r}$ and the condition in Lemma S.6 is fulfilled.

S.III.3 Detailed Proofs of Lemmas S.1 and S.2

In this subsection, we complete the proofs of Lemmas S.1 and S.2 using Lemmas S.3–S.8.

Proof of Lemma S.1. According to (14) of the main paper, it is equivalent to showing

$$\sup_{|t_{1}| \leq t'_{1}, |t_{2}| \leq t'_{2}} \left| \frac{1}{m} \sum_{s \in \mathcal{S}_{m}} \left[\int L\left\{t_{1}, t_{2}, x, \widehat{\rho}(s)\right\} d\widehat{G}_{\tilde{m}}(x) - \int L\left\{t_{1}, t_{2}, x, \rho(s)\right\} dG_{0}(x) \right] \right| = o_{\mathbb{P}}(1),$$
(S.16)

as $m \to \infty$. Due to the triangular inequality, the LHS of (S.16) can be written as

$$\left| \frac{1}{m} \sum_{s \in \mathcal{S}_{m}} \left\{ \int L\left\{t_{1}, t_{2}, x, \widehat{\rho}(s)\right\} d\widehat{G}_{\tilde{m}}(x) - \int L\left\{t_{1}, t_{2}, x, \rho(s)\right\} dG_{0}(x) \right\} \right|$$

$$\leq \left| \frac{1}{m} \sum_{s \in \mathcal{S}_{m}} \int \left[L\left\{t_{1}, t_{2}, x, \widehat{\rho}(s)\right\} - L\left\{t_{1}, t_{2}, x, \rho(s)\right\}\right] d\widehat{G}_{\tilde{m}}(x) \right|$$

$$+ \left| \frac{1}{m} \sum_{s \in \mathcal{S}_{m}} \int L\left\{t_{1}, t_{2}, x, \rho(s)\right\} \left\{d\widehat{G}_{\tilde{m}}(x) - dG_{0}(x)\right\} \right|.$$

Thus, we only need to prove

$$\sup_{|t_1| \le t_1', |t_2| \le t_2'} \left| \frac{1}{m} \sum_{s \in \mathcal{S}_m} \int \left[L\left\{ t_1, t_2, x, \widehat{\rho}(s) \right\} - L\left\{ t_1, t_2, x, \rho(s) \right\} \right] d\widehat{G}_{\tilde{m}}(x) \right| = o_{\mathbb{P}}(1) \quad (S.17)$$

and

$$\sup_{|t_1| \le t_1', |t_2| \le t_2'} \left| \frac{1}{m} \sum_{s \in \mathcal{S}_m} \int L\left\{ t_1, t_2, x, \rho(s) \right\} \left\{ d\widehat{G}_{\tilde{m}}(x) - dG_0(x) \right\} \right| = o_{\mathbb{P}}(1). \tag{S.18}$$

To simplify our presentation, we will prove (S.17) and (S.18) under the condition that $L(t_1, t_2, x, c)$ is uniformly continuous over $\mathbb{R}^3 \times [-1, 1]$. The justification of the uniform continuity of $L(t_1, t_2, x, c)$ is given later.

(i) Now, we prove (S.17) with the uniform continuity of $L(t_1, t_2, x, c)$. For an arbitrary $\epsilon > 0$, there exists $0 < \delta < 2$ such that

$$\sup_{(t_1, t_2, x) \in \mathbb{R}^3} |L(t_1, t_2, x, c_1) - L(t_1, t_2, x, c_2)| < \epsilon, \tag{S.19}$$

for any $c_1, c_2 \in [-1, 1]$ satisfying $|c_1 - c_2| < \delta$. Thus, we have

$$\sup_{(t_1,t_2,x)\in\mathbb{R}^3} \int |L\left(t_1,t_2,x,c_1\right) - L\left(t_1,t_2,x,c_2\right)| \, d\widehat{G}_{\tilde{m}}(x) < \epsilon.$$

It further implies that

$$\mathbb{P}\left(\left|\frac{1}{m}\sum_{s\in\mathcal{S}_m}\int\left[L\left\{t_1,t_2,x,\widehat{\rho}(s)\right\}-L\left\{t_1,t_2,x,\rho(s)\right\}\right]d\widehat{G}_{\tilde{m}}(x)\right|>\epsilon\right)$$

$$\leq \mathbb{P}\left\{\frac{1}{m}\sum_{s\in\mathcal{S}_m}\int |L\left\{t_1,t_2,x,\widehat{\rho}(s)\right\} - L\left\{t_1,t_2,x,\rho(s)\right\}|d\widehat{G}_{\tilde{m}}(x) > \epsilon; \sup_{s\in\mathcal{S}_m}|\rho(s) - \widehat{\rho}(s)| < \delta\right\} \\ + \mathbb{P}\left\{\sup_{s\in\mathcal{S}_m}|\rho(s) - \widehat{\rho}(s)| > \delta\right\} \\ = \mathbb{P}\left\{\sup_{s\in\mathcal{S}_m}|\rho(s) - \widehat{\rho}(s)| > \delta\right\} \to 0,$$

where the convergence in the last step is due to Assumptions 2 and 3(b).

(ii) To prove (S.18), it is sufficient to show that

$$\sup_{|t_1| \le t_1', |t_2| \le t_2'} \sup_{c \in [-1, 1]} \left| \int L(t_1, t_2, x, c) \left\{ d\widehat{G}_{\tilde{m}}(x) - dG_0(x) \right\} \right| = o_{\mathbb{P}}(1). \tag{S.20}$$

To show (S.20), we note that the following pointwise convergence,

$$\int L(t_1, t_2, x, c) \left\{ d\hat{G}_{\tilde{m}}(x) - dG_0(x) \right\} = o_{\mathbb{P}}(1), \tag{S.21}$$

can directly obtained according to the proof of (44) in Yi et al. (2021) when (t_1, t_2, c) is fixed. For any $\epsilon > 0$, we can split $[-t'_1, t'_1] \times [-t'_2, t'_2] \times [-1, 1]$ into B disjoint finite sets $\bigcup_{1 \le k \le B} C_k$ such that

$$\sup_{\substack{(t_1,t_2,c),(\tilde{t}_1,\tilde{t}_2,\tilde{c})\in\mathcal{C}_k}} \left| \int \left\{ L\left(t_1,t_2,x,c\right) - L\left(\tilde{t}_1,\tilde{t}_2,x,\tilde{c}\right) \right\} dG_0(x) \right| \leq \epsilon/2,$$

$$\sup_{\substack{(t_1,t_2,c),(\tilde{t}_1,\tilde{t}_2,\tilde{c})\in\mathcal{C}_k}} \left| \int \left\{ L\left(t_1,t_2,x,c\right) - L\left(\tilde{t}_1,\tilde{t}_2,x,\tilde{c}\right) \right\} d\widehat{G}_{\tilde{m}}(x) \right| \leq \epsilon/2,$$

according to the uniform continuity of $L(t_1, t_2, x, c)$. Fixing $(t_1^k, t_2^k, c^k) \in \mathcal{C}_k, 1 \leq k \leq B$, we have

$$\begin{split} \sup_{|t_1| \leq t_1', |t_2| \leq t_2'} \sup_{c \in [-1, 1]} \left| \int L\left(t_1, t_2, x, c\right) \left\{ d\widehat{G}_{\tilde{m}}(x) - dG_0(x) \right\} \right| \\ &= \sup_{(t_1, t_2, c) \in \cup_{1 \leq k \leq B} C_k} \left| \int L\left(t_1, t_2, x, c\right) \left\{ d\widehat{G}_{\tilde{m}}(x) - dG_0(x) \right\} \right| \\ &\leq \max_{1 \leq k \leq B} \sup_{(t_1, t_2, c) \in C_k} \left| \int L\left(t_1, t_2, x, c\right) - L\left(t_1^k, t_2^k, x, c^k\right) dG_0(x) \right| \\ &+ \max_{1 \leq k \leq B} \sup_{(t_1, t_2, c) \in C_k} \left| \int L\left(t_1, t_2, x, c\right) - L\left(t_1^k, t_2^k, x, c^k\right) d\widehat{G}_{\tilde{m}}(x) \right| \\ &+ \max_{1 \leq k \leq B} \left| \int L\left(t_1^k, t_2^k, x, c^k\right) \left\{ d\widehat{G}_{\tilde{m}}(x) - dG_0(x) \right\} \right| \\ &\leq \epsilon + \max_{1 \leq k \leq B} \left| \int L\left(t_1^k, t_2^k, x, c^k\right) \left\{ d\widehat{G}_{\tilde{m}}(x) - dG_0(x) \right\} \right|. \end{split}$$

Due to the pointwise convergence of (S.21) and the arbitrariness of $\epsilon > 0$, the uniform convergence of (S.20) stands from the above displayed inequality. Finally, the definition of $K_0(t_1, t_2)$ in Assumption 9 together with (S.16) implies the conclusion of Lemma S.1.

We now justify the uniform continuity to complete the proof of Lemma S.1. We first prove $L(t_1, t_2, x, c)$ is uniformly continuous over $\mathbb{R}^3 \times [-1 + \delta_{\rho}, 1 - \delta_{\rho}]$ for any $0 < \delta_{\rho} < 1$. Denote by f(u, v; c) the bivariate normal density with mean zero, variance one and correlation $c \in (-1, 1)$. Then we have

$$L(t_1, t_2, x, c) = \int_{t_2 - x}^{\infty} \int_{t_1}^{\infty} f(u, v; c) dv du$$

=
$$\int_{t_2 - x}^{\infty} du \int_{t_1}^{\infty} \frac{1}{2\pi \sqrt{(1 - c^2)}} \exp\left\{-\frac{u^2 - 2cuv + v^2}{2(1 - c^2)}\right\} dv.$$

Next, we prove that given δ_{ρ} , M > 0, c_1 and c_2 such that $|c_1 - c_2| < \delta$ and $0 < \delta < 2 - 2\delta_{\rho}$, the following inequalities hold

$$\sup_{(t_{1},t_{2},x)\in\mathbb{R}^{3};-1+\delta_{\rho}\leq c_{1},c_{2}\leq 1-\delta_{\rho}} |L(t_{1},t_{2},x,c_{1})-L(t_{1},t_{2},x,c_{2})|$$

$$\leq \sup_{-1+\delta_{\rho}\leq c_{1},c_{2}\leq 1-\delta_{\rho}} \int_{-\infty}^{\infty} \int_{-\infty}^{\infty} |f(u,v;c_{1})-f(u,v;c_{2})| dudv$$

$$\leq 8 \int_{M}^{\infty} \phi(u)du + \sup_{-1+\delta_{\rho}\leq c_{1},c_{2}\leq 1-\delta_{\rho}} \int_{-M}^{M} \int_{-M}^{M} \left|\frac{\partial f(u,v;c)}{\partial c}|_{c=\tilde{c}(c_{1},c_{2})}\right| |c_{1}-c_{2}| dudv$$

$$\leq 8 \int_{M}^{\infty} \phi(u)du + \delta \int_{-M}^{M} \int_{-M}^{M} \sup_{c\in[-1+\delta_{\rho},1-\delta_{\rho}]} \left|\frac{\partial f(u,v;c)}{\partial c}\right| dudv$$

$$\leq 8 \int_{M}^{\infty} \phi(u)du + \delta C(\delta_{\rho},M),$$

where the second inequality is achieved by covering $(-\infty, \infty)^2$ with five regions, namely $[-M, M]^2$, $(-\infty, -M) \times (-\infty, \infty)$, $(M, \infty) \times (-\infty, \infty)$, $(-\infty, \infty) \times (M, \infty)$ and $(-\infty, \infty) \times (-\infty, -M)$ and then applying the mean value theorem to the first region and using the fact $\int_{-\infty}^{\infty} f(u, v; c) dv = \phi(u)$ (and $\int_{-\infty}^{\infty} f(u, v; c) du = \phi(v)$) for the remaining four regions, and the last inequality stands because $\partial f(u, v; c)/\partial c$ is continuous and

$$C(M, \delta_{\rho}) = 4M^{2} \sup_{(u,v) \in [-M,M]^{2}, c \in [-1+\delta_{\rho}, 1-\delta_{\rho}]} \left| \frac{\partial f(u,v;c)}{\partial c} \right|$$

is a positive constant depending only on M and δ_{ρ} . For any $\epsilon>0$, we can choose M>0 large enough such that $8\int_{M}^{\infty}\phi(u)du<\epsilon/2$. We then take $\delta(M,\delta_{\rho})=\min\{2-2\delta_{\rho},\epsilon/2C(\delta_{\rho},M)\}>0$ to fulfill $|L(t_{1},t_{2},x,c_{1})-L(t_{1},t_{2},x,c_{2})|\leq\epsilon$ when $|c_{1}-c_{2}|<\delta(M,\delta_{\rho})$. We extend the uniform continuity for the correlation parameter c in $[-1+\delta_{\rho},1-\delta_{\rho}]$ to [-1,1]. To this end, it is sufficient to show that for any $\epsilon>0$, there exists $\delta_{\rho}>0$ such that

$$\sup_{\substack{(t_1,t_2,x)\in\mathbb{R}^3}} |L(t_1,t_2,x,1-\delta) - L(t_1,t_2,x,1)| \le \epsilon,$$

$$\sup_{\substack{(t_1,t_2,x)\in\mathbb{R}^3}} |L(t_1,t_2,x,-1+\delta) - L(t_1,t_2,x,-1)| \le \epsilon,$$

for any δ satisfying $0 < \delta \le \delta_{\rho}$. We present the proof of the first inequality above. The

proof for the second equality is similar and thus omitted. Letting $t_1 - x \le t_2$, we have

$$\begin{split} |L(t_1,t_2,x,1-\delta)-L(t_1,t_2,x,1)| &= |L(t_1,t_2,x,1-\delta)-\mathbb{P}(V_2(s)\geq t_2)|\\ &= |\mathbb{P}\left\{V_1(s)+x\geq t_1,V_2(s)\geq t_2\right\}-\mathbb{P}\left\{V_2(s)\geq t_2\right\}|\\ &= \mathbb{P}\left\{V_1(s)< t_1-x,V_2(s)\geq t_2\right\}\\ &< \mathbb{P}\left\{V_1(s)< V_2(s)\right\}, \end{split}$$

where $(V_1(s), V_2(s))$ follows a bivariate normal distribution with variance one and correlation $1 - \delta$. Similarly, when $t_1 - x > t_2$, we have

$$|L(t_1, t_2, x, 1 - \delta) - L(t_1, t_2, x, 1)| < \mathbb{P}\{V_1(s) > V_2(s)\},\$$

which implies

$$|L(t_1, t_2, x, 1 - \delta) - L(t_1, t_2, x, 1)| < \mathbb{P} \{V_1(s) \neq V_2(s)\}.$$

As $\mathbb{P}\{V_1(s) \neq V_2(s)\}$ as a function of the correlation δ is right continuous at $\delta = 0$, a proper $\delta_{\rho} > 0$ can always be selected. To sum up, we have verified the uniform continuity and the proof is thus completed.

Proof of Lemma S.2. To show the uniform convergence of $m_0^{-1}\widehat{V}_m(t_1,t_2)$ in (S.1), we begin with the pointwise convergence. In other words, we first show $|m_0^{-1}\widehat{V}_m(t_1,t_2) - K_0(t_1,t_2)| = o_{\mathbb{P}}(1)$ for any fixed (t_1,t_2) . It suffices to show that

$$\mathbb{P}\left\{m_0^{-1}\widehat{V}_m(t_1, t_2) \le K_0(t_1, t_2) + \delta_0\right\} \to 1$$
 (S.22)

and

$$\mathbb{P}\left\{m_0^{-1}\widehat{V}_m(t_1, t_2) \ge K_0(t_1, t_2) - \delta_0\right\} \to 1$$
 (S.23)

as $m \to \infty$.

We now focus on (S.22). Observe that

$$\widehat{V}_{m}(t_{1}, t_{2}) = \sum_{s \in S_{0,m}} \mathbf{1} \left\{ \widehat{T}_{1}(s) \geq t_{1}, \widehat{T}_{2}(s) \geq t_{2} \right\}$$

$$= \sum_{s \in S_{0,m}} \mathbf{1} \left\{ T_{1}(s) \geq \widehat{r}^{(1)}(s) t_{1}, T_{2}(s) \geq \widehat{r}^{(2)}(s) t_{2} \right\}$$

$$:= V_{m} \left(\widehat{\mathbf{r}}^{(1)} t_{1}, \widehat{\mathbf{r}}^{(2)} t_{2} \right),$$

where $\widehat{r}^{(1)}(s) = \widehat{\sigma}(s)/\sigma(s)$, $\widehat{r}^{(2)}(s) = \widehat{\tau}(s)/\tau(s)$ for $s \in \mathcal{S}_{0,m}$, and $\widehat{\mathbf{r}}^{(k)} = (\widehat{r}^{(k)}(s))_{s \in \mathcal{S}_{0,m}}$ for k = 1, 2. For an arbitrary $\delta > 0$, we define three events $\mathcal{A}_{k,\delta} = \{\sup_{s \in \mathcal{S}_{0,m}} |\widehat{r}^{(k)}(s) - 1| \le \delta \}$ for k = 1, 2, and

$$\mathcal{A}_{3,\delta}(t_1,t_2) = \left\{ \left| m_0^{-1} V_m(t_1,t_2) - K_0(t_1,t_2) \right| \le \delta \right\}.$$

It can be seen that $\mathbb{P}(\mathcal{A}_{k,\delta}) \to 1$ for k = 1, 2 due to Assumptions 2 and 3. Similarly, $\mathbb{P}\{\mathcal{A}_{3,\delta}(t_1,t_2)\} \to 1$ for any fixed $(t_1,t_2) \in \mathbb{R}^2$ as $m \to \infty$, because of Assumptions 2, 7, and 9. To verify (S.22), we notice that

$$\left\{ \frac{1}{m_0} \widehat{V}_m(t_1, t_2) \le K_0(t_1, t_2) + \delta_0 \right\}$$

$$\supseteq \left\{ \frac{1}{m_0} V_m \left(\widehat{\mathbf{r}}^{(1)} t_1, \widehat{\mathbf{r}}^{(2)} t_2 \right) \le K_0 \left(t_1, t_2 \right) + \delta_0 \right\} \cap \left(\mathcal{A}_{1,\delta} \cap \mathcal{A}_{2,\delta} \right) \\
\supseteq \left\{ \frac{1}{m_0} V_m \left(\widehat{\mathbf{r}}^{(1)} t_1, \widehat{\mathbf{r}}^{(2)} t_2 \right) \le \frac{1}{m_0} V_m \left((1 - \delta) t_1, (1 - \delta) t_2 \right) \right\} \cap \left(\mathcal{A}_{1,\delta} \cap \mathcal{A}_{2,\delta} \right) \\
\cap \left\{ \left| \frac{1}{m_0} V_m \left((1 - \delta) t_1, (1 - \delta) t_2 \right) - K_0 \left((1 - \delta) t_1, (1 - \delta) t_2 \right) \right| \le \delta_0 / 2 \right\} \\
\cap \left\{ \left| K_0 \left((1 - \delta) t_1, (1 - \delta) t_2 \right) - K_0 (t_1, t_2) \right| \le \delta_0 / 2 \right\} \\
\supseteq \left(\mathcal{A}_{1,\delta} \cap \mathcal{A}_{2,\delta} \right) \cap \mathcal{A}_{3,\delta_0/2} \left((1 - \delta) t_1, (1 - \delta) t_2 \right) \\
\cap \left\{ \left| K_0 \left((1 - \delta) t_1, (1 - \delta) t_2 \right) - K_0 (t_1, t_2) \right| \le \delta_0 / 2 \right\},$$

where the first inclusion is because of $\widehat{V}_m(t_1, t_2) = V_m(\widehat{\mathbf{r}}^{(1)}t_1, \widehat{\mathbf{r}}^{(2)}t_2)$; the second inclusion is due to the triangle inequality; as for the third inclusion, we used the fact that V_m is monotonically decreasing with respect (t_1, t_2) and

$$\left\{ \frac{1}{m_0} V_m \left(\widehat{\mathbf{r}}^{(1)} t_1, \widehat{\mathbf{r}}^{(2)} t_2 \right) \le \frac{1}{m_0} V_m \left((1 - \delta) t_1, (1 - \delta) t_2 \right) \right\}$$

holds true under $\mathcal{A}_{1,\delta} \cap \mathcal{A}_{2,\delta}$, and the definition of $\mathcal{A}_{3,\delta}$. Thus for an arbitrary $\delta_0 > 0$, we can choose $\delta > 0$ to guarantee

$$|K_0((1-\delta)t_1,(1-\delta)t_2)-K_0(t_1,t_2)| \leq \delta_0/2$$

because $K_0(t_1, t_2)$ is continuous, and (S.22) holds due to

$$\mathbb{P}\left(\mathcal{A}_{1,\delta} \cap \mathcal{A}_{2,\delta} \cap \mathcal{A}_{3,\delta_0/2}\left((1-\delta)t_1,(1-\delta)t_2\right)\right) \to 1.$$

For (S.23), it can be shown similarly and thus the pointwise convergence of $m_0^{-1}\widehat{V}_m(t_1,t_2)$ holds. The uniform convergence in (S.1) can be derived similarly as in the proof of Lemma S.1 after getting the pointwise convergence of $m_0^{-1}\widehat{V}_m(t_1,t_2)$. As for (S.2) and (S.3), these two results can be proved analogously as (S.1) and thus their proofs are omitted.

S.IV Proofs of Lemmas S.3–S.8

This section is organized as follows. Section S.IV.1 discusses how to choose a set $\widetilde{\mathcal{S}}_m$ used for NPEB such that Assumption 6 is satisfied. Section S.IV.2 presents the detailed proofs of Lemmas S.3–S.8.

S.IV.1 Justification of Assumption 6

Observe that $\{T_1^*(s;r): s \in \widetilde{\mathcal{S}}_m\}$ defined in (11) of the main paper are independent once (12) is fulfilled. Due to Assumptions 1 and 2, (12) holds as long as

$$\operatorname{dist}(s, s') \ge 2N_{nei}\Delta_u + 2r, \quad s, s' \in \widetilde{\mathcal{S}}_m. \tag{S.24}$$

It is because for any $w \in \bigcup_{v \in \mathcal{N}(s)} B(v; r)$, $\operatorname{dist}(s, w) \leq \operatorname{dist}(s, v) + \operatorname{dist}(v, w) \leq N_{nei} \Delta_u + r$, where we have used Assumption 2 that $\mathcal{N}(s)$ is the set of nearest neighbors with

uniformly bounded cardinality for each location s. With (S.24), r can be taken as large as $\widetilde{\Delta}_{l,m}/2 - N_{nei}\Delta_u$ to ensure the independence of $\{T_1^*(s;r): s \in \widetilde{\mathcal{S}}_m\}$, where $\widetilde{\Delta}_{l,m}$ is defined as in (13) of the main paper. In other words, r and $\widetilde{\Delta}_{l,m}$ are of the same order. We show that $\widetilde{\mathcal{S}}_m$ can be chosen such that

$$\tilde{m} = |\tilde{\mathcal{S}}_m| \times m/r^K.$$
 (S.25)

To this end, we pick all possible $s \in \mathcal{S}_m$ into $\widetilde{\mathcal{S}}_m$ which satisfies (S.24) for any $s' \in \widetilde{\mathcal{S}}_m$ until no more locations satisfy the condition. A typical choice is

$$\widetilde{\mathcal{S}}_{m} = \underset{\widetilde{\mathcal{S}}_{m} \in \widetilde{\mathcal{S}}_{m}}{\arg \max} |\widetilde{\mathcal{S}}_{m}| \quad \text{with} \quad \widetilde{\mathscr{S}}_{m} = \left\{ \widetilde{\mathcal{S}}_{m} \subset \mathcal{S}_{m} : \widetilde{\mathcal{S}}_{m} \text{ satisfies (S.24)} \right\}, \tag{S.26}$$

which can be viewed as the largest $2N_{nei}\Delta_u + 2r$ -packing, motivated by the definition of packing number (see e.g., Definition 5.4 of Wainwright, 2019). Borrowing the idea of volume comparison lemma, we construct m K-dimensional cubes centered at the locations in \mathcal{S}_m with the length $\Delta_l/2$, which are non-overlapping due to (S.24), and \tilde{m} K-dimensional cubes centered at the locations in $\tilde{\mathcal{S}}_m$ with the length $2(2N_{nei}\Delta_u + \Delta_u + 2r)$. It is straightforward to verify the cubes centered at $\tilde{\mathcal{S}}_m$ covers all cubes centered at \mathcal{S}_m ; otherwise, (S.26) will be violated. Thus m, \tilde{m} , and r satisfy

$$m\Delta_l^K/2^K \le \tilde{m}2^K (2N_{nei}\Delta_u + \Delta_u + 2r)^K$$
,

where the LHS is the total volume of cubes centered at \mathcal{S}_m and the RHS is the total volume of cubes centered at $\widetilde{\mathcal{S}}_m$. Hence, we obtain

$$\tilde{m} \ge m \frac{\Delta_l^K}{4^K (2N_{nei}\Delta_u + \Delta_u + 2r)^K} \propto m/r^K.$$

To satisfy the other side of (S.25), we just need to pick fewer locations into the $\widetilde{\mathcal{S}}_m$. This completes the proof of (S.25).

Next, we show that $\widetilde{\mathcal{S}}_m$ can be constructed such that $\tilde{m}^{1/(\lambda p)}\{\log(\tilde{m})\}^{-1/(2\lambda)} = o(\widetilde{\Delta}_{l,m})$ to fulfill (S.46) and $\tilde{m} \to \infty$ as $m \to \infty$, where $\lambda, p > 0$ are associated with the L_p -NED in Assumption 4. The above requirement on $\widetilde{\mathcal{S}}_m$ can be guaranteed when we take, for simplicity, $\widetilde{\Delta}_{l,m} \asymp \tilde{m}^{1/(\lambda p)}$, which implies $r \asymp \tilde{m}^{1/(\lambda p)}$. Combining with (S.25), we get

$$\tilde{m} \simeq m^{\frac{\lambda p}{K + \lambda p}}$$

which tends to infinity and $\tilde{m}^{1/(\lambda p)}\{\log(\tilde{m})\}^{-1/(2\lambda)} = o(\widetilde{\Delta}_{l,m})$ as $m \to \infty$.

S.IV.2 Detailed Proofs of Lemmas S.3–S.8

In this section, we provide the detailed proofs of Lemmas S.3–S.8 stated in Section S.III.2. We first present some results about the difference between $T_1(s;r)$ and $T_1^*(s;r)$. Suppose X is $L_p(\mathbf{d})$ -NED on the random field $Y = \{Y(s), s \in \mathcal{V}_m\}$. Then the L_p norm of the difference between $T_1(s)$ and $\mathbb{E}\left[T_1(s) \mid \mathfrak{F}\left\{\bigcup_{v \in \mathcal{N}(s)} B(v;r)\right\}\right]$ is controlled by

$$||T_1(s) - \mathbb{E}\left[T_1(s) \mid \mathfrak{F}\left\{\bigcup_{v \in \mathcal{N}(s)} B(v; r)\right\}\right]||_{n}$$

$$\leq \sum_{v \in \mathcal{N}(s)} \frac{\|X(v) - \mathbb{E}\left[X(v) \mid \mathfrak{F}\left\{\bigcup_{v \in \mathcal{N}(s)} B(v; r)\right\}\right]\|_{p}}{\tau(s)}$$

$$\leq \sum_{v \in \mathcal{N}(s)} \frac{d_{m}(v)}{\tau(s)} \psi(r) \tag{S.27}$$

due to the triangular inequality and the generalized non-decreasing property. Accordingly, the difference between the normalized variants is controlled by

$$||T_1(s;r) - T_1^*(s;r)||_p \le \sum_{v \in \mathcal{N}(s)} \frac{d_m(v)}{\tau(s)\zeta_r(s)} \psi(r) := \eta(s;r)\psi(r), \tag{S.28}$$

where $\eta(s;r) = \sum_{v \in \mathcal{N}(s)} d_m(v) / \{\tau(s)\zeta_r(s)\}$. Thus, it can be seen that

$$\mathbb{P}\left\{|T_1(s;r) - T_1^*(s;r)| > \delta\right\} \le \frac{1}{\delta^p} \|T_1(s;r) - T_1^*(s;r)\|_p^p \le \frac{\eta^p(s;r)\psi^p(r)}{\delta^p}$$

for any $\delta > 0$ due to the Markov inequality. Subsequently, we can establish the convergence of

$$\sup_{s \in \tilde{S}_m} |T_1(s;r) - T_1^*(s;r)| \quad \text{and} \quad \frac{1}{\tilde{m}} \sum_{s \in \tilde{S}_m} |T_1(s;r) - T_1^*(s;r)|.$$

In particular, for a fixed $\delta > 0$, the maximum difference between $T_1(s;r)$ and $T_1^*(s;r)$ is controlled by

$$\mathbb{P}\left\{\sup_{s\in\widetilde{\mathcal{S}}_m}|T_1(s;r)-T_1^*(s;r)|\leq\delta\right\} = \mathbb{P}\left\{\bigcap_{s\in\widetilde{\mathcal{S}}_m}|T_1(s;r)-T_1^*(s;r)|\leq\delta\right\} \\
\geq 1 - \frac{1}{\delta^p}\sum_{s\in\widetilde{\mathcal{S}}}\eta^p(s;r)\psi^p(r). \tag{S.29}$$

The mean difference is controlled by

$$\mathbb{P}\left\{\frac{1}{\tilde{m}}\sum_{s\in\tilde{\mathcal{S}}_{m}}|T_{1}(s;r)-T_{1}^{*}(s;r)|>\delta\right\} \leq \frac{1}{\tilde{m}^{p}\delta^{p}}\left\|\sum_{s\in\tilde{\mathcal{S}}_{m}}|T_{1}(s;r)-T_{1}^{*}(s;r)|\right\|_{p}^{p} \\
\leq \frac{1}{\tilde{m}^{p}\delta^{p}}\left\{\sum_{s\in\tilde{\mathcal{S}}_{m}}\|T_{1}(s;r)-T_{1}^{*}(s;r)\|_{p}\right\}^{p} \quad (S.30) \\
\leq \frac{1}{\tilde{m}^{p}\delta^{p}}\left\{\sum_{s\in\tilde{\mathcal{S}}_{m}}\eta(s;r)\psi(r)\right\}^{p},$$

where the first, second, and last inequalities are due to the Markov inequality, the triangular inequality, and (S.28), respectively.

Proof of Lemma S.3. First note that X is uniformly L_p -NED on Y for $p \geq 2$ implies that X is uniformly L_2 -NED on Y.

(a) Recall $\zeta_r^2(s) = \text{var}\left(\mathbb{E}\left[T_1(s) \mid \mathfrak{F}\left\{\bigcup_{v \in \mathcal{N}(s)} B(v; r)\right\}\right]\right)$ and $\text{var}\left\{T_1(s)\right\} = 1$. Then we have

$$\zeta_r^2(s) = \operatorname{var}\left(\mathbb{E}\left[T_1(s) \mid \mathfrak{F}\left\{\bigcup_{v \in \mathcal{N}(s)} B(v; r)\right\}\right]\right) \le \operatorname{var}\left\{T_1(s)\right\} = 1 \tag{S.31}$$

according to the law of total variance. Further, setting p=2 in (S.27), we obtain

$$||T_1(s) - \mathbb{E}\left[T_1(s) \mid \mathfrak{F}\left\{\bigcup_{v \in \mathcal{N}(s)} B(v; r)\right\}\right]||_2 \le \sum_{v \in \mathcal{N}(s)} \frac{d_m(v)}{\tau(s)} \psi(r) \le C\psi(r)$$

where the last inequality holds by Assumptions 2, 3(a) and 4. Therefore, we get

$$\begin{aligned} \left| \zeta_r^2(s) - 1 \right| &= \left| \operatorname{var} \left(\mathbb{E} \left[T_1(s) \mid \mathfrak{F} \left\{ \bigcup_{v \in \mathcal{N}(s)} B(v; r) \right\} \right] \right) - \operatorname{var} \left\{ T_1(s) \right\} \right| \\ &= \left| \mathbb{E} \left(\mathbb{E} \left[T_1(s) \mid \mathfrak{F} \left\{ \bigcup_{v \in \mathcal{N}(s)} B(v; r) \right\} \right] - T_1(s) \right)^2 \right| \\ &= \left\| T_1(s) - \mathbb{E} \left[T_1(s) \mid \mathfrak{F} \left\{ \bigcup_{v \in \mathcal{N}(s)} B(v; r) \right\} \right] \right\|_2^2 \\ &\leq C \psi^2(r), \end{aligned}$$

where the second equality stands because $\mathbb{E}\left(\mathbb{E}\left[T_1(s) \mid \mathfrak{F}\left\{\cup_{v \in \mathcal{N}(s)} B(v; r)\right\}\right]\right) = \mathbb{E}\left\{T_1(s)\right\}$. For the third equality, we have

$$\mathbb{E}\left(T_{1}(s)\mathbb{E}\left[T_{1}(s)\mid\mathfrak{F}\left\{\cup_{v\in\mathcal{N}(s)}B(v;r)\right\}\right]\right)$$

$$=\mathbb{E}\left\{\mathbb{E}\left(T_{1}(s)\mathbb{E}\left[T_{1}(s)\mid\mathfrak{F}\left\{\cup_{v\in\mathcal{N}(s)}B(v;r)\right\}\right]\mid\mathfrak{F}\left\{\cup_{v\in\mathcal{N}(s)}B(v;r)\right\}\right)\right\}$$

$$=\mathbb{E}\left(\mathbb{E}\left[T_{1}(s)\mid\mathfrak{F}\left\{\cup_{v\in\mathcal{N}(s)}B(v;r)\right\}\right]\right)^{2},$$

where $T_1(s)\mathbb{E}\left[T_1(s) \mid \mathfrak{F}\left\{\bigcup_{v \in \mathcal{N}(s)} B(v;r)\right\}\right] \in L_1$ is due to the Gaussianity from Assumption 5. Together with (S.31), for large enough r, we have

$$\left|1/\zeta_r^2(s)-1\right| \leq \left\{1-C\psi^2(r)\right\}^{-1}C\psi^2(r) \leq C\psi^2(r)$$

since $|1/x^2 - 1|$ decreases as $x^2 \in (0, 1]$ increases. This completes Part (a) of this lemma. (b) Assumptions 2 and 3 imply $|\hat{\tau}(s)/\tau(s) - 1| = o_{\mathbb{P}}(\tilde{m}^{-q})$ and $|\hat{\tau}^2(s)/\tau^2(s) - 1| = o_{\mathbb{P}}(\tilde{m}^{-q})$. For any $0 < \delta = C\tilde{m}^{-q} < 1$, combining with the proved conclusion in (a), we have

$$\begin{split} \left| \widehat{\tau}^2(s) / \tau_r^2(s) - 1 \right| &= \left| \widehat{\tau}^2(s) / \tau^2(s) \zeta_r^2(s) - 1 \right| \\ &\leq \left| \widehat{\tau}^2(s) / \tau^2(s) \zeta_r^2(s) - \widehat{\tau}^2(s) / \tau^2(s) \right| + \left| \widehat{\tau}^2(s) / \tau^2(s) - 1 \right| \\ &\leq \widehat{\tau}^2(s) / \tau^2(s) \left| 1 / \zeta_r^2(s) - 1 \right| + \left| \widehat{\tau}^2(s) / \tau^2(s) - 1 \right| \\ &\leq \left(1 + C \widetilde{m}^{-q} \right) C \psi^2(r) + C \widetilde{m}^{-q} \\ &\leq C \psi^2(r) + C \widetilde{m}^{-q} \end{split}$$

for large enough r with probability tending to one as $\tilde{m} \to \infty$.

For (c), we notice that

$$\sup_{m}\sup_{s\in\widetilde{\mathcal{S}}_{m}}\eta(s;r)=\sup_{m}\sup_{s\in\widetilde{\mathcal{S}}_{m}}\sum_{v\in\mathcal{N}(s)}\frac{d_{m}(v)}{\tau(s)\zeta_{r}(s)}\leq C\sup_{m}\sup_{s\in\widetilde{\mathcal{S}}_{m}}\frac{1}{\zeta_{r}(s)},$$

where the last inequality stands due to Assumptions 2, 3(a), and 4. Finally, $\sup_m \sup_{s \in \widetilde{\mathcal{S}}_m} \eta(s; r)$ is bounded away from zero for large enough r according to Part (a) of this lemma. \square

Proof of Lemma S.4. Note that

$$\mathbb{P}\left(\sup_{s\in\tilde{S}_{m}}|T_{1}^{*}(s;r) - \mathbb{E}\left\{T_{1}^{*}(s;r)\right\}| > \nu_{1}\delta_{1} \cup \sup_{s\in\tilde{S}_{m}}|T_{1}^{*}(s;r) - T_{1}(s;r)| > \nu_{1}\delta_{1}\right) \\
\qquad \cup \tilde{m}^{-1}\sum_{s\in\tilde{S}_{m}}|T_{1}(s;r) - T_{1}^{*}(s;r)| > \delta_{2}\right) \\
\leq \mathbb{P}\left[\sup_{s\in\tilde{S}_{m}}|T_{1}^{*}(s;r) - \mathbb{E}\left\{T_{1}^{*}(s;r)\right\}| > \nu_{1}\delta_{1}\right] \\
+ \mathbb{P}\left\{\sup_{s\in\tilde{S}_{m}}|T_{1}^{*}(s;r) - T_{1}(s;r)| > \nu_{1}\delta_{1}\right\} \\
+ \mathbb{P}\left\{\tilde{m}^{-1}\sum_{s\in\tilde{S}_{m}}|T_{1}(s;r) - T_{1}^{*}(s;r)| > \delta_{2}\right\} \\
\leq \tilde{m}\exp(-\nu_{s}^{2}\delta_{s}^{2}/2) + C\tilde{m}\psi^{p}(r)/\nu_{s}^{p}\delta_{s}^{p} + C\psi^{p}(r)/\delta_{s}^{p}$$

due to (S.29), (S.30), Lemma S.3(c), and the observation that

$$\mathbb{P}\left(\sup_{s\in\widetilde{\mathcal{S}}_m}|T_1^*(s;r)-\mathbb{E}\left\{T_1^*(s;r)\right\}|>\nu_1\delta_1\right)=\mathbb{P}\left(\bigcup_{s\in\widetilde{\mathcal{S}}_m}\left[T_1^*(s;r)-\mathbb{E}\left\{T_1^*(s;r)\right\}>\nu_1\delta_1\right]\right)$$

$$\leq \tilde{m}\exp(-\nu_1^2\delta_1^2/2)$$

implied directly by Assumption 5. Thus, to obtain Parts (a)–(c) of Lemma S.4 with probability at least (S.12), it suffices to show the desired upper bounds in Lemma S.4 can be derived from the complementary event of (S.32), i.e.,

$$\sup_{s \in \tilde{S}_m} |T_1^*(s;r) - \mathbb{E} \{T_1^*(s;r)\}| \le \nu_1 \delta_1, \tag{S.33}$$

$$\sup_{s \in \tilde{S}_m} |T_1^*(s;r) - T_1(s;r)| \le \nu_1 \delta_1, \tag{S.34}$$

and

$$\tilde{m}^{-1} \sum_{s \in \tilde{\mathcal{S}}_m} |T_1(s;r) - T_1^*(s;r)| \le \delta_2.$$
(S.35)

Now let us turn to the cumbersome details.

(a) First, $\sup_{s \in \widetilde{\mathcal{S}}_m} T_1^*(s;r)$ is upper bounded by $\nu_1(1+\delta_1)$ through

$$\sup_{s \in \tilde{S}_m} |T_1^*(s;r)| \le \sup_{s \in \tilde{S}_m} |T_1^*(s;r) - \mathbb{E} \{T_1^*(s;r)\}| + \sup_{s \in \tilde{S}_m} |\mathbb{E} \{T_1^*(s;r)\}| \le \nu_1(1+\delta_1), \quad (S.36)$$

where the second inequality is due to (S.10) and (S.33). For $T_1(s;r)$, we have

$$\sup_{s \in \tilde{\mathcal{S}}_m} |T_1(s;r)| \le \sup_{s \in \tilde{\mathcal{S}}_m} |T_1^*(s;r)| + \sup_{s \in \tilde{\mathcal{S}}_m} |T_1^*(s;r) - T_1(s;r)| \le \nu_1(1+2\delta_1), \tag{S.37}$$

where the second inequality is because of (S.34) and (S.36).

(b) To measure the difference between $T_1^2(s;r)$ and $\{T_1^*(s;r)\}^2$, we have

$$\tilde{m}^{-1} \left| \sum_{s \in \tilde{\mathcal{S}}_{m}} T_{1}^{2}(s;r) - \left\{ T_{1}^{*}(s;r) \right\}^{2} \right| \\
= \tilde{m}^{-1} \left| \sum_{s \in \tilde{\mathcal{S}}_{m}} \left\{ T_{1}(s;r) - T_{1}^{*}(s;r) \right\} \left\{ T_{1}(s;r) + T_{1}^{*}(s;r) \right\} \right| \\
\leq \left\{ \tilde{m}^{-1} \left| \sum_{s \in \tilde{\mathcal{S}}_{m}} T_{1}(s;r) - T_{1}^{*}(s;r) \right| \right\} \left\{ \sup_{s \in \tilde{\mathcal{S}}_{m}} |T_{1}(s;r) + T_{1}^{*}(s;r)| \right\} \\
\leq \left\{ \tilde{m}^{-1} \sum_{s \in \tilde{\mathcal{S}}_{m}} |T_{1}(s;r) - T_{1}^{*}(s;r)| \right\} \left\{ \sup_{s \in \tilde{\mathcal{S}}_{m}} |T_{1}(s;r)| + \sup_{s \in \tilde{\mathcal{S}}_{m}} |T_{1}^{*}(s;r)| \right\} \\
\leq \nu_{1} \delta_{2}(2 + 3\delta_{1}), \tag{S.38}$$

where the first inequality holds by the Hölder's inequality and the last inequality is due to (S.35)–(S.37).

(c) The upper bound for $\tilde{m}^{-1} \sum_{s \in \tilde{\mathcal{S}}_m} |T_1(s;r)|$ is obtained by

$$\tilde{m}^{-1} \sum_{s \in \tilde{S}_{m}} |T_{1}(s;r)|$$

$$= \tilde{m}^{-1} \sum_{s \in \tilde{S}_{m}} |T_{1}(s;r) - T_{1}^{*}(s;r) + T_{1}^{*}(s;r) - \mathbb{E}\{T_{1}^{*}(s;r)\} + \mathbb{E}\{T_{1}^{*}(s;r)\}|$$

$$\leq \tilde{m}^{-1} \sum_{s \in \tilde{S}_{m}} |T_{1}(s;r) - T_{1}^{*}(s;r)| + \sup_{s \in \tilde{S}_{m}} |T_{1}^{*}(s;r) - \mathbb{E}\{T_{1}^{*}(s;r)\}| + \sup_{s \in \tilde{S}_{m}} |\mathbb{E}\{T_{1}^{*}(s;r)\}|$$

$$\leq \nu_{1} (1 + \delta_{1}) + \delta_{2}$$
(S.39)

where the last step in (S.39) is due to (S.10), (S.33), and (S.35). As for $\tilde{m}^{-1} \sum_{s \in \tilde{\mathcal{S}}_m} T_1^2(s;r)$, the Hölder inequality implies

$$\tilde{m}^{-1} \sum_{s \in \tilde{S}_{m}} \left[\left\{ T_{1}^{*}(s;r) \right\}^{2} - \mathbb{E} \left\{ T_{1}^{*}(s;r) \right\}^{2} \right] \\
\leq \left| \tilde{m}^{-1} \sum_{s \in \tilde{S}_{m}} \left[T_{1}^{*}(s;r) - \mathbb{E} \left\{ T_{1}^{*}(s;r) \right\} \right] \right| \times \sup_{s \in \tilde{S}_{m}} \left| T_{1}^{*}(s;r) + \mathbb{E} \left\{ T_{1}^{*}(s;r) \right\} \right| \\
\leq \sup_{s \in \tilde{S}_{m}} \left| T_{1}^{*}(s;r) - \mathbb{E} \left\{ T_{1}^{*}(s;r) \right\} \right| \times \left\{ \sup_{s \in \tilde{S}_{m}} \left| T_{1}^{*}(s;r) \right| + \sup_{s \in \tilde{S}_{m}} \mathbb{E} \left| T_{1}^{*}(s;r) \right| \right\} \\
\leq \nu_{1}^{2} \delta_{1}(2 + \delta_{1}), \tag{S.40}$$

where the last line is due to (S.10), (S.33), and (S.36). We then have

$$\begin{split} \tilde{m}^{-1} & \sum_{s \in \tilde{S}_m} T_1^2(s; r) \\ &= \tilde{m}^{-1} \sum_{s \in \tilde{S}_m} \left[T_1^2(s; r) - \left\{ T_1^*(s; r) \right\}^2 \right] + \tilde{m}^{-1} \sum_{s \in \tilde{S}_m} \left[\left\{ T_1^*(s; r) \right\}^2 - \mathbb{E} \left\{ T_1^*(s; r) \right\}^2 \right] \end{split}$$

$$+ \tilde{m}^{-1} \sum_{s \in \tilde{\mathcal{S}}_{m}} \mathbb{E} \left\{ T_{1}^{*}(s;r) \right\}^{2}$$

$$\leq \tilde{m}^{-1} \left| \sum_{s \in \tilde{\mathcal{S}}_{m}} T_{1}^{2}(s;r) - \left\{ T_{1}^{*}(s;r) \right\}^{2} \right| + \tilde{m}^{-1} \sum_{s \in \tilde{\mathcal{S}}_{m}} \left[\left\{ T_{1}^{*}(s;r) \right\}^{2} - \mathbb{E} \left\{ T_{1}^{*}(s;r) \right\}^{2} \right]$$

$$+ \sup_{s \in \tilde{\mathcal{S}}_{m}} \mathbb{E} \left\{ T_{1}^{*}(s;r) \right\}^{2}$$

$$\leq \nu_{1}^{2} + \nu_{1} \delta_{2}(2 + 3\delta_{1}) + \nu_{1}^{2} \delta_{1}(2 + \delta_{1}), \qquad (S.41)$$

where we have used (S.10), (S.38), and (S.40) to obtain the last inequality in (S.41). The proof is thus completed.

Proof of Lemma S.5. The proof of Lemma S.4 has shown that with probability at least (S.12), the events of (S.35)–(S.41) hold. It is thus sufficient to show that (S.13) is upper bounded by $C\nu_1^2 \{\psi^2(r) + \tilde{m}^{-q}\} (1+\delta_1^2) + C\nu_1\delta_2 (1+\delta_1)$ under the events of (S.35)–(S.41). To show this, we divide (S.13) into four components and examine their upper bounds under the events of (S.35)–(S.41) separately.

To begin with, it can be shown

$$\begin{split} \left| \frac{1}{\tilde{m}} \sum_{s \in \tilde{S}_m} \log f_{\tilde{G}_{\tilde{m},r}} \{T_1(s;r)\} - \frac{1}{\tilde{m}} \sum_{s \in \tilde{S}_m} \log f_{\tilde{G}_{\tilde{m},r}} \{\hat{T}_1(s)\} \right| \\ &= \left| \frac{1}{\tilde{m}} \sum_{s \in \tilde{S}_m} \log \left[\frac{\sum_{i=1}^{\tilde{l}} \tilde{\pi}_i \phi \{T_1(s;r) - \tilde{v}_i\}}{\sum_{i=1}^{\tilde{l}} \tilde{\pi}_i \phi \{\hat{T}_1(s) - \tilde{v}_i\}} \right] \right| \\ &= \left| \frac{1}{\tilde{m}} \sum_{s \in \tilde{S}_m} \log \left(e^{-\left\{T_1^2(s;r) - \hat{T}_1^2(s)\right\}/2} \right. \\ &\qquad \qquad \times \frac{\sum_{i=1}^{\tilde{l}} \tilde{\pi}_i \exp \left\{\hat{T}_1(s) \tilde{v}_i - \hat{v}_i^2/2\right\} \exp \left[\left\{T_1(s;r) - \hat{T}_1(s)\right\} \tilde{v}_i\right\}}{\sum_{i=1}^{\tilde{l}} \tilde{\pi}_i \exp \left\{\hat{T}_1(s) \tilde{v}_i - \tilde{v}_i^2/2\right\}} \right) \right| \\ &\leq \left| \frac{1}{\tilde{m}} \sum_{s \in \tilde{S}_m} \left\{ \frac{\left|\hat{T}_1^2(s) - T_1^2(s;r)\right|}{2} + \left|\hat{T}_1(s) - T_1(s;r)\right| \max_{i=1,\cdots,\tilde{l}} |\tilde{v}_i| \right\} \right| \\ &\leq \left| \frac{1}{\tilde{m}} \sum_{s \in \tilde{S}_m} \left\{ \frac{\left|\hat{T}_1^2(s) - T_1^2(s;r)\right|}{2} + \left|\hat{T}_1(s) - T_1(s;r)\right| \sup_{s \in \tilde{S}_m} |T_1(s;r)| \right\} \right| \\ &\leq \frac{\sup_{s \in \tilde{S}_m} |\tilde{\tau}^2(s)/\tau_r^2(s) - 1|}{2\left\{1 - \sup_{s \in \tilde{S}_m} |\tilde{\tau}^2(s)/\tau_r^2(s) - 1|\right\}} \left\{ \frac{1}{\tilde{m}} \sum_{s \in \tilde{S}_m} T_1^2(s;r) + \sup_{s \in \tilde{S}_m} |T_1(s;r)| \left| \frac{1}{\tilde{m}} \sum_{s \in \tilde{S}_m} T_1(s;r) \right| \right\}, \end{split}$$

where the second inequality follows from the fact that the support of $\widetilde{G}_{\tilde{m}}$ is within the

range of $\{T_1(s;r): s \in \widetilde{\mathcal{S}}_m\}$. Plugging in (S.37), (S.39), and (S.41), we observe that

$$\left| \frac{1}{\tilde{m}} \sum_{s \in \tilde{S}_m} T_1^2(s;r) \right| + \sup_{s \in \tilde{S}_m} |T_1(s;r)| \left| \frac{1}{\tilde{m}} \sum_{s \in \tilde{S}_m} T_1(s;r) \right|$$

$$\leq \nu_1^2 + \nu_1 \delta_2 (2 + 3\delta_1) + \nu_1^2 \delta_1 (2 + \delta_1) + \nu_1 (1 + 2\delta_1) \left\{ \nu_1 (1 + \delta_1) + \delta_2 \right\}$$

$$= 2\nu_1^2 + \nu_1 \delta_2 (3 + 5\delta_1) + \nu_1^2 \delta_1 (5 + 3\delta_1).$$

Combining the above with (S.11), we immediately obtain that the first component of the target difference (S.13) is bound by

$$C\nu_1 \left\{ \psi^2(r) + \tilde{m}^{-q} \right\} \left\{ 2\nu_1 + \delta_2(3 + 5\delta_1) + \nu_1\delta_1(5 + 3\delta_1) \right\}.$$

Secondly, we have

$$\begin{split} \left| \frac{1}{\tilde{m}} \sum_{s \in \tilde{\mathcal{S}}_m} \log f_{\tilde{G}_{\tilde{m},r}^*} \{T_1(s;r)\} - \frac{1}{\tilde{m}} \sum_{s \in \tilde{\mathcal{S}}_m} \log f_{\tilde{G}_{\tilde{m},r}^*} \{T_1^*(s;r)\} \right| \\ &= \left| \frac{1}{\tilde{m}} \sum_{s \in \tilde{\mathcal{S}}_m} \log \left[\frac{\sum_{i=1}^{\tilde{I}^*} \tilde{\pi}_i^* \phi \{T_1(s;r) - \tilde{v}_i^*\}}{\sum_{i=1}^{\tilde{I}^*} \tilde{\pi}_i^* \phi \{T_1^*(s;r) - \tilde{v}_i^*\}} \right] \right| \\ &= \left| \frac{1}{\tilde{m}} \sum_{s \in \tilde{\mathcal{S}}_m} \log \left(e^{-\left[T_1^2(s;r) - \left\{T_1^*(s;r)\right\}^2\right]/2} \right. \\ &\qquad \times \frac{\sum_{i=1}^{\tilde{I}^*} \tilde{\pi}_i^* \exp\left\{T_1^*(s;r)\tilde{v}_i^* - \left(\tilde{v}_i^*\right)^2/2\right\} \exp\left[\left\{T_1(s;r) - T_1^*(s;r)\right\}\tilde{v}_i^*\right]}{\sum_{i=1}^{\tilde{I}^*} \tilde{\pi}_i^* \exp\left\{T_1^*(s;r)\tilde{v}_i^* - \left(\tilde{v}_i^*\right)^2/2\right\}} \\ &\leq \left| \frac{1}{\tilde{m}} \sum_{s \in \tilde{\mathcal{S}}_m} \frac{\left\{T_1^*(s;r)\right\}^2 - T_1^2(s;r)}{2} \right| + \frac{1}{\tilde{m}} \sum_{s \in \tilde{\mathcal{S}}_m} \left|T_1(s;r) - T_1^*(s;r)\right| \max_{i=1,\cdots,\tilde{I}^*} \left|\tilde{v}_i^*\right| \\ &\leq \left| \frac{1}{\tilde{m}} \sum_{s \in \tilde{\mathcal{S}}_m} \frac{\left\{T_1^*(s;r)\right\}^2 - T_1^2(s;r)}{2} \right| + \frac{1}{\tilde{m}} \sum_{s \in \tilde{\mathcal{S}}_m} \left|T_1(s;r) - T_1^*(s;r)\right| \sup_{s \in \tilde{\mathcal{S}}_m} \left|T_1^*(s;r)\right|, \end{split}$$

where the second inequality follows the fact that the support of $\widetilde{G}_{\tilde{m},r}^*$ is within the range of $\{T_1^*(s;r):s\in\widetilde{\mathcal{S}}_m\}$. Using (S.35), (S.36), and (S.38), we further obtain that $\nu_1\delta_2$ (3 + 4 δ_1) is an upper bound for the above difference. As for the third component of the target (S.13), we have

$$\begin{split} &\left|\frac{1}{\tilde{m}}\sum_{s\in\tilde{\mathcal{S}}_{m}}\log f_{\hat{G}_{\tilde{m}}}\{\hat{T}_{1}(s)\} - \frac{1}{\tilde{m}}\sum_{s\in\tilde{\mathcal{S}}_{m}}\log f_{\hat{G}_{\tilde{m}}}\{T_{1}(s;r)\}\right| \\ &\leq \frac{\sup_{s\in\tilde{\mathcal{S}}_{m}}|\hat{\tau}^{2}(s)/\tau_{r}^{2}(s) - 1|}{2\left\{1 - \sup_{s\in\tilde{\mathcal{S}}_{m}}|\hat{\tau}^{2}(s)/\tau_{r}^{2}(s) - 1|\right\}}\left\{\left|\frac{1}{\tilde{m}}\sum_{s\in\tilde{\mathcal{S}}_{m}}T_{1}^{2}(s;r)\right| + \sup_{s\in\tilde{\mathcal{S}}_{m}}\left|\hat{T}_{1}(s)\right|\left|\frac{1}{\tilde{m}}\sum_{s\in\tilde{\mathcal{S}}_{m}}T_{1}(s;r)\right|\right\} \\ &\leq \frac{\sup_{s\in\tilde{\mathcal{S}}_{m}}|\hat{\tau}^{2}(s)/\tau_{r}^{2}(s) - 1|}{2\left\{1 - \sup_{s\in\tilde{\mathcal{S}}_{m}}|\hat{\tau}^{2}(s)/\tau_{r}^{2}(s) - 1|\right\}} \end{split}$$

$$\times \left\{ \left| \frac{1}{\tilde{m}} \sum_{s \in \tilde{\mathcal{S}}_m} T_1^2(s;r) \right| + \frac{\sup_{s \in \tilde{\mathcal{S}}_m} |T_1(s;r)|}{1 - \sup_{s \in \tilde{\mathcal{S}}_m} |\widehat{\tau}^2(s)/\tau_r^2(s) - 1|} \left| \frac{1}{\tilde{m}} \sum_{s \in \tilde{\mathcal{S}}_m} T_1(s;r) \right| \right\}$$

$$\leq \frac{\sup_{s \in \tilde{\mathcal{S}}_m} |\widehat{\tau}^2(s)/\tau_r^2(s) - 1|}{2 \left\{ 1 - \sup_{s \in \tilde{\mathcal{S}}_m} |\widehat{\tau}^2(s)/\tau_r^2(s) - 1| \right\}}$$

$$\times \left\{ \left| \frac{1}{\tilde{m}} \sum_{s \in \tilde{\mathcal{S}}_m} T_1^2(s;r) \right| + C \sup_{s \in \tilde{\mathcal{S}}_m} |T_1(s;r)| \left| \frac{1}{\tilde{m}} \sum_{s \in \tilde{\mathcal{S}}_m} T_1(s;r) \right| \right\},$$

where the last inequality holds for the same reason as for (S.11). Combining (S.11), (S.37), (S.39), and (S.41), we get the upper bound

$$C\left\{\psi^{2}(r) + \tilde{m}^{-q}\right\}\left\{\nu_{1}^{2} + \nu_{1}\delta_{2}(2 + 3\delta_{1}) + \nu_{1}^{2}\delta_{1}\left(2 + \delta_{1}\right) + C\nu_{1}(1 + 2\delta_{1})\left\{\nu_{1}(1 + \delta_{1}) + \delta_{2}\right\}\right\}$$

$$= C\left\{\psi^{2}(r) + \tilde{m}^{-q}\right\}\left[\nu_{1}^{2}\left(1 + C\right) + \nu_{1}\delta_{2}\left\{2 + C + \delta_{1}\left(3 + 2C\right)\right\} + \nu_{1}^{2}\delta_{1}\left\{2 + 3C + \delta_{1}\left(1 + 2C\right)\right\}\right]$$

$$\leq C\nu_{1}\left\{\psi^{2}(r) + \tilde{m}^{-q}\right\}\left\{\nu_{1} + \delta_{2}\left(1 + \delta_{1}\right) + \nu_{1}\delta_{1}\left(1 + \delta_{1}\right)\right\}.$$

For the forth component, we obtain

$$\begin{split} \left| \frac{1}{\tilde{m}} \sum_{s \in \tilde{\mathcal{S}}_{m}} \log f_{\hat{G}_{\tilde{m}}} \{ T_{1}^{*}(s;r) \} - \frac{1}{\tilde{m}} \sum_{s \in \tilde{\mathcal{S}}_{m}} \log f_{\hat{G}_{\tilde{m}}} \{ T_{1}(s;r) \} \right| \\ & \leq \left| \frac{1}{\tilde{m}} \sum_{s \in \tilde{\mathcal{S}}_{m}} \frac{\{ T_{1}^{*}(s;r) \}^{2} - T_{1}^{2}(s;r)}{2} \right| + \frac{1}{\tilde{m}} \sum_{s \in \tilde{\mathcal{S}}_{m}} |T_{1}(s;r) - T_{1}^{*}(s;r)| \sup_{s \in \tilde{\mathcal{S}}_{m}} |\widehat{T}_{1}(s)| \\ & \leq \left| \frac{1}{\tilde{m}} \sum_{s \in \tilde{\mathcal{S}}_{m}} \frac{\{ T_{1}^{*}(s;r) \}^{2} - T_{1}^{2}(s;r)}{2} \right| + \frac{\sup_{s \in \tilde{\mathcal{S}}_{m}} |T_{1}(s;r)|}{1 - \sup_{s \in \tilde{\mathcal{S}}_{m}} |\widehat{\tau}^{2}(s) / \tau_{r}^{2}(s) - 1|} \\ & \times \left\{ \frac{1}{\tilde{m}} \sum_{s \in \tilde{\mathcal{S}}_{m}} |T_{1}(s;r) - T_{1}^{*}(s;r)| \right\} \\ & \leq \left| \frac{1}{\tilde{m}} \sum_{s \in \tilde{\mathcal{S}}_{m}} \frac{\{ T_{1}^{*}(s;r) \}^{2} - T_{1}^{2}(s;r)}{2} \right| + C \sup_{s \in \tilde{\mathcal{S}}_{m}} |T_{1}(s;r)| \left\{ \frac{1}{\tilde{m}} \sum_{s \in \tilde{\mathcal{S}}_{m}} |T_{1}(s;r) - T_{1}^{*}(s;r)| \right\}. \end{split}$$

Similarly, due to (S.35), (S.37), and (S.38), the upper bound of the above is

$$\nu_1 \delta_2 (2 + 3\delta_1) + C \nu_1 \delta_2 (1 + 2\delta_1) \le C \nu_1 \delta_2 (1 + \delta_1)$$
.

Finally, combining the four components with the triangular inequality, we get the upper bound

$$\frac{1}{\tilde{m}} \left| \sum_{s \in \tilde{S}_{m}} \log \left[\frac{f_{\tilde{G}_{\tilde{m},r}^{*}} \{T_{1}(s;r)\}}{f_{\tilde{G}_{\tilde{m},r}^{*}} \{T_{1}^{*}(s;r)\}} \frac{f_{\tilde{G}_{\tilde{m}},r} \{\hat{T}_{1}(s)\}}{f_{\tilde{G}_{\tilde{m}},r} \{T_{1}(s;r)\}} \frac{f_{\hat{G}_{\tilde{m}}} \{T_{1}^{*}(s;r)\}}{f_{\hat{G}_{\tilde{m}}} \{T_{1}(s;r)\}} \frac{f_{\hat{G}_{\tilde{m}}} \{T_{1}(s;r)\}}{f_{\hat{G}_{\tilde{m}}} \{\hat{T}_{1}(s)\}} \right] \right| \\
\leq C \nu_{1}^{2} \left\{ \psi^{2}(r) + \tilde{m}^{-q} \right\} \left\{ 1 + \delta_{1} \left(1 + \delta_{1} \right) \right\} + C \nu_{1} \delta_{2} \left(1 + \delta_{1} \right) \\
\leq C \nu_{1}^{2} \left\{ \psi^{2}(r) + \tilde{m}^{-q} \right\} \left(1 + \delta_{1}^{2} \right) + C \nu_{1} \delta_{2} \left(1 + \delta_{1} \right) ,$$

which finishes the proof.

Lemma S.6 is a direct consequence of Theorem 1 in Zhang (2009). Interested readers are referred to Zhang (2009) and references therein for more details.

Proof of Lemma S.7. First, notice that $d_H^2(f_{G_{\tilde{m},r}}, f_{G_{\tilde{m}}}) \leq d_{TV}(f_{G_{\tilde{m},r}}, f_{G_{\tilde{m}}})$, where d_{TV} denotes the total variation distance

$$d_{TV}(f_{G_{\tilde{m},r}}, f_{G_{\tilde{m}}}) = \frac{1}{2} \int \left| \int \phi(v-u) \{ dG_{\tilde{m},r}(u) - dG_{\tilde{m}}(u) \} \right| dv.$$

Plugging the definitions of $G_{\tilde{m},r}(u)$ and $G_{\tilde{m}}(u)$ into the above equation, $d_{TV}\left(f_{G_{\tilde{m},r}},f_{G_{\tilde{m}}}\right)$ can be written as

$$\frac{1}{2\tilde{m}} \int \left| \sum_{s \in \tilde{S}_m} \int \phi(v - u) [d\mathbf{1}\{\xi(s)/\zeta_r(s) \le u\} - d\mathbf{1}\{\xi(s) \le u\}] \right| dv$$

$$= \frac{1}{2\tilde{m}} \int \left| \sum_{s \in \tilde{S}_m} \phi\{v - \xi(s)/\zeta_r(s)\} - \phi\{v - \xi(s)\} \right| dv$$

$$\le \frac{1}{2\tilde{m}} \sum_{s \in \tilde{S}_m} \int |\phi\{v - \xi(s)/\zeta_r(s)\} - \phi\{v - \xi(s)\}| dv.$$

Note that $\phi\{v - \xi(s)/\zeta_r(s)\}$ and $\phi\{v - \xi(s)\}$ are symmetric about $x = \xi(s)\{\zeta_r(s) + 1\}/2\zeta_r(s)$. The above integral is equivalent to

$$\frac{1}{\tilde{m}} \sum_{s \in \tilde{\mathcal{S}}_m} \left| \int_{\xi(s)\{1+\zeta_r(s)\}/2\zeta_r(s)}^{\infty} [\phi\{v-\xi(s)/\zeta_r(s)\} - \phi\{v-\xi(s)\}] dv \right|
= \frac{1}{\tilde{m}} \sum_{s \in \tilde{\mathcal{S}}_m} \left| \Phi[\xi(s)\{1-\zeta_r(s)\}/2\zeta_r(s)] - \Phi[\xi(s)\{\zeta_r(s)-1\}/2\zeta_r(s)] \right|
= \frac{1}{\tilde{m}} \sum_{s \in \tilde{\mathcal{S}}_m} \left| \phi(u(s)) \right| |\xi(s)\{1-\zeta_r(s)\}/\zeta_r(s)|,$$

where u(s) is some value between $\xi(s)\{1-\zeta_r(s)\}/2\zeta_r(s)$ and $\xi(s)\{\zeta_r(s)-1\}/2\zeta_r(s)$ due to the mean value theorem. Finally, by Lemma S.3(a), (S.10), and the uniform boundedness of $\phi(x)$, $d_{TV}\left(f_{G_{\tilde{m},r}}, f_{G_{\tilde{m}}}\right)$ is upper bounded by $C\nu_1\psi^2(r)$. Taking the square root, we get

$$d_H(f_{G_{\tilde{m},r}}, f_{G_{\tilde{m}}}) \le d_{TV}^{1/2} \left(f_{G_{\tilde{m},r}}, f_{G_{\tilde{m}}} \right) \le C \nu_1^{1/2} \psi(r).$$

Assumption 8(b) states that $d_H(f_{G_{\tilde{m}}}, f_{G_0}) \leq \delta_3$ for any $\delta_3 > 0$ with probability tending to one. The desired result follows from the triangular inequality.

Proof of Lemma S.8. Due to the triangular inequality, the Hellinger distance $d_H := d_H(f_{\widehat{G}_{\widehat{m}}}, f_{G_0})$ is bounded by the summation of the following two components,

$$d_{H,1} := d_H \left(f_{\widehat{G}_{\tilde{m}}}, f_{G_{\tilde{m},r}} \right) \quad \text{and} \quad d_{H,2} := d_H \left(f_{G_{\tilde{m},r}}, f_{G_0} \right)$$

for any r > 0. Thus, for an arbitrary $\epsilon > 0$, it shows that

$$\mathbb{P}\left(d_{H} \geq \varepsilon\right) \leq \mathbb{P}\left(d_{H,1} \geq \epsilon/2\right) + \mathbb{P}\left(d_{H,2} \geq \epsilon/2\right)$$

$$\leq \mathbb{P}\left(d_{H,1} \geq t c_{\tilde{m}}\right) + \mathbb{P}\left\{d_{H,2} \geq C \nu_1 \phi^2(r) + \epsilon/4\right\},\tag{S.42}$$

where the first inequality is because of the triangular inequality and the second inequality is achieved once (i) choosing r such that $C\nu_1\phi^2(r) \leq \epsilon/4$; (ii) \tilde{m} is sufficient large that induces arbitrarily small $c_{\tilde{m}}$ with fixed b > 0 defined at (S.15) in Lemma S.6. The second term of the RHS in (S.42) tends to zero by setting $\delta_3 = \epsilon/4$ in Lemma S.7. As for the first term of the RHS in (S.42), we have

$$\mathbb{P}(d_{H,1} \ge tc_{\tilde{m}}) = \mathbb{P}\left(d_{H,1} \ge tc_{\tilde{m}}, \frac{1}{\tilde{m}} \sum_{s \in \tilde{S}_{m}} \log \left[\frac{f_{\hat{G}_{\tilde{m}}} \left\{ T_{1}^{*}(s;r) \right\}}{f_{G_{\tilde{m},r}} \left\{ T_{1}^{*}(s;r) \right\}} \right] \ge -2t^{2}c_{\tilde{m}}^{2}/15 \right) \\
+ \mathbb{P}\left(\frac{1}{\tilde{m}} \sum_{s \in \tilde{S}_{m}} \log \left[\frac{f_{\hat{G}_{\tilde{m}}} \left\{ T_{1}^{*}(s;r) \right\}}{f_{G_{\tilde{m},r}} \left\{ T_{1}^{*}(s;r) \right\}} \right] < -2t^{2}c_{\tilde{m}}^{2}/15 \right) \\
\le C\tilde{m}^{-2} + \mathbb{P}\left(\frac{1}{\tilde{m}} \sum_{s \in \tilde{S}_{m}} \log \left[\frac{f_{\hat{G}_{\tilde{m}}} \left\{ T_{1}^{*}(s;r) \right\}}{f_{G_{\tilde{m},r}} \left\{ T_{1}^{*}(s;r) \right\}} \right] < -2t^{2}c_{\tilde{m}}^{2}/15 \right) \quad (S.43)$$

when t is large enough due to Lemma S.6. As for the second term of the RHS in (S.43), notice that

$$\frac{1}{\tilde{m}} \sum_{s \in \tilde{S}_{m}} \log \left[\frac{f_{\tilde{G}_{\tilde{m}}} \{T_{1}^{*}(s;r)\}}{f_{G_{\tilde{m},r}} \{T_{1}^{*}(s;r)\}} \right] \\
= \frac{1}{\tilde{m}} \sum_{s \in \tilde{S}_{m}} \log \left[\frac{f_{\tilde{G}_{\tilde{m},r}^{*}} \{T_{1}^{*}(s;r)\}}{f_{G_{\tilde{m},r}^{*}} \{T_{1}^{*}(s;r)\}} \frac{f_{\tilde{G}_{\tilde{m},r}^{*}} \{T_{1}(s;r)\}}{f_{\tilde{G}_{\tilde{m},r}^{*}} \{T_{1}^{*}(s;r)\}} \frac{f_{\tilde{G}_{\tilde{m},r}^{*}} \{T_{1}(s;r)\}}{f_{\tilde{G}_{\tilde{m},r}^{*}} \{T_{1}(s;r)\}} \right] \\
\times \frac{f_{\tilde{G}_{\tilde{m},r}} \{\hat{T}_{1}(s)\}}{f_{\tilde{G}_{\tilde{m},r}} \{T_{1}(s;r)\}} \frac{f_{\hat{G}_{\tilde{m}}} \{\hat{T}_{1}(s)\}}{f_{\tilde{G}_{\tilde{m}},r} \{\hat{T}_{1}(s;r)\}} \frac{f_{\hat{G}_{\tilde{m}}} \{T_{1}^{*}(s;r)\}}{f_{\tilde{G}_{\tilde{m}}} \{T_{1}(s;r)\}} \frac{f_{\hat{G}_{\tilde{m}}} \{T_{1}(s;r)\}}{f_{\tilde{G}_{\tilde{m}}} \{T_{1}(s;r)\}} \frac{f_{\tilde{G}_{\tilde{m}}} \{T_{1}(s;r)\}}{f_{\tilde$$

where the last inequality is due to the definitions of $\widetilde{G}_{\tilde{m},r}^*$, $\widetilde{G}_{\tilde{m},r}$, and $\widehat{G}_{\tilde{m}}$. In addition, (S.15) implies

$$2t^{2}c_{\tilde{m}}^{2}/15 = 2t^{2}\tilde{m}^{-b/(1+b)} \left(\log \tilde{m}\right)^{(2+3b)/(2+2b)} \left(1 \vee \nu_{1}\right)^{b/(1+b)}/15. \tag{S.45}$$

Plugging (S.44) and (S.45) into the second probability of the RHS of (S.43) yields

$$\mathbb{P}\left(\left|\frac{1}{\tilde{m}}\sum_{s\in\tilde{\mathcal{S}}_{m}}\log\left[\frac{f_{\tilde{G}_{\tilde{m},r}^{*}}\left\{T_{1}(s;r)\right\}}{f_{\tilde{G}_{\tilde{m},r}^{*}}\left\{T_{1}^{*}(s;r)\right\}}\frac{f_{\tilde{G}_{\tilde{m},r}}\left\{\widehat{T}_{1}(s)\right\}}{f_{\tilde{G}_{\tilde{m},r}}\left\{T_{1}(s;r)\right\}}\frac{f_{\hat{G}_{\tilde{m}}}\left\{T_{1}^{*}(s;r)\right\}}{f_{\hat{G}_{\tilde{m}}}\left\{T_{1}(s;r)\right\}}\frac{f_{\hat{G}_{\tilde{m}}}\left\{T_{1}(s;r)\right\}}{f_{\hat{G}_{\tilde{m}}}\left\{\widehat{T}_{1}(s)\right\}}\right| > C\tilde{m}^{-a}\right),$$

for some a such that $b/(1+b) < a < \min(q, 1/p)$ when \tilde{m} is large enough.

Next, we shall show that the above probability goes to zero as $m \to \infty$ when the subset $\widetilde{\mathcal{S}}_m$ used for NPEB fulfills Assumption 6. Using Lemma S.5, we only need to show for $\delta > 0$,

$$\tilde{m} \exp(-\nu_1^2 \delta_1^2/2) \leq \delta, \quad C \tilde{m} \psi^p(r) / \nu_1^p \delta_1^p \leq \delta, \quad \text{and} \quad C \psi^p(r) / \delta_2^p \leq \delta,$$

as well as

$$C\nu_1^2 \left\{ \psi^2(r) + \tilde{m}^{-q} \right\} \left(1 + \delta_1^2 \right) = O(\tilde{m}^{-a}) \quad \text{and} \quad C\nu_1 \delta_2 \left(1 + \delta_1 \right) = O(\tilde{m}^{-a})$$

for some $\delta_1, \delta_2 > 0$. Note that $\tilde{m} \exp(-\nu_1^2 \delta_1^2/2) \le \delta$ is equivalent to $\delta_1 \ge \sqrt{2 \ln(\tilde{m}/\delta)}/\nu_1$. We set

$$\delta_1 = \frac{1}{\nu_1} \sqrt{2 \ln(\tilde{m}/\delta)}$$

in the following calculations. For δ_2 , $C\nu_1\delta_2(1+\delta_1) \leq \tilde{m}^{-a}$ implies $\delta_2 \leq C\tilde{m}^{-a}/\nu_1(1+\delta_1)$. With the choice of δ_1 , we set

$$\delta_2 = \frac{C\tilde{m}^{-a}}{\nu_1 + \sqrt{2\ln(\tilde{m}/\delta)}}.$$

Similarly, with the above choice of δ_1 , the constraint $C\nu_1^2\tilde{m}^{-q}(1+\delta_1^2)\leq \tilde{m}^{-a}$ becomes

$$\tilde{m}^{-q} \le \frac{C\tilde{m}^{-a}}{\nu_1^2 + 2\ln(\tilde{m}/\delta)},$$

which can be achieved according to the upper and lower bounds of a. As $C\tilde{m}\psi^p(r)/\nu_1^p\delta_1^p \leq \delta$, $C\psi^p(r)/\delta_2^p \leq \delta$, and $C\nu_1^2\psi^2(r)(1+\delta_1^2) \leq \tilde{m}^{-a}$, we require

$$r^{-\lambda} \approx \psi(r) \leq \min \left[C\delta \tilde{m}^{-1/p} \sqrt{\ln(\tilde{m}/\delta)}, \ C\delta^{1/p} \tilde{m}^{-a} / \left\{ \nu_1 + \sqrt{2\ln(\tilde{m}/\delta)} \right\}, \\ \tilde{m}^{-a/2} / \sqrt{\nu_1^2 + 2\ln(\tilde{m}/\delta)} \right]$$
(S.46)

after plugging in δ_1 and δ_2 with Assumption 4. Again, according to the upper bounds of a, the RHS of (S.46) is dominated by its first term when \tilde{m} is large enough. Thus (S.46) is a consequence of Assumption 6 when we take $r = \widetilde{\Delta}_{l,m}/2$, which completes the proof.

In the proof of Lemma S.8, (S.46) requires r increases as \tilde{m} increases for non-degenerating $\psi(r)$. A special case is m-dependent, that is $\psi(r)=0$, whenever r>R for some R>0. According to (S.46), the choice of r is free of \tilde{m} and only depends on R in this special case.

S.V Covariance Estimation

We discuss the estimation of the covariance matrix. Suppose the error process has the decomposition

$$\epsilon(s) = \epsilon_1(s) + \epsilon_2(s),$$

where $\epsilon_1(s)$ is a spatial process modeling the spatial correlation and $\epsilon_2(s)$ is an independent error process, known as the nugget effect, modeling measurement error. It is common to assume that (i) $\epsilon_1(s)$ is a spatial Gaussian process with the covariance function $c(\cdot,\cdot)$; (ii) $\epsilon_2(s)$ independently follows the normal distribution with mean zero and

variance γ^2 at every location. For example, a popular choice of the spatial correlation function is the Matérn family of stationary correlation functions, i.e.,

$$\rho(s, s'; \nu, \phi) = \frac{1}{2^{\nu - 1} \Gamma(\nu)} \left\{ \frac{2\nu^{1/2} \operatorname{dist}(s, s')}{\phi} \right\}^{\nu} J_{\nu} \left(\frac{2\nu^{1/2} \operatorname{dist}(s, s')}{\phi} \right), \quad \nu > 0, \phi > 0,$$

where Γ is the Gamma function, $J_{\nu}(\cdot)$ is the modified Bessel function of the second kind with order ν , and dist (\cdot, \cdot) denotes the Euclidean distance. Here, ν controls the degree of smoothness and ϕ is the range parameter.

Generally, we can specify $c(\cdot,\cdot) = \sigma^2 \rho(\cdot,\cdot;\theta)$ for a correlation function ρ parameterized by θ , e.g., $\theta = (\nu,\phi)$ for the Matérn family. Recall that $\mathcal{S}_m = \{s_1,\ldots,s_m\}$ and let $C_m(\theta,\sigma^2) = (\sigma^2 \rho(s_i,s_j;\theta))_{i,j=1}^m$. The log-likelihood function of $\mathbf{X} = (X(s_1),\ldots,X(s_m))^{\top}$ is

$$l_m(\boldsymbol{\mu}, \theta, \sigma^2, \gamma^2) = -\frac{m}{2} \log(2\pi) - \frac{1}{2} \log \det\{C_m(\theta, \sigma^2) + \gamma^2 I_m\}$$
$$-\frac{1}{2} (\mathbf{X} - \boldsymbol{\mu})^{\mathsf{T}} \{C_m(\theta, \sigma^2) + \gamma^2 I_m\}^{-1} (\mathbf{X} - \boldsymbol{\mu}),$$

where $\boldsymbol{\mu} = (\mu_1, \dots, \mu_m)^{\top}$. Jointly estimating $(\boldsymbol{\mu}, \theta, \sigma^2, \gamma^2)$ without special structure for $\boldsymbol{\mu}$ is challenging. Some constraints are typically needed to regularize the form of $\boldsymbol{\mu}$. For example, when external covariates $\mathbf{Z} = (\mathbf{Z}(s_1), \dots, \mathbf{Z}(s_m))^{\top}$ with $\mathbf{Z}(s_j) = (Z_1(s_j), \dots, Z_p(s_j))^{\top}$ is available, we can model the signal by $\boldsymbol{\mu} = \mathbf{Z}\boldsymbol{\beta}$ for $\boldsymbol{\beta} \in \mathbb{R}^p$. Then, the parameters are estimated by

$$\underset{\boldsymbol{\beta}, \boldsymbol{\theta}, \sigma^2, \gamma^2}{\operatorname{arg \, min}} \log \det \{ C_m(\boldsymbol{\theta}, \sigma^2) + \gamma^2 I_m \} + (\mathbf{X} - \mathbf{Z}\boldsymbol{\beta})^{\top} \{ C_m(\boldsymbol{\theta}, \sigma^2) + \gamma^2 I_m \}^{-1} (\mathbf{X} - \mathbf{Z}\boldsymbol{\beta}).$$

Profiling out β , we can obtain the estimates for the target parameters $(\theta, \sigma^2, \gamma^2)$ by solving the following problem

$$\underset{\theta, \sigma^2, \gamma^2}{\operatorname{arg \, min}} \ \log \det \{ C_m(\theta, \sigma^2) + \gamma^2 I_m \} + \{ \mathbf{X} - \mathbf{Z} \widehat{\boldsymbol{\beta}}(\theta, \sigma^2, \gamma^2) \}^{\top}$$

$$\times \{C_m(\theta, \sigma^2) + \gamma^2 I_m\}^{-1} \{\mathbf{X} - \mathbf{Z}\widehat{\boldsymbol{\beta}}(\theta, \sigma^2, \gamma^2)\},$$

where
$$\widehat{\boldsymbol{\beta}}(\theta, \sigma^2, \gamma^2) = \arg\min_{\boldsymbol{\beta}} (\mathbf{X} - \mathbf{Z}\boldsymbol{\beta})^{\top} \{ C_m(\theta, \sigma^2) + \gamma^2 I_m \}^{-1} (\mathbf{X} - \mathbf{Z}\boldsymbol{\beta}).$$

Remark S.3. In some applications, we have multiple observations from the spatial random field

$$X_i(s) = \mu(s) + \epsilon_i(s), \quad i = 1, 2, \dots, n.$$

The joint log-likelihood function is given by

$$l_{n,m}(\boldsymbol{\mu}, \boldsymbol{\theta}, \sigma^2, \gamma^2) = -\frac{mn}{2} \log(2\pi) - \frac{n}{2} \log \det\{C_m(\boldsymbol{\theta}, \sigma^2) + \gamma^2 I_m\}$$
$$-\frac{1}{2} \sum_{i=1}^n (\mathbf{X}_i - \boldsymbol{\mu})^{\top} \{C_m(\boldsymbol{\theta}, \sigma^2) + \gamma^2 I_m\}^{-1} (\mathbf{X}_i - \boldsymbol{\mu}),$$

with $\mathbf{X}_i = (X_i(s_1), \dots, X_i(s_m))^{\top}$. In this case, we can estimate the covariance parameters by solving the problem

$$\underset{\theta, \sigma^2, \gamma^2}{\operatorname{arg \, min}} \ n \log \det \{ C_m(\theta, \sigma^2) + \gamma^2 I_m \} + \sum_{i=1}^n (\mathbf{X}_i - \bar{\mathbf{X}})^\top \{ C_m(\theta, \sigma^2) + \gamma^2 I_m \}^{-1} (\mathbf{X}_i - \bar{\mathbf{X}})$$

with
$$\bar{\mathbf{X}} = n^{-1} \sum_{i=1}^{n} \mathbf{X}_i$$
.

S.VI Searching Algorithm

This section provides more details about Algorithm 1 in Section 3 of the main paper. Finding the optimal thresholds requires solving the constrained optimization problem (9). Due to the discrete nature of the problem, the solution can be obtained if we replace \mathcal{F}_q by

$$\{(t_1, t_2) \in \mathcal{T} : \widehat{\text{FDP}}_{\lambda, \widetilde{\mathcal{S}}}(t_1, t_2) \le q\},$$

where $\mathcal{T} = \{(\widehat{T}_1(s), \widehat{T}_2(s')) : s, s' \in \mathcal{S}\}$ is the set of all candidate cutoff values. A naive grid search algorithm would require evaluating $\widehat{\text{FDP}}_{\lambda,\widetilde{\mathcal{S}}}$ at $|\mathcal{S}|^2$ different values, which is computationally prohibitive for a large number of spatial locations. Interestingly, we show that there exists a faster algorithm that retains an exact maximization of (9). We derive our algorithm in three steps utilizing the specific structure of the optimization problem. For the ease of presentation, we assume that there is no tie among $\{\widehat{T}_j(s) : s \in \mathcal{S}\}$ for j = 1, 2.

Step 1. We partition the candidate set \mathcal{T} into I subsets (say $\{\mathscr{S}_i\}_{i=1}^I$) such that the rejection set remains unchanged using the cutoffs within the same subset. For example, let $\mathcal{D}(t_1,t_2)=\{s\in\mathcal{S}:\widehat{T}_1(s)\geq t_1,\widehat{T}_2(s)\geq t_2\}$ be the set of locations rejected using the cutoff (t_1,t_2) . Then we have $\mathcal{D}(t_1,t_2)=\mathcal{D}(t'_1,t'_2)$ for $(t_1,t_2),(t'_1,t'_2)\in\mathscr{S}_i$. As $L(t_1,t_2,x,\widehat{\rho}(s))$ is a non-increasing function of (t_1,t_2) , we know that $\widehat{\mathrm{FDP}}_{\lambda,\widetilde{\mathcal{S}}}(t_1,t_2)$ is a non-increasing function within each \mathscr{S}_i (note that $\widehat{R}(t_1,t_2)$ is a constant over \mathscr{S}_i). For $(t_1,t_2)\in\mathscr{S}_i$, $\widehat{\mathrm{FDP}}_{\lambda,\widetilde{\mathcal{S}}}(t_1,t_2)$ achieves its minimum value at $(\max_{(t_1,t_2)\in\mathscr{S}_i}t_1,\max_{(t_1,t_2)\in\mathscr{S}_i}t_2)$. Thus we can reduce the candidate set from \mathcal{T} to

$$\mathcal{T}' = \left\{ \left(\max_{(t_1, t_2) \in \mathscr{S}_i} t_1, \max_{(t_1, t_2) \in \mathscr{S}_i} t_2 \right) : 1 \le i \le I \right\},\tag{S.47}$$

where the maximum is defined to be infinity when $\mathscr{S}_i = \emptyset$. For each \mathscr{S}_i , we let $\mathcal{D}_i \subseteq \mathcal{S}$ be the set of locations associated with the hypotheses being rejected. It is not hard to verify that

$$\left(\max_{(t_1,t_2)\in\mathscr{S}_i} t_1, \max_{(t_1,t_2)\in\mathscr{S}_i} t_2\right) = \left(\min_{s\in\mathcal{D}_i} \widehat{T}_1(s), \min_{s\in\mathcal{D}_i} \widehat{T}_2(s)\right). \tag{S.48}$$

Below we derive an alternative expression for \mathcal{T}' which facilitates the implementation of our fast algorithm. Without loss of generality, let us assume that $\mathcal{S} = \{s_1, s_2, \cdots, s_m\}$ and

$$\widehat{T}_2(s_1) > \widehat{T}_2(s_2) > \dots > \widehat{T}_2(s_m).$$
 (S.49)

We claim that

$$\mathcal{T}' = \left\{ (\widehat{T}_1(s_l), \widehat{T}_2(s_k)) : \widehat{T}_1(s_l) \le \widehat{T}_1(s_k) \text{ and } l \le k, \ k = 1, 2, \dots, m \right\} \cup \left\{ (\infty, \infty) \right\}.$$
 (S.50)

To prove the above result, let us consider any cutoff $(\widehat{T}_1(s_l), \widehat{T}_2(s_k))$ from the set defined in the RHS of (S.50). There exists an $1 \leq i \leq I$ such that the corresponding set of rejected locations is given by \mathcal{D}_i . Then we have

$$\min_{s \in \mathcal{D}_i} \widehat{T}_1(s) \ge \widehat{T}_1(s_l) \quad \text{and} \quad \min_{s \in \mathcal{D}_i} \widehat{T}_2(s) \ge \widehat{T}_2(s_k). \tag{S.51}$$

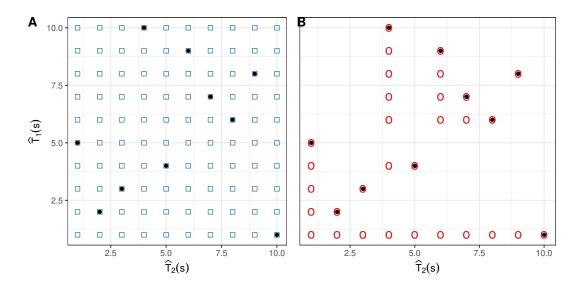


Figure S.13: The black points denote the values of the test statistics. The blue squares in Panel A denote all the candidate cutoffs in \mathcal{T} . The red circles in Panel B correspond to the cutoffs in $\mathcal{T}' \setminus \{(\infty, \infty)\}$.

Also note that \mathcal{H}_{s_l} and \mathcal{H}_{s_k} are both rejected as $\widehat{T}_2(s_l) \geq \widehat{T}_2(s_k)$ for $l \leq k$ and $\widehat{T}_1(s_l) \leq \widehat{T}_1(s_k)$ by the requirement in (S.50). Hence, both inequalities in (S.51) become equalities, i.e., $\min_{s \in \mathcal{D}_i} \widehat{T}_1(s) = \widehat{T}_1(s_l)$ and $\min_{s \in \mathcal{D}_i} \widehat{T}_2(s) = \widehat{T}_2(s_k)$, which shows the RHS of (S.50) belongs to \mathcal{T}' . To show the other direction, we note that for any $1 \leq i \leq I$, there exist $1 \leq k, l \leq m$ such that $s_k, s_l \in \mathcal{D}_i$, $\widehat{T}_1(s_l) = \min_{s \in \mathcal{D}_i} \widehat{T}_1(s)$ and $\widehat{T}_2(s_k) = \min_{s \in \mathcal{D}_i} \widehat{T}_2(s)$. Therefore, we get $\widehat{T}_1(s_l) \leq \widehat{T}_1(s_k)$ and $\widehat{T}_2(s_k) \leq \widehat{T}_2(s_l)$. In view of (S.49), we must have $l \leq k$ and thus $(\widehat{T}_1(s_l), \widehat{T}_2(s_k))$ is an element of the set in the RHS of (S.50).

To understand the complexity of \mathcal{T}' , we point out two extreme cases. In the first case, we assume that $\widehat{T}_1(s_1) > \widehat{T}_1(s_2) > \cdots > \widehat{T}_1(s_m)$. Then we have $\mathcal{T}' = \{(\widehat{T}_1(s_k), \widehat{T}_2(s_k)) : k = 1, 2, \ldots, m\} \cup \{(\infty, \infty)\}$ and hence $|\mathcal{T}'| = m+1$. In the second case, suppose $\widehat{T}_1(s_1) < \widehat{T}_1(s_2) < \cdots < \widehat{T}_1(s_m)$. Then $\mathcal{T}' = \{(\widehat{T}_1(s_l), \widehat{T}_2(s_k)) : l \leq k, k = 1, 2, \ldots, m\} \cup \{(\infty, \infty)\}$ and $|\mathcal{T}'| = m(m+1)/2 + 1$. In general, the cardinality of \mathcal{T}' is between these extreme cases. See Figure S.13 for an illustration about \mathcal{T}' in the intermediate case.

Step 2. Suppose that we have found some cutoff $(t_1, t_2) \in \mathbb{R}^2$ such that $\widehat{\text{FDP}}_{\lambda, \widetilde{\mathcal{S}}}(t_1, t_2) \leq q$. Then we can reduce the candidate set by removing those cutoffs whose rejection numbers are less than $\widehat{R}(t_1, t_2)$. For example, let

$$\widetilde{t}_2^\# = \min \underset{t_2: \widehat{\text{FDP}}_{\lambda, \widetilde{\mathcal{S}}}(-\infty, t_2) \leq q}{\arg \max} \widehat{R}(-\infty, t_2),$$

which can be efficiently computed using the usual BH procedure. Clearly, $\widehat{R}(t_1, t_2) \leq \widehat{R}(-\infty, \widetilde{t}_2^{\#})$ for $t_2 > \widetilde{t}_2^{\#}$. Thus we can further reduce \mathcal{T}' to $\mathcal{T}'' = \left\{ (t_1, t_2) \in \mathcal{T}' : t_2 \leq \widetilde{t}_2^{\#} \right\}$.

Step 3. Searching over \mathcal{T}'' can still be computationally expensive. Here we show that pruning can be used to increase the computational efficiency whilst still ensuring that the method finds a global optimum of (9) of the main paper. The essence of pruning in this context is to remove those cutoffs which can never deliver the best number of rejections.

To introduce pruning, we denote the elements in \mathcal{T}'' by $(t_{1,i,j},t_{2,i})$ for $i=1,2\ldots,\check{m}$ and $1\leq j\leq m_i$, where \check{m} is the number of $\widehat{T}_2(s)$'s that are no larger than $\widehat{t}_2^\#$. Suppose the points are sorted in the following way: (1) $t_{2,1}>t_{2,2}>\cdots>t_{2,\check{m}}$; (2) $t_{1,i,1}>t_{1,i,2}>\cdots>t_{1,i,m_i}$ for all $1\leq i\leq \check{m}$. We then examine the candidate cutoffs in a sequential way. As described in Algorithm 1 below, in the outer loop, we consider $t_{2,i}$ for i running from 1 to \check{m} . In the inner loop, for a given i, we consider $t_{1,i,j}$ for j running from 1 to m_i . Let (t_1^C,t_2^C) be the best cutoff value we have found so far that delivers the largest number of rejections while controlling $\widehat{\mathrm{FDP}}_{\lambda,\widetilde{S}}$ at the desired level q. We skip all the remaining cutoffs whose rejection numbers are less than $\widehat{R}(t_1^C,t_2^C)$. We replace (t_1^C,t_2^C) by $(t_{1,i,j},t_{2,i})$ if one of the following two conditions is satisfied:

1.
$$\widehat{R}(t_{1,i,j}, t_{2,i}) = \widehat{R}(t_1^C, t_2^C)$$
 and $\widehat{\text{FDP}}_{\lambda, \widetilde{\mathcal{S}}}(t_{1,i,j}, t_{2,i}) < \widehat{\text{FDP}}_{\lambda, \widetilde{\mathcal{S}}}(t_1^C, t_2^C) \le q$;

2.
$$\widehat{R}(t_{1,i,j}, t_{2,i}) > \widehat{R}(t_1^C, t_2^C)$$
 and $\widehat{\text{FDP}}_{\lambda, \widetilde{S}}(t_{1,i,j}, t_{2,i}) \leq q$.

When the cutoff $(t_{1,i,j}, t_{2,i})$ being examined satisfies neither conditions, instead of moving directly to the next cutoff on the list, we can use the statistics we have computed in the current step to decide the minimum number of rejections required for the next cutoff. Specifically, note that

$$\frac{\int L\left(t_{1,i,j},t_{2,i},x,\widehat{\rho}(s)\right)d\widehat{G}_{\widetilde{\mathcal{S}}}(x)}{\widehat{R}(t_{1,i,j'},t_{2,i})} \leq \frac{\int L\left(t_{1,i,j'},t_{2,i},x,\widehat{\rho}(s)\right)d\widehat{G}_{\widetilde{\mathcal{S}}}(x)}{\widehat{R}(t_{1,i,j'},t_{2,i})} = \widehat{\mathrm{FDP}}_{\lambda,\widetilde{\mathcal{S}}}(t_{1,i,j'},t_{2,i}).$$

For a cutoff to be valid, we need $\widehat{\text{FDP}}(t_{1,i,j'},t_{2,i}) \leq q$, which implies that

$$\begin{split} \widehat{R}(t_{1,i,j'},t_{2,i}) &\geq \left\lceil \frac{1}{q} \int L\left(t_{1,i,j},t_{2,i},x,\widehat{\rho}(s)\right) d\widehat{G}_{\widetilde{\mathcal{S}}}(x) \right\rceil \\ &= \left\lceil \frac{1}{q} \widehat{\text{FDP}}_{\lambda,\widetilde{\mathcal{S}}}(t_{1,i,j},t_{2,i}) \widehat{R}(t_{1,i,j},t_{2,i}) \right\rceil \\ &:= R_{\text{reg.}}. \end{split}$$

where $\lceil \cdot \rceil$ denotes the ceiling function. When there is no tie, increasing j by k brings k more rejections. Thus we must have

$$j' - j \ge \max \left\{ 1, R_{\text{req}} - \widehat{R}(t_{1,i,j}, t_{2,i}) \right\}.$$
 (S.52)

This observation is used to prune the candidate set, which improves the efficiency. Combining the insights from the above discussions, we propose Algorithm 1, the fast step-down algorithm.

Remark S.4. Algorithm 1 can be modified to find the optimal cutoffs for the 2d procedure coupled with various weighted BH procedures (wBH) as discussed in Section 2.7 of the main paper. Recall that the rejection rule for the hypothesis at location s is given by $p_1(s) \leq \min\{\tau, w(s)t_1\}$ and $p_2(s) \leq \min\{\tau, w(s)t_2\}$ (or equivalently $p_1(s) \leq \tau$, $p_2(s) \leq \tau$, $p_1(s)/w(s) \leq t_1$, and $p_2(s)/w(s) \leq t_2$), where $p_j(s) = 1 - \Phi(\widehat{T}_j(s))$ for j = 1, 2. Thus the set of all candidate cutoff values is

$$\{(p_1(s)/w(s), p_2(s)/w(s)) : p_1(s) \le \tau, p_2(s) \le \tau, s \in \mathcal{S}\}.$$

Algorithm 1 in the main paper can be modified to find the optimal thresholds (t_1, t_2) for the weighted p-values.

Remark S.5. When there exist ties among $\{\widehat{T}_j(s): s \in \mathcal{S}\}$ for j = 1, 2, Algorithm 1 still manages to find the target threshold. The key here is to argue that line 11 of Algorithm 1 does not skip any cutoff whose rejection number is no less than R_{req} . To see this, suppose

$$t_{1,i,1} = \dots = t_{1,i,j_1} > t_{1,i,j_1+1} = \dots = t_{1,i,j_2} > \dots > t_{1,i,j_{m'_i-1}+1} = \dots = t_{1,i,j_{m'_i}},$$

where $j_0 = 0$ and $j_{m'_i} = m_i$. Obviously, the rejection numbers of the nearby cutoffs satisfy that $\widehat{R}(t_{1,i,j},t_{2,i}) = \widehat{R}(t_{1,i,j_k},t_{2,i})$ for $j_{k-1} < j \le j_k$ and $\widehat{R}(t_{1,i,j_k},t_{2,i}) - \widehat{R}(t_{1,i,j_{k-1}},t_{2,i}) = j_k - j_{k-1}$ for all $0 < k \le m'_i$. For non-nearby cutoffs, suppose they locate between $j_{k-1} < j = j_k - l \le j_k$ and $j_{k'-1} < j' = j_{k'} - l' \le j_{k'}$ for some j < j' and $0 < k, k' \le m'_i$. Then,

$$\widehat{R}(t_{1,i,j'}, t_{2,i}) - \widehat{R}(t_{1,i,j}, t_{2,i}) = \widehat{R}(t_{1,i,j_{k'}}, t_{2,i}) - \widehat{R}(t_{1,i,j_{k}}, t_{2,i})$$

$$= \sum_{l=k}^{k'-1} (j_{l+1} - j_{l})$$

$$= j_{k'} - j_{k}.$$

We now show that the rejection numbers of the skipped cutoffs are no more than R_{req} . Start with an arbitrary cutoff $(t_{1,i,j},t_{2,i})$ whose rejection number is less than R_{req} , i.e., $\widehat{R}(t_{1,i,j},t_{2,i}) < R_{\text{req}}$. Line 11 in Algorithm 1 suggests $j' = j + R_{\text{req}} - \widehat{R}(t_{1,i,j},t_{2,i})$. As $j = j_k - l$, $j' = j_{k'} - l'$ and $\widehat{R}(t_{1,i,j'},t_{2,i}) - \widehat{R}(t_{1,i,j},t_{2,i}) = j_{k'} - j_k$, we have

$$\widehat{R}(t_{1,i,j'},t_{2,i}) - \widehat{R}(t_{1,i,j},t_{2,i}) = j_{k'} - j_k = l' - l + R_{\text{req}} - \widehat{R}(t_{1,i,j},t_{2,i}),$$

which implies that

$$\widehat{R}(t_{1,i,j'}, t_{2,i}) = R_{\text{req}} + l' - l.$$

We thus only need to verify that the rejection number of $(t_{1,i,j_{k'-1}},t_{2,i})$ is less than R_{req} . Indeed, when $l' \leq l$,

$$\widehat{R}(t_{1,i,j_{k'-1}},t_{2,i}) < \widehat{R}(t_{1,i,j'},t_{2,i}) \le R_{\text{reg}}.$$

When l < l',

$$\widehat{R}(t_{1,i,j_{k'-1}},t_{2,i}) = R_{\text{req}} + l' - l - (j_{k'} - j_{k'-1}) < R_{\text{req}} - l \le R_{\text{req}}.$$

In both cases, the skipped cutoffs induce no more than R_{reg} rejections.

References

Jiang, W. and Zhang, C.-H. (2009), "General maximum likelihood empirical Bayes estimation of normal means," *The Annals of Statistics*, 37, 1647–1684.

Wainwright, M. J. (2019), High-Dimensional Statistics: A Non-Asymptotic Viewpoint, Cambridge Series in Statistical and Probabilistic Mathematics, Cambridge: Cambridge University Press.

Yi, S., Zhang, X., Yang, L., Huang, J., Liu, Y., Wang, C., Schaid, D. J., and Chen, J. (2021), "2dFDR: A new approach to confounder adjustment substantially increases detection power in omics association studies," *Genome Biology*, 22, 208.

Zhang, C.-H. (2009), "Generalized maximum likelihood estimation of normal mixture densities," *Statistica Sinica*, 19, 1297–1318.